THE CLIMATOLOGY OF SPRINGTIME FREEZE EVENTS IN THE CENTRAL AND EASTERN USA

By

Ting Wang

A THESIS

Submitted to
Michigan State University
in partial fulfillment of the requirements
for the degree of

Geography – Master of Science

2021

ABSTRACT

THE CLIMATOLOGY OF SPRINGTIME FREEZE EVENTS IN THE CENTRAL AND EASTERN USA

By

Ting Wang

The agricultural productions in the central and eastern United States are sensitive to springtime freeze events. As a result of global warming, increasing temperatures have led to earlier shifted springs, usually called false springs, which have resulted in disastrous damage on premature plants exposed to subsequent freeze events. This study analyzes the climatology of springtime freezes and their impacts on agriculture in the Midwestern United States for the period of 1981-2018. The study began by evaluating two potential datasets for the purpose of this analysis: the PRISM (Parameter-elevation Regressions on Independent Slopes Model, http://prism.oregonstate.edu) analysis and the ERA5 (the fifth major global reanalysis produced by European Centre for Medium-Range Weather Forecasts, Hersbach et al., 2018) reanalysis. The PRISM data are found to be a better representation of the observed freezing events and therefore used for establishing freeze events climatology, while the ERA5 reanalysis is used to understand the weather conditions and climate background of the freeze events. Freezing days in March show a decreasing trend across our study region from 1981 to 2018. EOF analysis of freezing days in March shows a relatively larger variation in the Ohio Valley, and the first EOF time series shows substantial interannual variability. The positive phase of NAO (North Atlantic Oscillation) is usually associated with less freezing risk in March across the study region. A crop yield simulation model is used to investigate the historical impacts of false springs and subsequent freeze events on fruit crop yields using apple as an example. Damage tends to occur at the early growing stages of apples when they are more vulnerable. Damage is generally occurring on earlier and warmer days, which could be due to the more frequent false spring occurrences. The Upper Midwest and the Northeast are regions that are less vulnerable to freeze damage.

ACKNOWLEDGEMENTS

I would like to thank my advisors, Drs. Jeff Andresen and Shiyuan Zhong, and committee member and graduate director, Nathan Moore, for their help and guidance in this research. They have been very supportive and instructive, and I am so grateful to have the opportunity to work with them.

I would like to acknowledge the Department of Geography, Environment and Spatial Sciences for giving me the opportunity to pursue my graduate study and to thank all my fellow graduate students and collaborators for their help and encouragement. It is a wonderful experience being a geographer here. I have learned a lot and expanded my interests.

I would like to thank researchers in the Forest Service Northern Research Station Lansing Office, particularly Xindi Bian, Warren Heilman, Joseph Charney, and Mike Kiefer, for their scientific discussions and for providing computational and data storage resources and office space.

Last but not least, I would like to thank the beauty of Michigan. The gorgeous views here attract me to choose to stay here for two years. I love the sapphire shines of the Great Lakes; I love the fantastic biking trails around the Mackinac Island; I love the melodious sound of lake waves I recorded at the impressive Airbnb house; I love the thick carpet of fallen leaves in Picture Rocks; I love the spectacular sunset of the Lake Lansing North.

So long as men can breathe or eyes can see,

So long lives this, and this gives life to thee.

TABLE OF CONTENTS

LIST OF TABLES vi

LIST OF FIGURES viii

CHAPTER 1 INTRODUCTION 1

CHAPTER 2 EVALUATION OF THE ERA5 AND PRISM DATASETS 7
- 2.1 Background 7
  - 2.1.1 Necessity of evaluating gridded datasets 7
  - 2.1.2 PRISM analysis and ERA5 reanalysis datasets 8
  - 2.1.3 Study objective 9
- 2.2 Data and Method 10
  - 2.2.1 Study region 10
  - 2.2.2 Gridded datasets 10
  - 2.2.3 Observational datasets 11
  - 2.2.4 Evaluation Methods 14
- 2.3 Results 15
  - 2.3.1 Assessment of weather variables 15
  - 2.3.2 Assessment of derived variables 30
- 2.4 Summary 34

CHAPTER 3 FREQUENCY AND SEVERITY OF SPRINGTIME FREEZE EVENTS . . 36
- 3.1 Background 36
  - 3.1.1 False Springs and Springtime Freeze Events 36
  - 3.1.2 Spatiotemporal Variability of Springtime Freeze Events 37
  - 3.1.3 Study Objectives 38
- 3.2 Data and Method 39
- 3.3 Results 41
  - 3.3.1 Temporal and spatial variability of freeze events 41
  - 3.3.2 Freezing Area Percentage 43
  - 3.3.3 Result of EOF analysis for freezing days in springtime months 51
- 3.4 Summary 56

CHAPTER 4 SPRINGTIME FREEZE EVENTS IMPACTS ON AGRICULTURE 58
- 4.1 Background 58
  - 4.1.1 Springtime freeze types and their impacts on perennials 58
  - 4.1.2 False spring occurrences and impacts on crops 59
  - 4.1.3 Influence of phenology on freeze damage 60
  - 4.1.4 Study objectives 61
- 4.2 Dataset and methods 62
  - 4.2.1 PRISM dataset 62
  - 4.2.2 Apple yield simulation model 62

4.3 Results 64
4.3.1 Characteristics of the yearly results 64
4.3.2 Daily Results and some derived indices 68
4.4 Summary 83
CHAPTER 5 CONCLUSION 85
APPENDIX 88
BIBLIOGRAPHY 98

LIST OF TABLES

Table 2.1: Percent of hourly observations missing at six stations 13

Table 2.2: Hourly summary statistics, root mean square difference (RMSD), and Bias between ERA5 product and observational networks at six locations 23

Table 2.3: Daily summary statistics, RMSD between ERA5 product and observational networks, at six locations 24

Table 2.4: Daily summary statistics, RMSD between PRISM product and observational networks, at six locations 25

Table 2.5: Seasonal summary statistics, RMSD between ERA5 product and observational networks, at six locations 27

Table 2.6: Seasonal summary statistics, RMSD between PRISM product and observational networks, at six locations 28

Table 2.7: Annual summary statistics, RMSD between ERA5 product and observational networks, at six locations 29

Table 2.8: Annual summary statistics, RMSD between PRISM product and observational networks, at six locations 29

Table 2.9: Growing degree day (Base 4 °C) summary statistics 30

Table 2.10: Freeze events captured ratios at East Lansing of ERA5 31

Table 2.11: Freeze events captured ratios at East Lansing of PRISM 32

Table 2.12: Freeze events below 0 °C captured ratios at six stations without detailed categories of ERA5 33

Table 2.13: Freeze events below 0 °C captured ratios at six stations without detailed categories of PRISM 33

Table 3.1: 39-year mean of regional averaged monthly FAP 46

Table 3.2: Theil-Sen Slope for monthly FAP. 46

Table 3.3: Pearson correlation values (r) comparing monthly FAP for the months of March, April, and May to NAO values 0-3 months earlier 48

Table 3.4: Pearson correlation values (r) comparing monthly FAP for the months of March, April, and May to PNA values 0-3 months earlier 50

Table A.1.1:. RMSDs of air temperature between WRF and observations at three locations for 48 hours from May12th to May13th with different vertical resolutions 91

Table A.1.2:. RMSDs of wind speed between WRF and observations at three locations for 48 hours from May12th to May13th with different vertical resolutions 93

LIST OF FIGURES

Figure 2.1: Study comparison site locations 12

Figure 2.2: Difference between ERA5 and observations for daily maximum temperature in 2010, 2012, and 2014 16

Figure 2.3: Difference between ERA5 and observations for daily minimum temperature in 2010, 2012, and 2014 17

Figure 2.4: Difference between PRISM and observations for daily maximum temperature in 2010, 2012, and 2014 18

Figure 2.5: Difference between PRISM and observations for daily minimum temperature in 2010, 2012, and 2014 19

Figure 2.6: Time series of the difference between ERA5 monthly mean daily mean temperature and observed values at six locations 20

Figure 2.7: Time series of the difference between PRISM monthly mean daily mean temperature and observed values at six locations 21

Figure 2.8: Scatter plot of daily minimum and maximum temperature between observations and reanalysis datasets 22

Figure 3.1: Average, standard deviation, and trend of freezing days in spring (March, April, May) from 1981 to 2019 42

Figure 3.2: Time series of springtime freeze events count from 1981 to 2019 43

Figure 3.3: Subset regions defined in Karl and Knight (1998) 44

Figure 3.4: Time series of monthly FAP values 45

Figure 3.5: The leading two EOF modes and PC times series for freezing days in March . . 52

Figure 3.6: The leading two EOF modes and PC times series for freezing days in April . . . 53

Figure 3.7: The first PC times series for freezing days in March related to atmospheric variables 54

Figure 3.8: The second PC times series for freezing days in March related to atmospheric variables 55

Figure 3.9: Times series of NAO in March related to atmospheric variables 55

Figure 4.1: Average, absolute variation, relative variation, and trend of the first green date (Julian date) from 1981 to 2018 64

Figure 4.2: Average, absolute variation, relative variation, and trend of the bloom date (Julian date) from 1981 to 2018 66

Figure 4.3: Average, absolute variation, relative variation, and trend of the yearly poor pollination days from 1981 to 2018 67

Figure 4.4: Average, absolute variation, relative variation, and trend of the yield (bud survival chance) from 1981 to 2018 68

Figure 4.5: Average, absolute variation, relative variation, and trend of damage days from 1981 to 2018 69

Figure 4.6: Average of damage days at each growth stage from 1981 to 2018 70

Figure 4.7: The trend of damage days at each growth stage from 1981 to 2018 71

Figure 4.8: The average of freeze damage occurring date at each growth stage from 1981 to 2018 72

Figure 4.9: The trend of freeze damage occurring date at each growth stage from 1981 to 2018 73

Figure 4.10: The average daily minimum temperature during damage occurring date at each growth stage from 1981 to 2018 74

Figure 4.11: The trend of daily minimum temperature during damage occurring date at each growth stage from 1981 to 2018 75

Figure 4.12: The time series of area-averaged damage days in six subregions from 1981 to 2018 77

Figure 4.13: The sum of damage days at each growth stage in six subregions from 1981 to 2018 78

Figure 4.14: The average of damage values at each growth stage in six subregions from 1981 to 2018 79

Figure 4.15: The average daily minimum temperature at each growth stage in six subregions from 1981 to 2018 80

Figure 4.16: The average daily minimum temperature during damage days at each growth stage in six subregions from 1981 to 2018 81

Figure 4.17: The average damage-occurring dates at each growth stage in six subregions from 1981 to 2018 82

Figure A.1.1:. Differences of soil moisture between WRF outputs and observations at Williamsburg 91

Figure A.1.2:. Differences of air temperature between WRF outputs and observations at three locations 92

Figure A.1.3:. Comparison of daily minimum air temperature between WRF and PRISM on May 8th 92

Figure A.1.4:. Daily minimum temperature changes in response to increased soil moisture by a factor of 1.05 on May 8th and May 9th 94

Figure A.1.5:. Daily minimum temperature changes in response to increased soil moisture by a factor of 1.05 on May 12th and May 13th 95

Figure A.1.6:. Major soil categories in our study region 96

Figure A.1.7:. Soil moisture change based on soil types on May 8th and May 9th 96

Figure A.1.8:. Soil moisture change based on soil types on May 12th and May 13th 97

CHAPTER 1

INTRODUCTION

The Midwestern US (including the states of Illinois, Indiana, Iowa, Michigan, Minnesota, Missouri, Ohio, and Wisconsin) ranks among the most intensive and extensive agricultural production areas in the world and affects the global economy consistently and dynamically. Among the various weather- and climate-related threats to agricultural production systems in the region are abnormally mild winters followed by warm, early springs, usually called false springs, which have resulted in disastrous damage to crops phenologically advanced by the early warmth but then exposed to subsequent freeze events (Gu et al., 2008; O'Brien et al., 2019). For example, springtime freeze events in 2002 and 2012 caused dramatic losses in regional agricultural production, including a yield reduction of more than 95% of sour cherry yields in Michigan in 2002 and a loss of more than 85% of apple production in Michigan in 2012 (NASS, 2002; Marino et al., 2011; O'Brien et al., 2019; Labe et al., 2015; Kistner et al., 2018; Gu et al., 2008). While the economic impacts of false springs and subsequent freeze events are significant, there is a general lack of previous research investigating the nature, extent, and impacts of such events, which is the primary objective of the study presented in this thesis.

Understanding the statistical characteristics of springtime freeze events requires continuous, long-term (decades) climate data from both station observations and gridded analysis/reanalysis. Gridded datasets may provide considerable advantages over single site station observations with continuous coverage over space and time, especially in areas with sparse meteorological stations or restricted data accessibility and availability (Ceglar et al., 2017). Gridded datasets include analysis or reanalysis products, both of which involve performing data assimilation, a process relying on both observations from a variety of sources and forecasts from numerical weather prediction models (Parker et al., 2016). Initially, some type of objective analysis is applied on a myriad of observations to an irregular grid to represent the atmospheric state (Dee et al., 2011). As a follow-up process, model-based reanalysis can be performed with individual data layers from the data assimilation system to provide a multivariate, spatially complete, and coherent record of the global atmospheric circulation (Dee et al., 2011). A reanalysis is a particular type of analysis done with a fixed software system. However, both reanalyses and analyses are sensitive to changes in observational systems (Dee et al., 2011). Reanalyses are potentially more attractive since they provide more comprehensive gridded estimates of atmospheric conditions at regular intervals over long periods of time (Parker et al., 2016). Gridded reanalyses and analyses have been used in a wide range of applications, including understanding atmospheric dynamics of jet streams (Kidston et al., 2010), investigating the impact of climate variability on agriculture, air pollution applications, and wind energy development (Toreti et al., 2019; Essou et al., 2017; Gleixner et al., 2020; Cannon et al., 2015), and evaluating climate models (Gleckler et al., 2008).

There are also limitations. Despite their popularity, gridded datasets represent area-averaged, and in some cases, time-averaged estimates of meteorological variables and hence may not accurately represent meteorological conditions at a particular location or time (Tetzner et al., 2019; Bosilovich et al., 2013). It is, therefore, necessary before a specific application to assess how the gridded datasets represent the local variability in a region of interest. This necessity is the motivation for the work presented in Chapter 2 that evaluates two gridded datasets used for the studies in the later chapters: The analysis product PRISM (Parameter-elevation Regressions on Independent Slopes Model, http://prism.oregonstate.edu), a gridded analysis dataset provided by the PRISM climate group from Oregon State University, and a reanalysis product, ERA5, the fifth major global reanalysis produced by the European Centre for Medium-Range Weather Forecasts (ECMWF; Hersbach et al., 2018). PRISM estimates temperatures over space using empirical statistical relationships with observed single site climate data from nearby stations adjusted for elevation (Walton and Hall et al., 2018). Station observations are given higher weights if they are geographically closer to the target grid cell and have similar coastal proximity or topographic position, considering all other factors (Walton and Hall et al., 2018). Previous research suggests that consideration of these factors resulted in greater accuracy for PRISM in complex terrain and along coastlines compared to other gridded analyses, including Daymet and WorldClim (Walton and Hall et al., 2018). ERA5 is a global reanalysis extending back to 1979 with a horizontal resolution of 30 km and has been evaluated for a number of regions and historical periods. For example, Tetzner et al. (2019) evaluated ERA5 in the southern Antarctic Peninsula and Ellsworth Land, Antarctica, and concluded that ERA5 is highly accurate in representing the magnitude and variability of near-surface air temperature. They also revealed that the higher spatial and temporal resolution of ERA5 compared to its predecessor, ERA-Interim, significantly reduced the cold coastal bias. Gleixner et al. (2020) concluded that ERA5 reduced statistical biases and improved the representation of interannual variability over most of Africa. However, few studies have specifically evaluated PRISM and ERA5 over the Midwestern and Eastern United States, necessitating an assessment of how both datasets represent the local climatic variability of temperature prior to their application as a proxy for observations to investigate the historical frequency of freeze events. In an evaluation of the two gridded datasets across the region from 2001 to 2018, PRISM was found to more accurately represent historical observations compared to ERA5 and was used as a proxy for observations across the study region in a study of springtime freeze events (Chapter 3) and their impacts on agriculture (Chapter 4).

To investigate the statistical characteristics of springtime freeze events, we need first to consider the physical and causal mechanisms associated with them. There are two main types of freeze events, advection freezes and radiation freezes. Advection freezes tend to occur in a well-mixed boundary layer with strong winds associated with cold fronts or the leading edges of polar-origin high-pressure systems (Winkler et al., 2012). Radiation freezes tend to be associated with surface anticyclones located across the region characterized by relatively cloud-free and calm conditions in which the earth's surface cools more rapidly than the atmosphere above (Winkler et al., 2012). Radiation freezes occur more frequently and are comparatively easier to predict due to the association with a temperature inversion. On the contrary, advection freezes are less frequent and occur without inversion developing and thus are difficult to predict.

There are also temporal changes in springtime freeze frequency to consider. Daily minimum temperatures across the region have warmed in recent decades (Andresen et al. 2012), in many areas more quickly than maximum temperatures, resulting in a decrease in the diurnal temperature range (Qu et al., 2014). There have also been changes at both ends of the temperature distribution. Rowe et al. (2012) noted that the days with record low daily minimum temperatures had been significantly and steadily decreasing nearly everywhere across the United States, while the days with record high daily minimum temperatures increased considerably. There have also been decreases in the number of days with freezing temperatures. DeGaetano (1996) detected an overall decreasing trend in freezing days in the Northeastern United States from 1959 to 1993, while Easterling et al. (2002) observed a significant reduction in springtime freezing days across the western and north-central US from 1948 to 1999. In the same study, first fall freeze occurrences was found to be occurring later in the year with time; the occurrences of the last spring freeze were trending earlier, resulting in an overall increase in the length of the frost-free season (Easterling et al., 2002). Yu et al. (2014) also revealed the same trend for first fall freeze dates, last spring freeze dates, and the frost-free season length from 1980 to 2010 in the Midwest. Their study also identified lesser interannual variability of these dates in the Great Lakes region versus other portions of the Midwest (Yu et al., 2014).

Projected future changes in the frequency and severity of false spring events and subsequent freeze events associated with a warming world may be complex (Allstadt et al., 2015). Both first green dates and first bloom dates will likely continue to shift earlier in the year with rising global temperatures, but the complex nature of this process complicates making a priori estimates of how temperature changes will affect spring onset (Allstadt et al., 2015). Results from previous studies suggest that the intermountain West, Great Plains, and upper Midwest regions of the United States may experience increases in the frequency of false springs (Allstadt et al., 2015; Peterson and Abatzoglou 2014; O'Brien et al., 2019). However, Winkler et al. (2012) concluded that projections of freeze risk after false springs in Michigan are associated with high uncertainty.

Following an examination of historical freeze events across the region in Chapter 3, we study potential associated agricultural impacts in Chapter 4. Springtime freeze events can cause severe damage to crops, especially following false springs. The pattern of abnormal early warmth will not directly cause damage, but the timing of any subsequent freeze events, particularly in relation to the crop phenological stage, is critical (Augspurger et al., 2007; Longstroth et al., 2012). For example, in the early phenological stages of temperate tree fruit crops such as apple and cherry, cold injury and damage begin at temperatures near -6°C, but as the bloom stage approaches, temperatures as warm as -2°C can cause considerable damage (Longstroth, 2005). Therefore, the magnitude of cold injury may vary greatly depending on the crop phenological phase and the level of observed minimum temperatures at the time of the freeze (Hufkens et al., 2012). Extensive damage in both 2007 and 2012 freeze events was associated with record-breaking warm temperatures during the month of March, which led to abnormally advanced and vulnerable crop phenological stages, followed by a series of both advective and radiational freezes in April (Augspurger et al., 2007; Kistner et al., 2017). Since changes in extreme weather events such as freeze events depend more on variability than overall temperature trends, studies reveal that there is an increased risk of freeze damage on crops with more significant temperature variability related to global climate change (Rigby et al., 2008; Augspurger et al., 2013).

Deterministic or semi-deterministic crop simulation models are frequently applied to better understand the potential impacts of climate variability and change on agricultural production systems. However, the relatively slow growth and complexity of perennials tend to limit the number and types of available crop simulation models (Lobell and Field, 2011). The growth and development of vegetation is generally a function of many environmental variables, with the most substantial contribution is typically associated with temperature (Rigby et al., 2008). Rigby et al. (2008) used a simple Thermal Time (or Degree Day) model to estimate the phenology of bud break, and their results revealed that frost risk to vegetation is as sensitive to increases in daily temperature variance as to increases in the mean temperature. Similarly, Marino et al. (2011) used a model to approximate the timing of leaf-out to reconstruct the seasonal start of the season over the period 1901-2007 across the southeastern United States and noted a decreasing trend of false spring occurrences over the study region (Marino et al., 2011). Various studies have focused on how the phenological stages of plants respond to the temperature change with warming trends, but far fewer have investigated possible tree fruit production impacts. In Chapter 4 of this study, the approach of Zavalloni et al. (2006) was applied over the Midwestern and Eastern United States to estimate the yield response of apple, with phenological development based on the methodology of Rijal (2017).

Given their importance in describing yield variability of tree fruit production over time, a better understanding of the climatology of springtime freezes and their impacts on agriculture is highly desirable. This study considers production areas across the central and eastern United States. In Chapter 2, ERA5 reanalysis and PRISM analysis datasets are compared to single station observations at different temporal scales for several relevant climate variables and then evaluated to determine how these datasets capture freeze events with specified criteria. Chapter 3 investigates the frequency, severity, and potential causes of springtime freeze event occurrences across the study region using ERA5 reanalysis to understand the weather conditions and climate background of the freeze events represented by the PRISM analysis dataset. In Chapter 4, we investigate the historical impacts of springtime freeze event damage on apple in the Midwestern US from 1981 to 2018 with a crop simulation model with input data from PRISM, including temporal changes in associated agroclimatic variables. Finally, in Chapter 5, we summarize the main results from Chapter 2 to Chapter 4 and also the limitations.

CHAPTER 2

EVALUATION OF THE ERA5 AND PRISM DATASETS

2.1 Background

2.1.1 Necessity of evaluating gridded datasets

Many environmental-themed applications including crop simulation models require detailed and comprehensive weather and climate data as inputs (Ceglar et al., 2017). Such input data are usually obtained from various sources, including direct observations from networks of weather or climate stations, gridded analyses of station observations, or gridded reanalyses blending observations with numerical weather or climate model outputs. Gridded analyses/reanalyses datasets have advantages over station observations as they can provide reasonable estimates of missing data over space and time, allowing for continuous pattern analysis (Ceglar et al., 2017). The gridded analyses of station observations are typically generated by means of spatial and temporal interpolation techniques (Daly et al., 2008; Walton et al., 2018), while gridded reanalyses generate gridded data surfaces primarily with model simulations and their outputs. Because of the continuous spatial and temporal coverage, gridded analyses or reanalyses datasets have been widely used for understanding weather phenomena, climate variability and trends, and other related applications such as agriculture, air pollution, wind energy (Toreti et al., 2019; Essou et al., 2017; Gleixner et al., 2020; Cannon et al., 2015). There are also challenges in their application. In particular, gridded datasets represent area-averaged, and in some cases, time-averaged estimates of meteorological variables and hence may not accurately represent meteorological conditions at a particular location or time (Tetzner et al., 2019). Consequently, these datasets should be evaluated against actual observations to document if biases or errors exist before being used to understand weather or climate conditions for a particular application.

2.1.2 PRISM analysis and ERA5 reanalysis datasets

PRISM (Parameter-elevation Regressions on Independent Slopes Model; Daly et al., 2008), a gridded analysis dataset of surface climate variables provided by the PRISM climate group from Oregon State University, was utilized to characterize freeze events in the study domain. The dataset was first evaluated by comparing it with observational datasets at different locations in the region. The PRISM climate group incorporates climate observations from a wide range of monitoring networks and develops continuous spatial climate datasets by applying sophisticated quality control measures. PRISM provides long-term (from 1981 to present) daily climate variables, including daily minimum/maximum/mean temperature, precipitation, and vapor pressure deficit (VPD) at a uniform 4 km grid spacing. The comparison of the freeze characteristics derived from the PRISM data with those derived from station observations will determine whether it is a good proxy for observations of freeze occurrences.

Because the PRISM dataset only contains daily surface variables, another dataset that provides information above the surface is necessary to explain the variability and trends of freezing events from the perspective of large-scale atmospheric conditions. The recently released climate reanalysis dataset, ERA5, by the European Centre for Medium-Range Weather Forecasts (ECMWF) will be used for this purpose. ERA refers to 'ECMWF Re-Analysis,' with ERA5 being the fifth major global reanalysis produced by ECMWF. ERA5 provides hourly data from 1979 until present at 139 pressure levels from 1000 hPa to 1 hPa with a horizontal resolution of 30 km. As the latest global reanalysis dataset, ERA5 benefited from a decade of developments in model physics, core dynamics, and data assimilation relative to earlier reanalysis datasets such as ERA-Interim (Hersbach et al., 2019). The ERA5 dataset significantly enhances horizontal resolution with the 30 km grid spacing at different pressure levels and 9 km grid spacing at the surface on land compared to 79 km for ERA-Interim. A number of studies have evaluated the accuracy and applicability of ERA5 and ERA-Interim. For example, Tarek et al. (2019) reveal that the ERA-Interim and ERA5 temperatures are generally similar to site observations over North-America, and ERA5 demonstrates a substantial reduction in warmer biases compared to those in the ERA-Interim dataset. Also, with a good representation of observational precipitation data, the dry/wet bias pattern of ERA-Interim is sharply reduced in ERA5 (Tarek et al., 2019). In this study, we will examine the accuracy of ERA5 in representing freeze events in our study region.

2.1.3 Study objective

The primary objective of this study is to compare ERA5 reanalysis and PRISM analysis datasets with single-site observations at different temporal scales for several relevant climate variables and then evaluate how these datasets capture freeze events with specified criteria.

2.2 Data and Method

2.2.1 Study region

The study domain is the central and eastern United States encompassing the region from 105º W to 75º W longitude and from 35º N to 50º N latitude. This region encompasses one of the largest and most intensive agricultural production areas in the world, including large areas of specialty-crop agriculture such as tree fruit which are highly vulnerable to spring freezes.

2.2.2 Gridded datasets

ERA5 is the fifth generation reanalysis from ECMWF. The reanalysis is produced at a 1-hourly time step using a significantly more advanced 4D-var assimilation scheme (Terek et al., 2019). The ERA5-Land reanalysis dataset provides a consistent view of the evolution of land variables over several decades at an enhanced resolution (9km) compared to ERA5 (Muñoz Sabater et al., 2019). Hourly temperature, relative humidity, and precipitation from 2001 to 2018 across our study region are obtained from ERA5-Land. Data from the centers of grid boxes from the reanalysis nearest to the observational stations were then extracted for comparison. Also, it is noteworthy that variable outputs in grid boxes containing adjacent water areas (e.g., along the shores of the Great Lakes) only represent spatial averages across the land areas and do not include the water-covered surfaces (Muñoz Sabater et al., 2019).

The Parameter-elevation Regressions on Independent Slopes Model (PRISM; Daly et al. 1994) is used to derive gridded surface variables for the conterminous United States. At each grid cell, an elevation regression function, considering multiple physical factors that reflect their similarity to the target grid cell, is fit to stational observations using a moving window (Walton et al., 2018). These factors include distance, cluster, elevation, coastal proximity, topographic facet, vertical layer, topographic position, and effective terrain height (Walton et al., 2018). PRISM incorporates data from a wide range of networks, as many as possible, including COOP, RAWS, the California Data Exchange Center (CDEC), Agrimet, NRCS, the California Irrigation Management

Information System (CIMIS), and more (see http://prism.oregonstate.edu for details). We obtained daily minimum and maximum temperatures from PRISM from 2001 to 2018 across our study region for this comparison.

2.2.3 Observational datasets

Three stational observation datasets are used in the study. They are respectively the Michigan Enviroweather (EW) network, the NOAA National Weather Service Automated Surface Observing System (ASOS), and the US Climate Reference Network (USCRN). The Michigan Enviroweather (EW) network is an interactive information system linking real-time weather data from a statewide mesonetwork, forecasts, and biological and other process-based models for assistance in operational decision-making and risk management associated with Michigan's agriculture and natural resource industries. It aims to develop a sustainable weather-based information system that helps users make pests, plant production, and natural resource management decisions in Michigan (https://www.canr.msu.edu/resources/enviroweather_weather_data_and_pest-_modeling). The Automated Surface Observing System (ASOS) units are automated sensor suites designed to serve as a primary meteorological observing network in the United States. There are currently more than 900 ASOS sites with one-minute and five-minute data at hourly intervals in the United States (https://www.ncdc.noaa.gov/data-access/land-based-station-data/land-based-datasets/automated-surface-observing-system-asos). Five-minute data was obtained for use in this study. The US Climate Reference Network (USCRN) is a systematic and sustained network of climate monitoring stations with sites across the conterminous US, Alaska, and Hawaii. It incorporates high-quality instruments to measure temperature, precipitation, wind speed, soil conditions, and more. The USCRN program aims at maintaining a sustainable, high-quality climate observation network to provide a continuous series of climate observations for monitoring trends in the nation's climate and supporting climate-related research (https://www.ncdc.noaa.gov/crn/).

For the purpose of evaluating gridded weather products, six single site stations across Michigan were chosen for reference observations: East Lansing, Gaylord, East Leland, South Haven, Grand

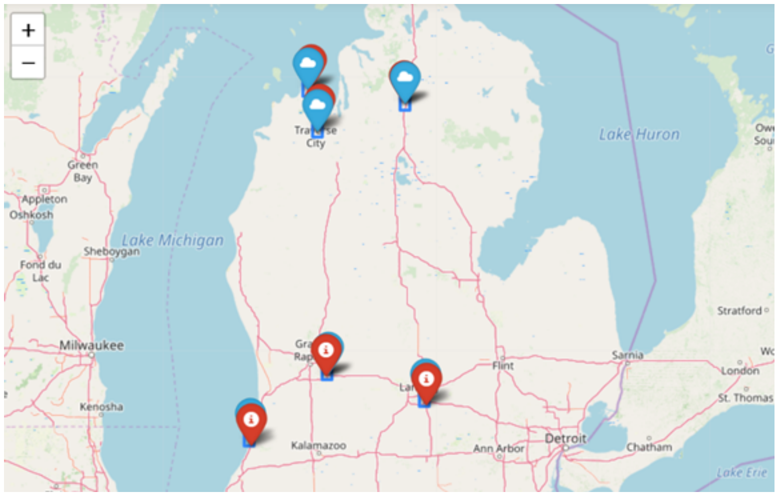

Figure 2.1: *Study comparison site locations.* The red icons in the figure refer to the points of the stational observation datasets, while the blue icons represent the centroids of the rectangles in ERA5-land datasets which contain the stational points.

Rapids, and Traverse City (Figure 2.1). East Leland and South Haven were both chosen to reflect the areas of the study domain near the Great Lakes, where the lakes may significantly modify local climate (Andresen and Winkler, 2009). It is important to note that the comparisons of gridded areal averages to individual point observations are not at identical spatial and temporal scales but still close enough to determine their representativeness and relative applicability.

We evaluate the gridded datasets with the point observations at hourly, daily, monthly, annual, and decadal scales. Missing hourly temperature, relative humidity, and precipitation observations for the six chosen stations were omitted from the comparison and are summarized in table 2.1. The fewest overall missing observations were found at East Lansing, East Leland, and South Haven sites. The ASOS network misses more than half of the precipitation record. With a focus on freeze events that are more related to temperature, we are not going to provide many results of evaluating precipitation data. Also, we notice that more than a quarter of the relative humidity data is not recorded at Gaylord.

Network	Station	Lat	Lon	Date	Atmp missing	Relh missing	Prcp missing
EW	East Lansing	42.67°	-84.49°	1/1/2001 to 12/31/2018	1.38%	0%	0.13%
EW	East Leland	45.03°	-85.67°	5/1/2003 to 12/31/2018	0.37%	0.37%	0.96%
EW	South Haven	42.36°	-86.29°	4/6/2006 to 12/31/2018	0.94%	0.99%	0.8%
ASOS	Grand Rapids	42.881°	-85.523°	1/1/2001 to 12/31/2018	1.97%	2.39%	54.91%
ASOS	Traverse City	44.742°	-85.582°	1/1/2001 to 12/31/2018	3.06%	3.88%	54.11%
USCRN	Gaylord	44.91°	-84.72°	9/19/2007 to 12/31/2018	0.06%	26.63%	0.69%

Table 2.1: *Percent of hourly observations missing at six stations.*

2.2.4 Evaluation Methods

To quantify the differences between gridded datasets and point observations, several statistics were computed. Root Mean Squared Difference (RMSD), a common metric used to measure the accuracy of variables, is the square root of the average of squared differences between estimations and actual observations. In this study, estimations are the gridded datasets (ERA5 and PRISM) and observations are the stational datasets (EW, ASOS, and USCRN). The definition for RMSD is as follows. y_j and $\widehat{y_j}$ are observations and estimations, respectively.

$$RMSD = \sqrt{\frac{1}{n}\sum_{j=1}^{n}(y_j - \widehat{y_j})^2}$$

And the definition for Bias is:

$$Bias = \frac{1}{n}\sum_{j=1}^{n}(y_j - \widehat{y_j})$$

2.3 Results

2.3.1 Assessment of weather variables

We first provide time series plots by comparing the reanalysis datasets and the observational datasets (Figure 2.2 - Figure 2.5). We select three years, 2010, 2012, and 2014 (randomly selected; all three years have complete data from observations), and plot the daily differences between the reanalysis datasets and the observations. The conclusions from the time series of DmaxT (daily maximum temperature) and DminT (daily minimum temperature) for both ERA5 and PRISM reveal that ERA5 shows larger perturbations than PRISM for both DmaxT and DminT, indicating the smaller RMSDs (Root Mean Squared Differences) of PRISM. Also, ERA5 underestimates DmaxT for near-lake stations, especially for late springs, which period we care about most. The time series of DminT for ERA5 shows that it dramatically overestimates DminT for stations near the lake. Also, the DminT of ERA5 is consistently warmer than the observations near the lake during the summertime for our selected three years. The difference between ERA5 and observations of DmaxT shows overall smaller perturbations than DminT.

The time series of DminT and DmaxT for PRISM also reveal that DminT has noticeably larger errors than DmaxT. And the time series of DmaxT shows much smoother patterns for all six stations for three selected years. The differences between PRISM and observations for DminT reveal that PRISM is consistently warmer than observations for the two near-lake stations. Also, since the ASOS network is incorporated into the PRISM reanalysis dataset, Grand Rapids and Traverse city show noticeably smaller perturbations than other stations.

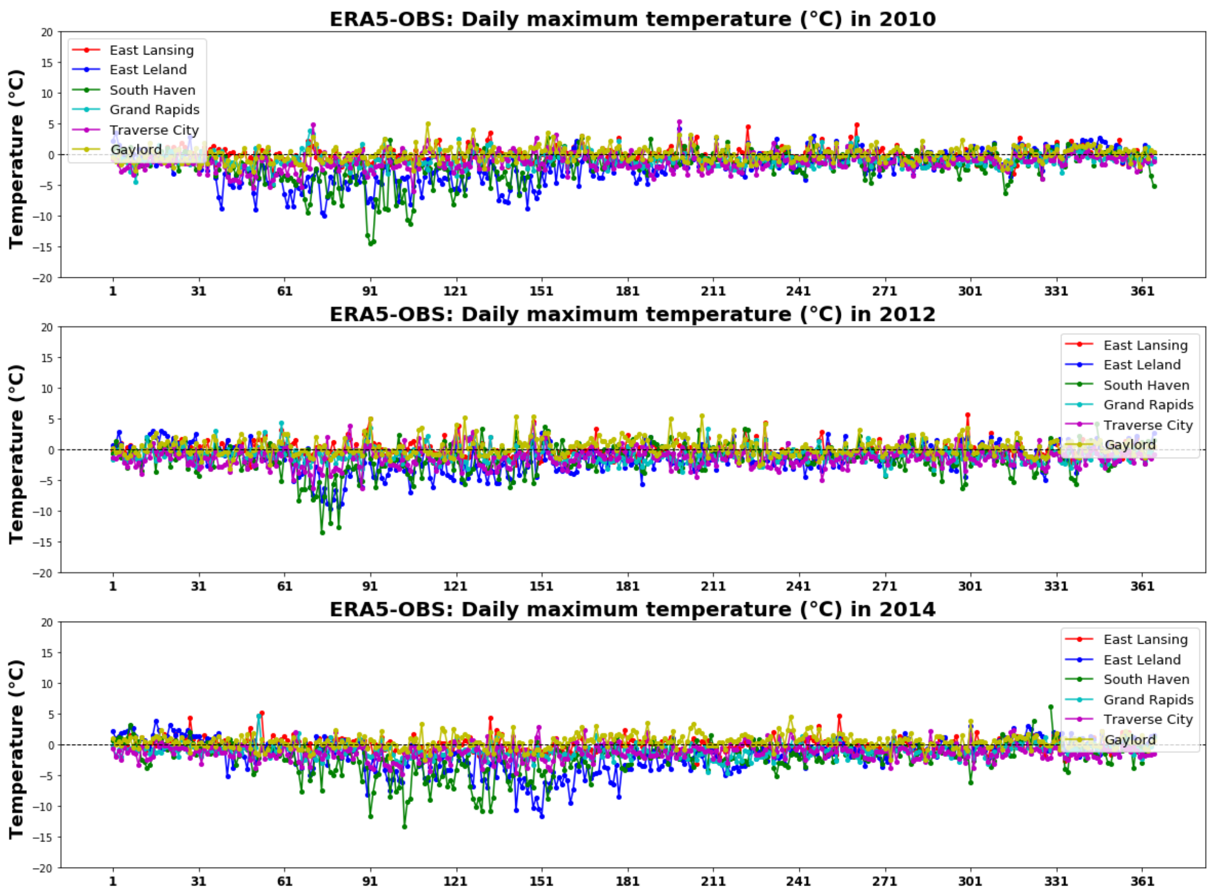

Figure 2.2: *Difference between ERA5 and observations for daily maximum temperature in 2010, 2012, and 2014.*

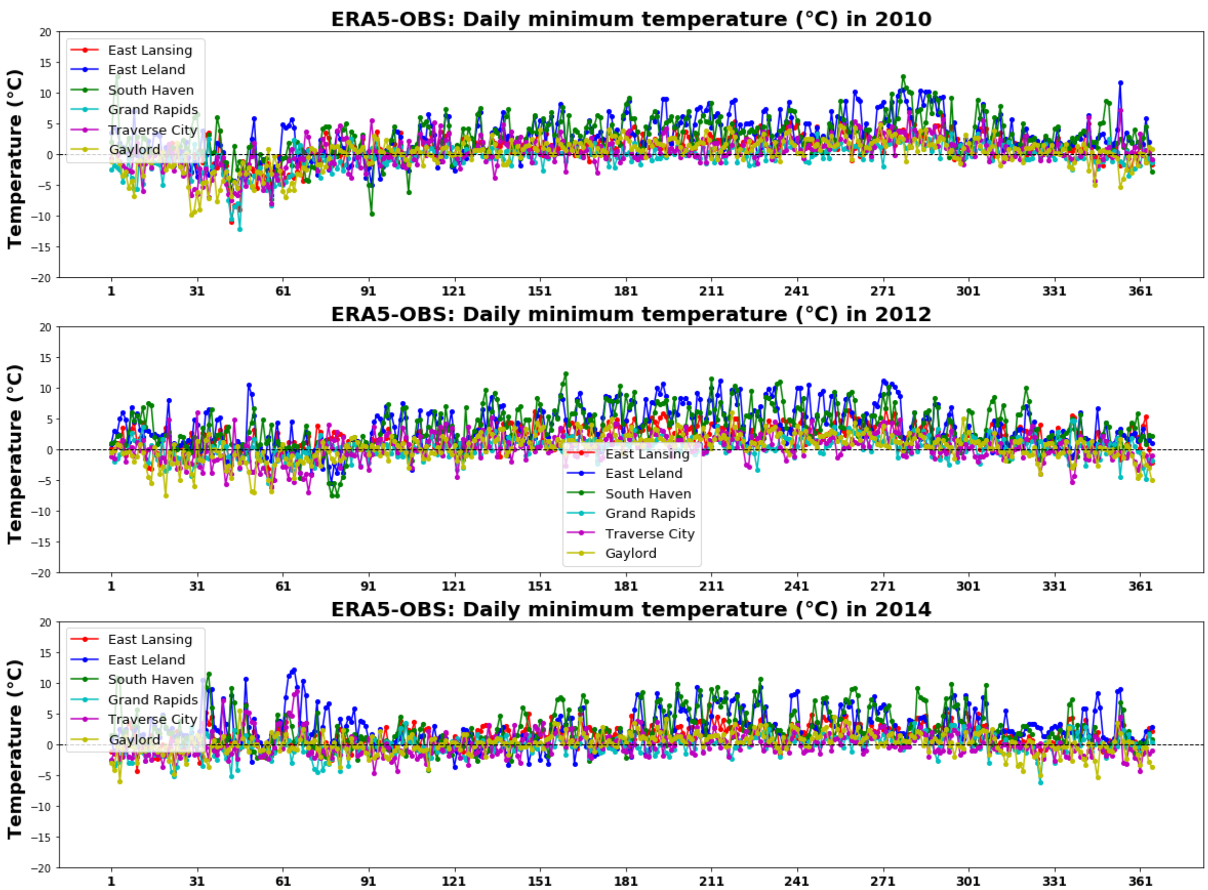

Figure 2.3: *Difference between ERA5 and observations for daily minimum temperature in 2010, 2012, and 2014.*

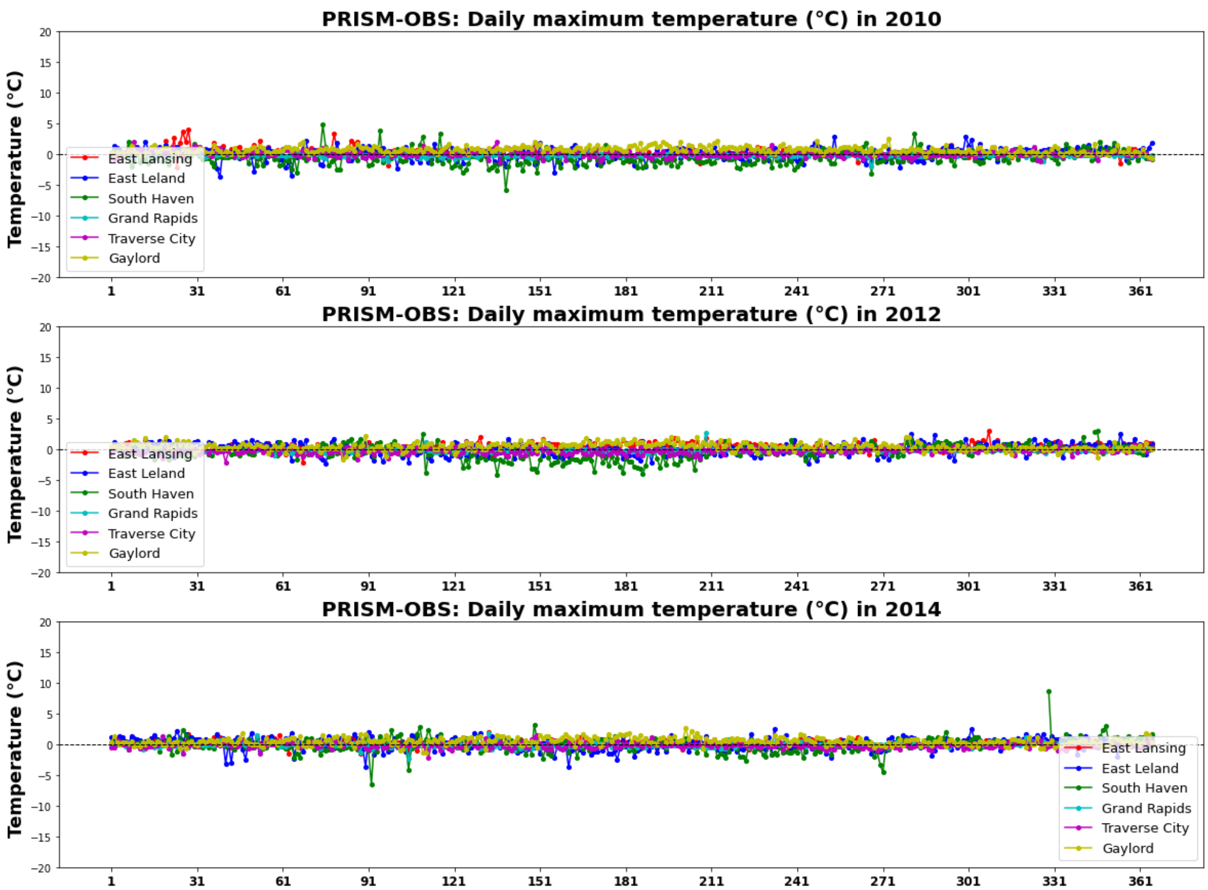

Figure 2.4: *Difference between PRISM and observations for daily maximum temperature in 2010, 2012, and 2014.*

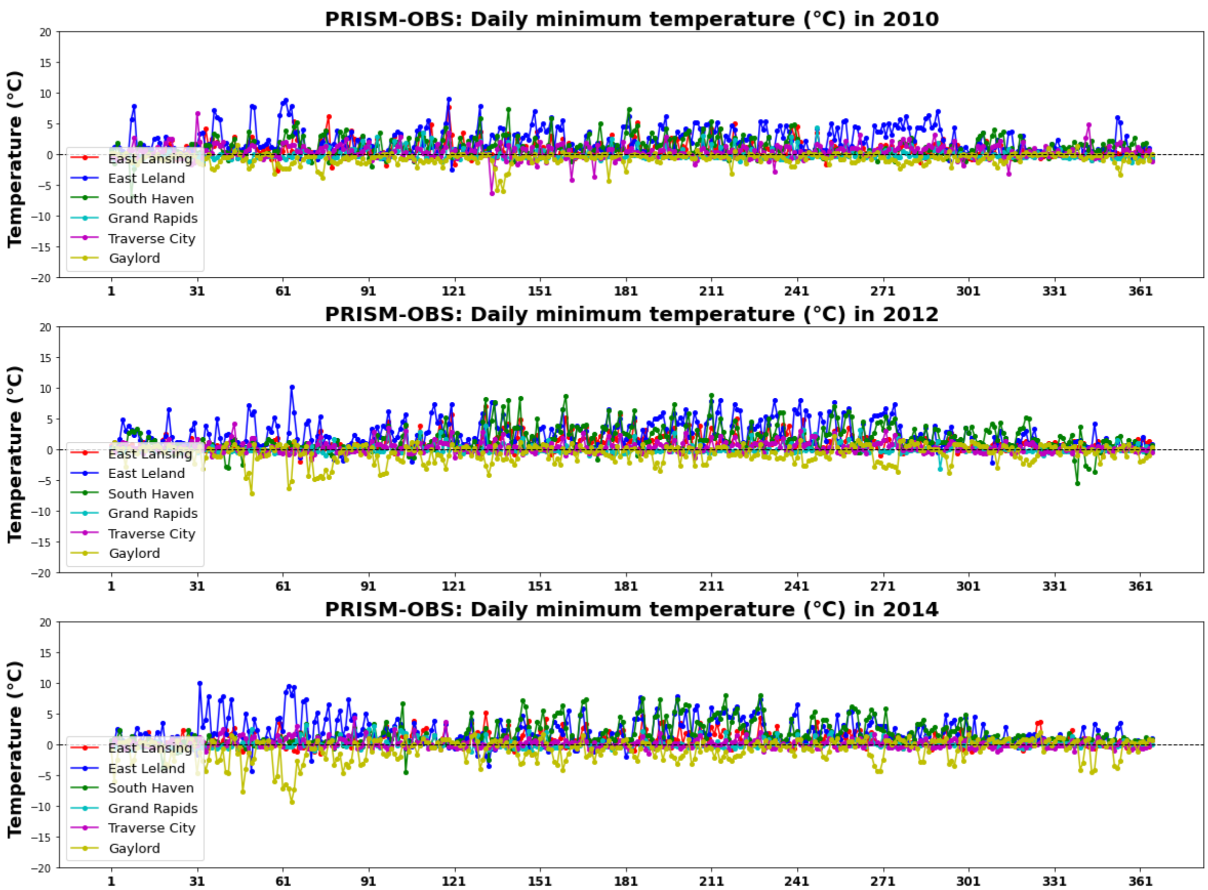

Figure 2.5: *Difference between PRISM and observations for daily minimum temperature in 2010, 2012, and 2014.*

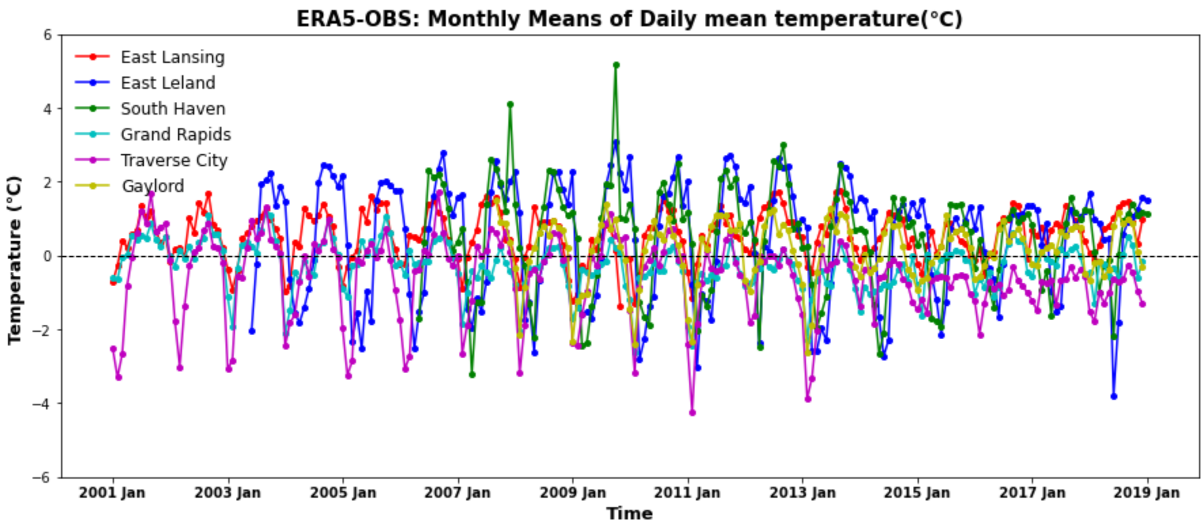

Figure 2.6: *Time series of the difference between ERA5 monthly mean daily mean temperature and observed values at six locations.*

We also evaluate the reanalysis datasets on a monthly scale. The differences between ERA5 reanalysis and observations of monthly means of daily mean temperature show noticeable annual cycles (Figure 2.6). ERA5 reanalysis tends to overestimate daily mean temperature during summer seasons and underestimate during winter seasons, which is out of our expectation. We think that reanalysis datasets should reduce the cycle since they are area-averaged. And the two near-lake stations still show larger amplitudes. Since the ASOS network is not incorporated into ERA5 reanalysis datasets, we don't observe better agreements between the reanalysis and observations. The differences between PRISM reanalysis and observations of monthly means of daily mean temperature reveal that the lake effect tends to get PRISM consistently higher than observations (Figure 2.7). Also, the two ASOS stations are showing overall smaller perturbations around zero. We observe abnormally large differences between observations and both ERA5 and PRISM reanalysis datasets in September of 2009 and November of 2007 at South Haven. The reanalysis datasets both greatly overestimate the daily mean temperature for these two months. We then check the observational data, and there are no missing data for these two months. The abnormal value between gridded datasets and observations for East Lansing in December of 2009 is due to the missing data in the stational observations.

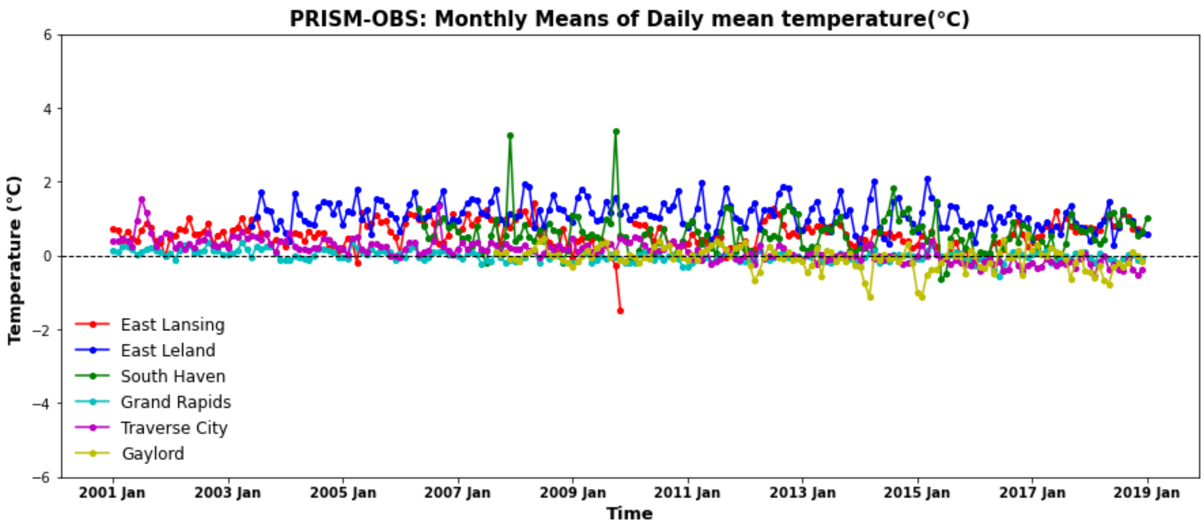

Figure 2.7: *Time series of the difference between PRISM monthly mean daily mean temperature and observed values at six locations.*

To demonstrate the agreement between observations and reanalysis datasets in a more straightforward way, we provide scattered plots at daily scales between them for the selected six stations (Figure 2.8). In this scatter plot, if the points are on the red line, it means that gridded data agree with the observations. If the points are above the red line, it means that gridded data are larger than observations; if below, smaller. Comparing ERA5 and PRISM, we observe that the DmaxT and DminT of PRISM are in overall better agreements with observations. The shapes of DminT of EAR5 tell us that the ERA5 reanalysis dataset tends to overestimate DminT during summertime when DminT is higher and underestimate DminT during wintertime when DminT is lower. The agreement between ERA5 and observations for DmaxT is better than DminT, and the two near-lake stations are overall underestimated. For PRISM, DmaxT also agrees better with observations than DminT. The same as ERA5, PRISM tends to overestimate DminT of East Leland and South Haven. Most of the DminT and DmaxT of PRISM are scattered around the red line with small variations. The two ASOS stations, Grand Rapids and Traverse City show great shapes of the agreement since they are incorporated into the PRISM group model.

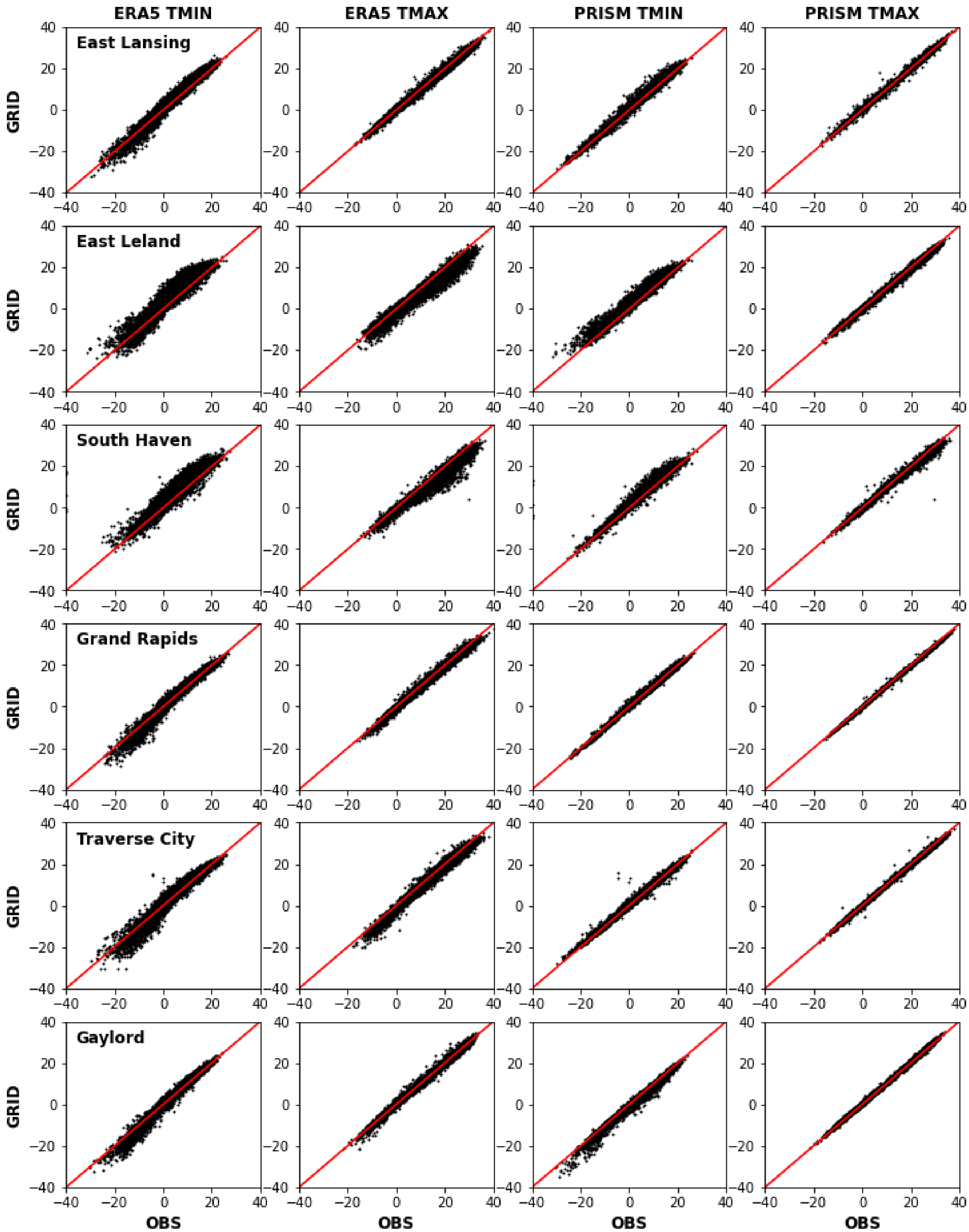

Figure 2.8: *Scatter plot of daily minimum and maximum temperature between observations and reanalysis datasets.*

Station	Number	RMSD Temp °C	RMSD Rel Hum %	RMSD Precip mm	Bias Temp °C	Bias Rel Hum %	Bias Precip mm
East Lansing	157770	1.81	11.26	0.43	0.37	-3.75	0.1
East Leland	137346	3.05	11.85	0.4	0.27	0.33	0.11
South Haven	111666	3.18	12.97	0.51	0.3	3.45	0.12
Grand Rapids	157751	1.57	9.06	NaN	-0.32	-0.09	NaN
Traverse City	157751	2.16	9.59	NaN	-0.69	2.76	NaN
Gaylord	98905	1.71	9.59	0.6	0.23	-0.15	0
Median	147548	1.99	10.43	0.51	0.25	0.12	0.1

Table 2.2: *Hourly summary statistics, root mean square difference (RMSD), and Bias between ERA5 product and observational networks at six locations.*

Since the ERA5 reanalysis dataset has hourly products, we are able to examine the performance of the ERA5 on an hourly timescale (Table 2.2). Since more than half of the precipitation data at Grand Rapids and Traverse City are not recorded by the network system, we do not assess precipitation data at these two stations. ERA5 products overall overestimate temperature, relative humidity, and precipitation for our six stations. Also, it is noteworthy that the Root Mean Squared Errors (RMSDs) are large for relative humidity, which also reflected the Bias in temperature. Our results also reveal that the two near-lake stations, East Leland and South Haven, have noticeably larger RMSD for temperature and relative humidity. Since PRISM only has daily data, we could not evaluate it on an hourly scale.

We also evaluate ERA5 products on a daily scale. To compare with the PRISM dataset, we provide the assessment for daily minimum temperature (DminT) and daily maximum temperature (DmaxT) (Table 2.3). PRISM defines a day as the 24 hours ending at Greenwich Mean Time (GMT, or 7:00 a.m. Eastern Standard Time). This means that PRISM data, like daily minimum temperature, for May 26th, refers to the 24 hours ending at 7:00 a.m. on May 26th. For consistency, we use this method to define a day for the data of ERA5 as well. We observe PRISM has overall smaller RMSDs and Bias for both the DminT and DmaxT compared to ERA5, showing a better agreement with observations. The RMSD for DmaxT of ERA5 could be as large as 4.49 degrees. ERA5 overall overestimates the DminT and underestimates the DmaxT, while PRISM

Station	Days	RMSD DminT °C	RMSD DmaxT °C	Bias DminT °C	Bias DmaxT °C
East Lansing	6573	2.49	1.14	1.23	-0.1
East Leland	5722	4.27	3.15	2.76	-1.82
South Haven	4652	4.49	2.98	2.82	-1.83
Grand Rapids	6572	1.88	1.33	0.05	-0.6
Traverse City	6572	2.52	1.98	0.08	-1.23
Gaylord	4120	2.12	1.27	-0.05	0.34
Median	6147	2.51	1.66	0.66	-0.92

Table 2.3: *Daily summary statistics, RMSD between ERA5 product and observational networks, at six locations.*

overestimates both the DminT and DmaxT. The underestimation for DmaxT and overestimation for DminT of EAR5 are reasonable since the reanalysis data are area-averaged values across the gridded boxes, which could reduce the diurnal cycle of observations. The lake effects are reflected by the dramatically large RMSD and Bias at East Leland and South Haven from the EAR5 dataset, which could be as three times large as those of other stations. The lake effects also have significant but smaller influences on the PRISM dataset, which might be due to PRISM incorporates more of the observational datasets. Also, it is noteworthy that PRISM has a larger RMSD and Bias of DminT than that of DmaxT (Table 2.4). This might be due to that DmaxT is usually measured at stable conditions, resulting in a smaller bias in the area-averaged reanalysis datasets. Also, we observed overall better estimates of PRISM at the ASOS network stations than the EW network since stations of the ASOS network are incorporated into the reanalysis datasets.

Station	Days	RMSD DminT °C	RMSD DmaxT °C	Bias DminT °C	Bias DmaxT °C
East Lansing	6573	1.49	0.91	0.65	0.5
East Leland	5722	2.98	0.96	2.13	0.08
South Haven	4652	2.84	1.27	1.51	-0.34
Grand Rapids	6572	0.73	0.33	-0.01	-0.01
Traverse City	6572	1.03	0.58	0.29	-0.04
Gaylord	4120	1.62	0.83	-0.74	0.6
Median	6147	1.56	0.87	0.47	0.04

Table 2.4: *Daily summary statistics, RMSD between PRISM product and observational networks, at six locations.* The unit for temperature is °C.

We also provide seasonal and annual summary statistics for both ERA5 and PRISM datasets. We calculate the seasonal and annual averages for both daily minimum and maximum temperatures. The seasons are defined with a continuous winter season from December to February. For example, the winter season of 2001 is defined as December 2001, January 2002, and February 2002. The table results (Table 2.5-2.8) tell us that from daily scale to annual scale, values of RMSDs are overall reduced, and values of Bias are not significantly affected. In addition, PRISM always shows overall better agreements with observations no matter what time scales. It is noteworthy that from daily to annual, the RMSDs of DminT and DmaxT, especially for the two near-lake stations, for the ERA5 are considerably decreasing, that is, at an annual scale, the RMSDs of ERA5 are comparable to those of PRISM. The seasonal RMSDs and Bias are varied by season. Both PRISM and ERA5 tend to generally overestimate DminT and underestimate DmaxT during the spring and summer seasons. ERA5 also underestimates DmaxT during the fall and winter seasons. However, ERA5 overestimates DminT during fall and underestimates DminT during winter. The magnitudes of Bias of ERA5 overall show smaller values during the cold season, spring and winter, comparing to larger values during the warm season, summer and fall. This characteristic is especially observed for East Leland and South Haven. For fall and winter, PRISM overestimates both DmaxT and DminT. The magnitudes of Bias of PRISM are similar for all seasons. RMSDs of DmaxT are overall smaller than (half of the magnitude) those of DminT for both PRISM and ERA5. However, the RMSDs of DminT are smaller than those of DmaxT, especially for the two near-lake stations. In addition, ERA5 generally shows the best comparison results for DminT in the spring season compared to other seasons considering both RMSDs and Bias. In contrast, PRISM generally shows the best comparison results for DminT in the winter season compared to other seasons considering both RMSDs and Bias. Still, PRISM shows more reliable results for both DmaxT and DminT throughout all the seasons.

Station	season	years	RMSD DminT °C	RMSD DmaxT °C	Bias DminT °C	Bias DmaxT °C
East Lansing	Spring	18	0.92	0.30	0.85	-0.11
East Leland	Spring	16	1.32	3.97	1.18	-3.92
South Haven	Spring	13	1.49	3.71	1.34	-3.67
Grand Rapids	Spring	18	0.44	0.63	-0.20	-0.51
Traverse City	Spring	18	0.78	1.36	-0.55	-1.33
Gaylord	Spring	11	0.78	0.36	-0.67	0.20
Median	Spring	17	0.85	1.00	0.33	-0.92
East Lansing	Summer	18	2.39	0.35	2.36	-0.23
East Leland	Summer	16	4.46	2.57	4.39	-2.51
South Haven	Summer	13	4.51	1.52	4.46	-1.40
Grand Rapids	Summer	18	0.63	0.90	0.54	-0.83
Traverse City	Summer	18	1.14	1.23	0.96	-1.15
Gaylord	Summer	11	1.12	0.54	1.10	0.47
Median	Summer	17	1.77	1.07	1.73	-0.99
East Lansing	Fall	18	2.05	0.76	1.95	-0.34
East Leland	Fall	16	3.99	0.82	3.92	-0.69
South Haven	Fall	13	4.08	1.31	3.97	-1.26
Grand Rapids	Fall	18	1.16	0.67	1.07	-0.58
Traverse City	Fall	18	1.45	1.03	1.29	-0.94
Gaylord	Fall	12	0.97	0.52	0.91	0.47
Median	Fall	17	1.75	0.79	1.62	-0.64
East Lansing	Winter	19	0.76	0.31	-0.36	0.19
East Leland	Winter	16	1.58	0.60	1.38	-0.25
South Haven	Winter	13	1.54	1.04	1.46	-0.98
Grand Rapids	Winter	19	1.36	0.54	-1.19	-0.44
Traverse City	Winter	19	1.62	1.57	-1.42	-1.53
Gaylord	Winter	12	1.71	0.33	-1.56	0.21
Median	Winter	17.5	1.56	0.57	-0.78	-0.35

Table 2.5: *Seasonal summary statistics, RMSD between ERA5 product and observational networks, at six locations.* The unit for temperature is °C.

Station	season	years	RMSD DminT °C	RMSD DmaxT °C	Bias DminT °C	Bias DmaxT °C
East Lansing	Spring	18	0.89	0.62	0.82	0.50
East Leland	Spring	16	2.34	0.23	2.32	-0.10
South Haven	Spring	13	1.45	0.49	1.41	-0.40
Grand Rapids	Spring	18	0.20	0.16	0.14	-0.04
Traverse City	Spring	18	0.38	0.21	0.31	-0.01
Gaylord	Spring	11	1.06	0.66	-1.02	0.63
Median	Spring	17	0.98	0.36	0.57	-0.03
East Lansing	Summer	18	1.03	0.61	0.94	0.43
East Leland	Summer	16	2.76	0.36	2.74	-0.31
South Haven	Summer	13	2.30	1.04	2.25	-0.90
Grand Rapids	Summer	18	0.11	0.15	-0.08	-0.02
Traverse City	Summer	18	0.46	0.40	0.31	-0.07
Gaylord	Summer	11	0.73	0.93	-0.70	0.92
Median	Summer	17	0.88	0.51	0.63	-0.05
East Lansing	Fall	18	0.78	0.84	0.40	0.32
East Leland	Fall	16	1.99	0.34	1.92	0.06
South Haven	Fall	13	1.81	0.36	1.61	-0.22
Grand Rapids	Fall	18	0.09	0.14	0.07	0.01
Traverse City	Fall	18	0.47	0.26	0.36	-0.10
Gaylord	Fall	12	0.56	0.51	-0.53	0.47
Median	Fall	17	0.67	0.35	0.38	0.04
East Lansing	Winter	19	0.54	0.72	0.36	0.65
East Leland	Winter	16	1.45	0.60	1.39	0.58
South Haven	Winter	13	0.83	0.41	0.71	0.19
Grand Rapids	Winter	19	0.22	0.11	-0.18	0.02
Traverse City	Winter	19	0.31	0.27	0.17	0.02
Gaylord	Winter	12	0.83	0.42	-0.71	0.37
Median	Winter	17.5	0.69	0.42	0.27	0.28

Table 2.6: *Seasonal summary statistics, RMSD between PRISM product and observational networks, at six locations.* The unit for temperature is °C.

Station	years	RMSD	RMSD	Bias	Bias
		DminT °C	DmaxT °C	DminT °C	DmaxT °C
East Lansing	18	1.23	0.57	1.11	-0.24
East Leland	16	2.77	1.87	2.75	-1.86
South Haven	13	2.85	1.87	2.81	-1.85
Grand Rapids	18	0.35	0.66	0.05	-0.6
Traverse City	18	0.35	1.25	0.08	-1.23
Gaylord	12	0.29	0.41	0	0.36
Median	17	0.79	0.96	0.6	-0.92

Table 2.7: *Annual summary statistics, RMSD between ERA5 product and observational networks, at six locations.* The unit for temperature is °C.

Station	years	RMSD	RMSD	Bias	Bias
		DminT °C	DmaxT °C	DminT °C	DmaxT °C
East Lansing	18	0.71	0.71	0.55	0.36
East Leland	16	2.11	0.22	2.1	0.03
South Haven	13	1.52	0.46	1.49	-0.38
Grand Rapids	18	0.07	0.12	-0.01	-0.01
Traverse City	18	0.38	0.26	0.29	-0.04
Gaylord	12	0.75	0.61	-0.73	0.59
Median	17	0.73	0.36	0.42	0.01

Table 2.8: *Annual summary statistics, RMSD between PRISM product and observational networks, at six locations.* The unit for temperature is °C.

Station	Days	RMSD ERA5	RMSD PRISM	Bias ERA5	Bias PRISM
East Lansing	6573	0.99	0.77	0.49	0.38
East Leland	5722	1.79	1.07	0.2	0.59
South Haven	4652	1.96	1	0.27	0.36
Grand Rapids	6572	0.71	0.34	-0.07	0
Traverse City	6572	0.99	0.47	-0.13	0.05
Gaylord	4120	0.8	0.49	0.3	0.02
Median	6147	0.99	0.63	0.24	0.21

Table 2.9: *Growing degree day (Base 4 °C) summary statistics.*

2.3.2 Assessment of derived variables

Freeze events could result in differentiated risks on crops with different phenological stages. Growing Degree Day (GDD) is a commonly used agro-climatic index to simulate plant phenologies. We calculate the GDD with a base temperature of 4 °C (Table 2.9). The results show that calculations based on DmaxT and DminT from PRISM have a relatively smaller RMSD and smaller Bias than those from ERA5. Both ERA5 and PRISM overestimate GDD values. ERA5 still shows larger RMSDs at these two near-lake stations and the same case for PRISM.

Since we care most about how the reanalysis datasets represent freeze occurrences, we need to assess how they are captured or missed. For precipitation variable evaluation, some forecast scores are utilized to measure the ability of a product. Here we use different criteria to define freeze events and then calculate how reanalysis products capture these events. Tables 2.10 and 2.11 show an example of how we examine this. We first define five levels of freeze events, ranging from 0°C to -25°C with 5-degree steps. And then, we count these events for each month (July and August are not showing here since no defined freeze events occurred). Here 107/131=0.82 means that throughout the data period, from 1/1/2001 to 12/31/2018, there are 6573 days, and 131 days of which in January have DminT between -5 degrees and 0 degrees. And of these 131 events, ERA5 captured 107 events with a ratio of 0.82. PRISM shows better results by capturing 112 events with a ratio of 0.85. By comparing ERA5 and PRISM, we observe that PRISM overall behaves very well in capturing different types of events throughout different months. The harder the freeze events, the

month	Type1	Type2	Type3	Type4	Type5
	-5 to 0 °C	-10 to -5 °C	-15 to -10 °C	-20 to -15 °C	-25 to -20 °C
1	107/131=0.82	91/141=0.65	67/101=0.66	49/84=0.58	17/28=0.61
2	88/122=0.72	80/141=0.57	66/108=0.61	43/70=0.61	11/23=0.48
3	151/173=0.87	93/170=0.55	40/68=0.59	10/17=0.59	5/6=0.83
4	120/193=0.62	7/32=0.22	0/0=nan	0/0=nan	0/0=nan
5	3/20=0.15	0/0=nan	0/0=nan	0/0=nan	0/0=nan
6	0/0=nan	0/0=nan	0/0=nan	0/0=nan	0/0=nan
9	0/0=nan	0/0=nan	0/0=nan	0/0=nan	0/0=nan
10	26/114=0.23	0/0=nan	0/0=nan	0/0=nan	0/0=nan
11	122/188=0.65	36/95=0.38	3/7=0.43	2/2=1.00	0/0=nan
12	171/192=0.89	98/159=0.62	26/59=0.44	13/21=0.62	3/4=0.75

Table 2.10: *Freeze events captured ratios at East Lansing of ERA5.* Freeze events are categorized into five types, which are, respectively, from -5 °C to 0 °C, from -10 °C to -5 °C, from -15 °C to -10 °C, from -20 °C to -15 °C, and from -25 °C to -20 °C.

overall lower the capturing ratio for EAR5, which is not the case for PRISM. PRISM still shows high capturing ratios for hard freeze events. Also, it is noteworthy that both ERA5 and PRISM show better results for wintertime freeze events than springtime freeze events. For springtime freeze events, we definitely see the advantages of PRISM. Even though not as good as wintertime ratios, the springtime freeze events, especially for the late spring, are captured pretty well by PRISM. In May, 20 days are reported to have freeze events throughout 18 years. And PRISM captures 13 of 20, which is much better than ERA5, which only captures 3 of 20. Therefore, generally, PRISM demonstrates an advantageous ability to capture freeze events for different types and for different occurring times. This benefit of PRISM leads to our later choice of using PRISM as a proxy for observations to represent the surface freeze events as an excellent gridded dataset.

For the other five stations, we don't present the detailed tables here since the results and conclusions are similar. PRISM shows much better results than ERA5 for all categories of freeze events. Also, for the two near-lake stations, even PRISM misses a lot of events for hard freezes and late spring freezes. And the two stations from the ASOS network show excellent ratios of PRISM, as we expect. We provide a summary table without detailed categories for six stations. In tables 2.12 and 2.13, we count all the freeze events, defined as DminT less than 0 degrees. For

month	Type1	Type2	Type3	Type4	Type5
	-5 to 0 °C	-10 to -5 °C	-15 to -10 °C	-20 to -15 °C	-25 to -20 °C
1	112/131=0.85	119/141=0.84	77/101=0.76	73/84=0.87	22/28=0.79
2	114/122=0.93	123/141=0.87	91/108=0.84	57/70=0.81	13/23=0.57
3	147/173=0.85	129/170=0.76	48/68=0.71	10/17=0.59	5/6=0.83
4	128/193=0.66	20/32=0.62	0/0=nan	0/0=nan	0/0=nan
5	13/20=0.65	0/0=nan	0/0=nan	0/0=nan	0/0=nan
6	0/0=nan	0/0=nan	0/0=nan	0/0=nan	0/0=nan
9	0/0=nan	0/0=nan	0/0=nan	0/0=nan	0/0=nan
10	86/114=0.75	0/0=nan	0/0=nan	0/0=nan	0/0=nan
11	159/188=0.85	62/95=0.65	6/7=0.86	0/2=0.00	0/0=nan
12	170/192=0.89	136/159=0.86	53/59=0.90	15/21=0.71	4/4=1.00

Table 2.11: *Freeze events captured ratios at East Lansing of PRISM.* Freeze events are categorized into five types, which are, respectively, from -5 °C to 0 °C, from -10 °C to -5 °C, from -15 °C to -10 °C, from -20 °C to -15 °C, and from -25 °C to -20 °C.

example, at East Lansing, from 1/1/2001 to 12/31/2018 with 6573 days, 493 days in January has a DminT no higher than 0 degrees. The 493 days are more than the sum of five defined freeze event days because there are days less than -25 degrees that are not counted above. Comparing ratios throughout different months, we conclude that both ERA5 and PRISM show better freeze event capturing behavior during wintertime freezes than springtime and fall freezes. ERA5 only captures an overall 17 percent of the total freeze occurrences in May and 13 percent of the total freezes in October. PRISM behaves better with an overall 63 percent in May and 65 percent in October. For the months of January, February, March, and December, both ERA5 and PRISM show excellent ratios from 0.97 to 0.99. Comparing ratios between different stations, the two near-lake stations, East Leland and South Haven, show the lowest ratios for both ERA5 and PRISM. And Gaylord, which is in the USCRN network, shows the best ratio for both EAR5 and PRISM. The several freeze occurrences in June and September are not captured by either ERA5 or PRISM. Therefore, we hope to understand how the springtime freeze events are determined in the later chapters.

month	East Lansing	East Leland	South Haven	Grand Rapids	Traverse City	Gaylord	Median
1	490/493=0.99	416/435=0.96	313/330=0.95	502/508=0.99	516/519=0.99	333/334=1.00	0.99
2	471/475=0.99	406/410=0.99	295/301=0.98	472/474=1.00	483/486=0.99	305/305=1.00	0.99
3	427/435=0.98	388/396=0.98	244/269=0.91	427/433=0.99	453/459=0.99	296/296=1.00	0.98
4	157/225=0.70	174/276=0.63	53/127=0.42	143/164=0.87	230/292=0.79	186/197=0.94	0.74
5	3/20=0.15	0/71=0.00	0/15=0.00	3/12=0.25	8/41=0.20	13/32=0.41	0.17
6	0/0=nan	0/6=0.00	0/0=nan	0/0=nan	0/1=0.00	0/1=0.00	0
9	0/0=nan	0/4=0.00	0/4=0.00	0/0=nan	0/3=0.00	0/1=0.00	0
10	26/114=0.23	0/83=0.00	0/34=0.00	12/70=0.17	9/96=0.09	48/98=0.49	0.13
11	230/292=0.79	104/253=0.41	50/169=0.30	207/265=0.78	198/281=0.70	229/252=0.91	0.74
12	429/437=0.98	370/436=0.85	239/304=0.79	449/461=0.97	458/472=0.97	347/351=0.99	0.97

Table 2.12: *Freeze events below 0 °C captured ratios at six stations without detailed categories of ERA5.*

month	East Lansing	East Leland	South Haven	Grand Rapids	Traverse City	Gaylord	Median
1	484/493=0.98	426/435=0.98	320/330=0.97	503/508=0.99	518/519=1.00	333/334=1.00	0.99
2	472/475=0.99	403/410=0.98	291/301=0.97	474/474=1.00	484/486=1.00	305/305=1.00	0.99
3	414/435=0.95	362/396=0.91	241/269=0.90	424/433=0.98	451/459=0.98	295/296=1.00	0.97
4	162/225=0.72	156/276=0.57	65/127=0.51	144/164=0.88	242/292=0.83	188/197=0.95	0.77
5	13/20=0.65	6/71=0.08	1/15=0.07	10/12=0.83	25/41=0.61	31/32=0.97	0.63
6	0/0=nan	0/6=0.00	0/0=nan	0/0=nan	0/1=0.00	0/1=0.00	0
9	0/0=nan	0/4=0.00	0/4=0.00	0/0=nan	0/3=0.00	1/1=1.00	0
10	86/114=0.75	13/83=0.16	8/34=0.24	57/70=0.81	52/96=0.54	91/98=0.93	0.65
11	266/292=0.91	174/253=0.69	108/169=0.64	255/265=0.96	259/281=0.92	246/252=0.98	0.92
12	423/437=0.97	416/436=0.95	275/304=0.90	456/461=0.99	466/472=0.99	348/351=0.99	0.98

Table 2.13: *Freeze events below 0 °C captured ratios at six stations without detailed categories of PRISM.*

2.4 Summary

This study compares ERA5 and PRISM reanalysis products to stational observations. We conclude that the PRISM dataset, with a higher horizontal resolution of 4km, overall demonstrates a better agreement of temperatures with observations. However, ERA5 outperforms PRISM in its availability of various weather variables. The major findings are as follows.

1) Both reanalysis datasets show better results for DmaxT than DminT, as shown in the lower DmaxT perturbations of the time series and the smaller values of DmaxT RMSDs.

2) Gridded reanalysis datasets tend to reduce the observed daily cycles. ERA5 underestimates DmaxT while overestimates DminT, resulting in reduced daily cycles. In contrast, PRISM tends to overestimate both DminT and DmaxT. However, on a monthly scale, ERA5 reanalysis tends to overestimate daily mean temperature during summer seasons and underestimate it during winter seasons in the time series, which is consistent with the scatter plot results.

3) The ASOS network stations, which are incorporated into the PRISM analysis, show excellent comparing results for both direct weather variables and derived variables. This behavior is not observed in the evaluation of the ERA5 dataset.

4) The two near-lake stations show large RMSDs and Bias and also large perturbations of time series for both reanalysis products. But PRISM still shows a better agreement.

5) PRISM also shows a better behavior in capturing the derived variables. With a base temperature of 4 °C, both ERA5 and PRISM overestimate GDD values. PRISM shows excellent ability in capturing different types of freeze events throughout different months. Both PRISM and ERA5 show better freeze event capture during wintertime than other seasons.

In conclusion, we will use PRISM as a proxy of observations to represent freeze events in later chapters. Since the whole thesis is focused on freeze events, we just evaluate temperatures and temperature-derived variables. However, to assess both ERA5 and PRISM datasets, more work needs to be done in the future. For example, with the availability and accessibility of precipitation data in the ERA5 and PRISM, we could evaluate how precipitation events are captured by computing analytical scores like the bias score (BS), the threat score (TS), and the Heidke skill score (HSS). In addition, since wind conditions also have a profound impact on freeze formation, it is a necessity to assess the wind speed and direction of the ERA5 (PRISM does not provide wind data). Also, ERA5 provides land-only datasets with a better resolution of 9km than the single-level datasets with 30km. It is significant to evaluate how this resolution improvement affects the overall agreement with observations.

CHAPTER 3

FREQUENCY AND SEVERITY OF SPRINGTIME FREEZE EVENTS

3.1 Background

3.1.1 False Springs and Springtime Freeze Events

As a consequence of the global warming trend, earlier springs induce premature plant development, resulting in vulnerable and susceptible crops exposed to subsequent springtime freeze events (Gu et al., 2008; Allstadt et al., 2015). In the early phenological stages, temperatures near -6°C begin to cause damage to the crops, but as the bloom stage approaches, temperatures as warm as -2°C could cause considerable damage (Longstroth, 2005). Springtime freeze events, especially those after an untimely extended period of warmer temperatures known as "false spring", could have devastating consequences to agriculture production. Prominent examples include freeze events that occurred in late spring of 2002, 2007, and 2012 following an extended period of warm weather and wiped out more than 90% of fruit production and other crops across the US Midwest, which resulted in an agricultural loss of more than 2 billion dollars (NASS, 2002; Marino et al., 2011; O'Brien et al., 2019; Labe et al., 2015; Kistner et al., 2018; Gu et al., 2008). These events share two characteristics: they occurred following an extended period of unusually warm conditions, and they caused disastrous consequences to premature developing vegetation and crops.

Earlier springs could result in the earlier development of crops and might increase the vulnerability of crops to freeze event damage (Winkler et al., 2013). Allstadt et al. (2015) projected that the widespread historical advances in spring plant phenology would extend into the future, with an increased risk of false springs in the Midwestern US. Besides, Katz and Brown (1992) also emphasized that changes in variability were more important to extreme event frequencies than changes in averages with statistical models.

Findings from previous research also revealed that false springs and subsequent freeze events could be related to large-scale atmospheric circulation patterns. When a relative low-pressure system emerges over the North Pacific Ocean, creating a ripple effect downstream, warm air mass intrudes, and then early spring occurs across much of western North America (Ault et al., 2013). Kunkel et al. (2004) speculated that the shorter growing seasons in the early 1900s were characterized by drier air masses and more global solar radiation while the longer growing seasons in recent years may be associated with air masses that are moister in comparison and result in less global solar radiation.

3.1.2 Spatiotemporal Variability of Springtime Freeze Events

Many previous studies have considered the spatiotemporal variability and trend of the springtime freeze events. DeGaetano (1996) detected a decreasing trend of freezing days in the Northeastern United States from 1959 to 1993, with different thresholds at an individual station level. Easterling et al. (2002) suggested that the springtime freezing days significantly decreased for the period 1948-1999 in western and north-central US. They also noted that the regional trends in frost days are substantially related to the mean annual temperature changes. Yu et al. (2014) revealed earlier occurrences of the Last Spring Frost, delayed events of the First Fall Frost, and lengthening periods of the Frost-Free Season from 1980 to 2010. Their study also showed weaker interannual variability of these dates in the Great Lakes region than other regions in the Midwest (Yu et al., 2014).

Most of these freeze event studies were carried out at the individual station level. Nevertheless, the gridded 4-km dataset released by the PRISM (Parameter-elevation Regressions on Independent Slopes Model) climate group from Oregon State University (PRISM Climate Group, Oregon State University, http://prism.oregonstate.edu, created Feb 2020) allows continuous spatiotemporal analysis of springtime freeze events across the Midwestern US. Besides, little research has focused on freeze events in the individual springtime months.

3.1.3 Study Objectives

With the necessity of understanding the climatology of springtime freeze events, we try to investigate the frequency, severity, and potential causes of springtime freeze event occurrences. This study aims to use ERA5 reanalysis (the fifth major global reanalysis produced by the European Centre for Medium-Range Weather Forecasts) to understand the weather conditions and climate background of the freeze events represented by the PRISM analysis dataset.

3.2 Data and Method

The study domain is the central and eastern United States encompassing the region from 105º W to 75º W longitude and from 35º N to 50º N latitude. This region covers one of the most intensive and extensive areas of agricultural production in the world. Since the agricultural production in this region is substantially sensitive to climate variability, especially freeze events, it is worthwhile to study the frequency and severity of freeze events represented by the gridded datasets over this region.

PRISM, a gridded analysis dataset provided by the PRISM climate group from Oregon State University, has a better agreement with the observational freezing events and provides estimates of six basic climate elements: precipitation (ppt), minimum temperature (tmin), maximum temperature (tmax), mean dew point (tdmean), minimum vapor pressure deficit (vpdmin), and maximum vapor pressure deficit (vpdmax). PRISM has an excellent spatial resolution of 4 km. But it just provides climate variables at daily scales with time coverage from 1981 until the present. We obtain daily minimum and mean air temperature from PRISM datasets to represent the frequency and severity of freeze events on the surface. ERA5 is a climate reanalysis dataset released by the European Centre for Medium-Range Weather Forecasts (ECMWF), covering the period from 1950 to the present. The name ERA refers to 'ECMWF ReAnalysis', with ERA5 being the fifth major global reanalysis produced by ECMWF (after FGGE, ERA-15, ERA-40, ERA-Interim) (Hennermann et al., 2020). The global ERA5 reanalysis dataset includes gridded datasets with a horizontal resolution of 30 km at 37 pressure levels. We use ERA5 datasets for understanding the weather conditions and climate background in the upper levels that occur simultaneously with the freeze events in the surface.

We define the freeze days as days by different criteria when the daily minimum air temperature is below different degrees Celsius, including the commonly used one, 0 ºC. The freeze events are identified using the PRISM dataset that is comprised of 357 × 722 horizontal grid points with a 4 km grid spacing across the study region.

We obtain the teleconnection indices from the Climate Prediction Center (CPC). Niño-3.4 is an index indicating the SST anomalies across the region spans 5°N-5°S, 120°-170°W in the tropical Pacific Ocean. Both the NAO (North Atlantic Oscillation) and PNA (Pacific North American) indices are based on the leading rotated principal component analyses of mean 500-mb heights in the Northern Hemisphere (20°–90°N latitude) (Dixon et al., 2007).

We also use the Empirical Orthogonal Function (EOF) technique to identify the spatial patterns of the freezing days in different months. The EOF analysis produces a set of mutually orthogonal modes that consist of spatial structures (EOFs) with corresponding time series (principal components or PCs) (Yu et al., 2014). The corresponding eigenvalue of each mode describes the variance explained by the mode (Yu et al., 2014). In this study, we analyse the first two modes that together explain more than 60% of the variance.

3.3 Results

3.3.1 Temporal and spatial variability of freeze events

We first examine the spatial variability of freeze events across the central and Midwestern United States. The mean, standard deviation, and trend of freezing days in March, April, and May across our study region from 1981 to 2019 are shown in Figure 3.1. The average numbers of freezing days for the three months all show a latitude-dependent pattern, and also decreases as the month proceeds. In May, some areas are moving toward the frost-free season, resulting in near-zero freeze events there. The standard deviation here is divided by the average numbers of freezing days at each grid point to represent the relative variations of the freezing days. Our results reveal that freezing days in March have the least variation across the region throughout the study period, and those in April show a relatively higher variation in the southern region. Freezing days in May show a high variation in the central-southern region, which is dominated by the small mean values in these areas. We also conduct trend analyses by linear least-squares regression. The results reveal that freezing days in March show a decreasing trend across the central and Midwestern United States, which is consistent with the decreasing trend in springtime freeze events in the previous studies (DeGaetano, 1996; Easterling et al., 2002). However, nearly half of the region shows an upward trend in April, which is especially significant in Northern Michigan, part of western Wisconsin, and central Oklahoma. Freezing days in May show a significant downward trend in most of the Northeast, in contrast to an upward trend in the western region. We try to understand why these differentiated results are observed in April and May in the following part.

Figure 3.2 shows the time series of Spatially Averaged Freezing Days (defined as the days with daily minimum temperatures below 0 ºC) Counts (SAFDC) and Spatially Averaged Daily Minimum Temperature (SADMT) in spring (March, April, May) from 1981 to 2019. We calculate the Theil-Sen slope, which is the median of all the paired values, to avoid having outliers' effects on the trend of the time series. A negative slope of -0.043 for SAFDC is observed, indicating a general decreasing trend of springtime freeze events across the central and Midwestern US, which

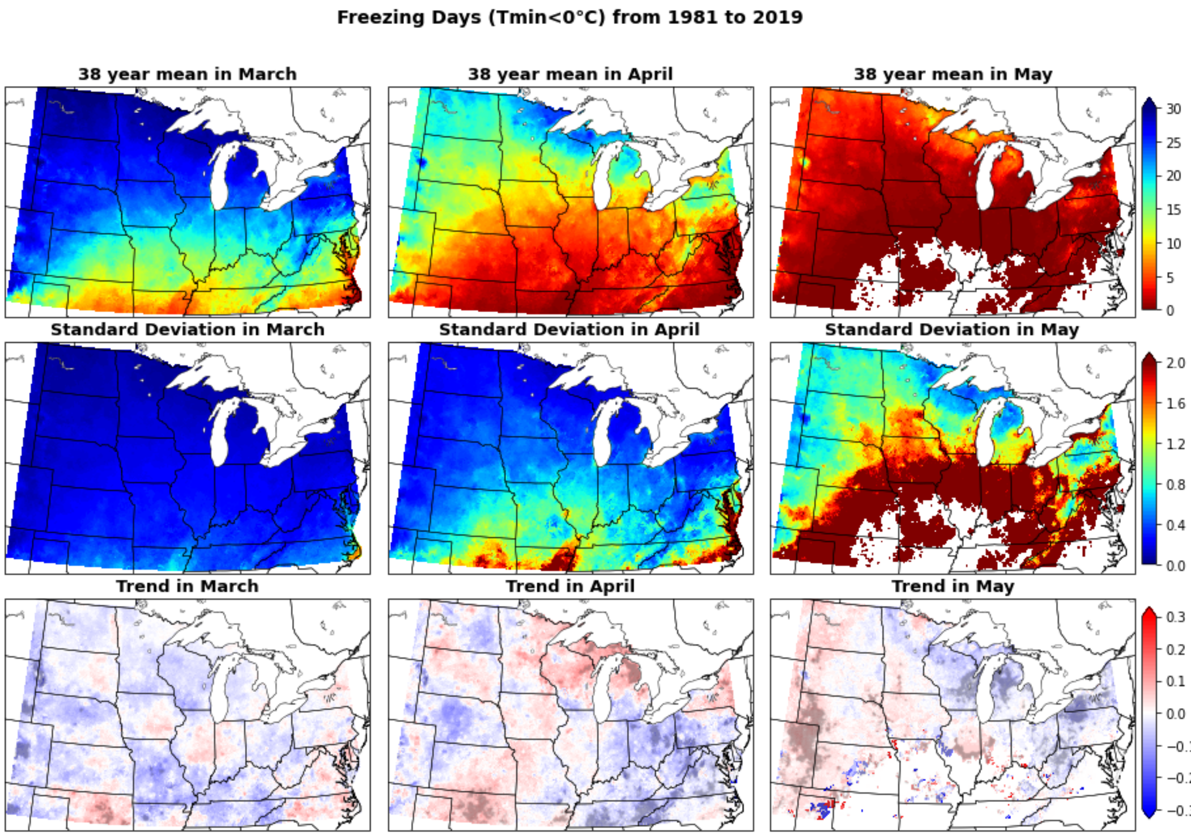

Figure 3.1: *Average, standard deviation, and trend of freezing days in spring (March, April, May) from 1981 to 2019.*

agrees with previous studies (DeGaetano, 1996; Easterling et al., 2002). The year 1996, 2013 and 2018 all show abruptly high values of SAFDC, while the year 2012 shows the lowest SAFDC. The results of SADMT were exactly on the contrary, as expected. It is noteworthy that, although both the years 2007 and 2012 show a low frequency of freeze events, considerable crop damage was observed in these two years, which were likely a consequence of false springs exposing the earlier developed crops to the subsequent freeze events. As we expect, the SADMT shows an exact opposite phase to the SAFDC with a positive Theil-Sen slope of 0.005. We also relate the SAFDC to the spatially averaged daily minimum and mean temperature. The result reveals both significant negative relationships with R-squared values of 0.7894 and 0.7414, indicating a deterministic relationship between the monthly averaged daily minimum/mean temperature and freezing days in that correspondent month. The significant tests for these relationships show that

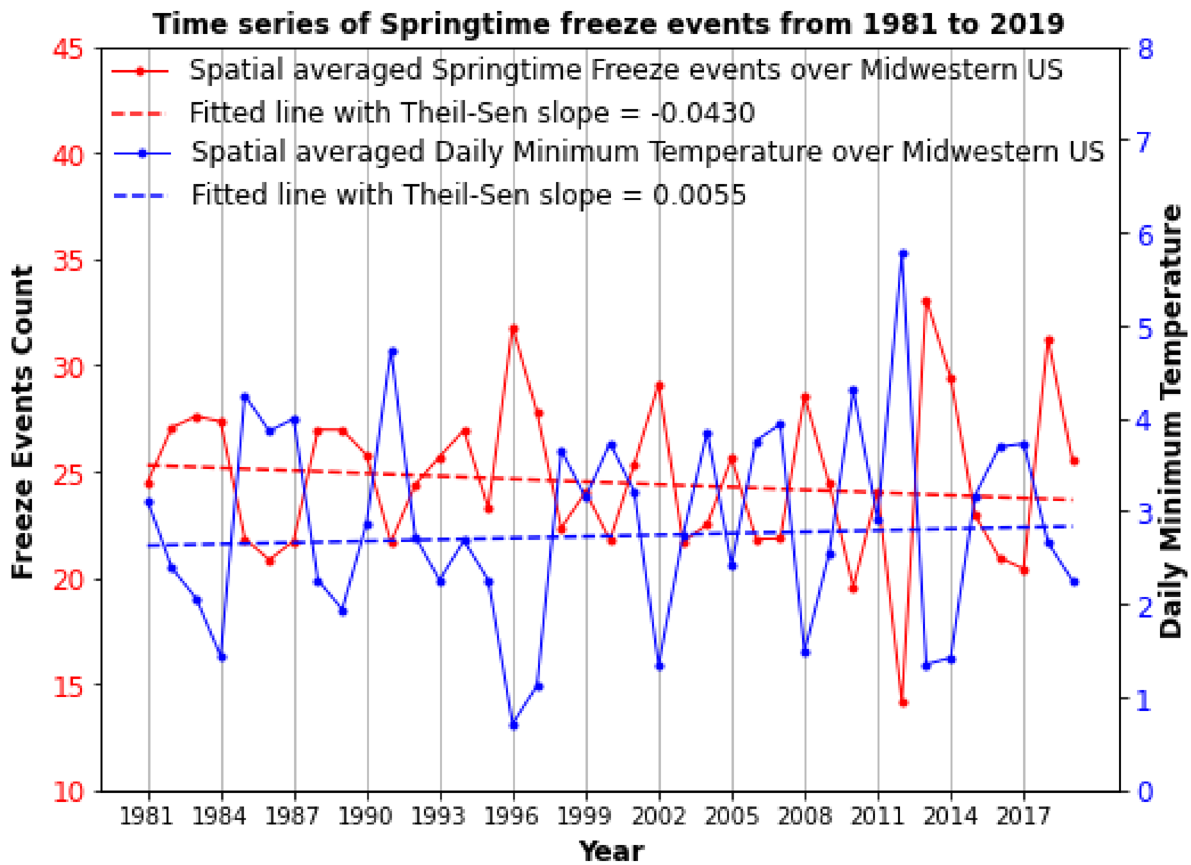

Figure 3.2: *Time series of springtime freeze events count from 1981 to 2019.* The fitted line was fitted without the year 2018.

all these trends are not significant.

3.3.2 Freezing Area Percentage

To further understand and explain variations in some regions of interest, we introduce a variable called Freezing Area Percentage (FAP), which is defined as the percentage of grid points whose daily minimum temperature is below 0 ºC on each day in a pre-defined subset of the study region. Here we use the regions defined in Karl and Knight (1998) and also used as climate regions by NOAA (National Oceanic and Atmospheric Administration) as the subsets (Figure 3.3). We calculate the FAP in each subregion respectively on each day and sum up the daily values for three springtime months (Table 3.1). The larger the FAP, the more areas of that region are likely to

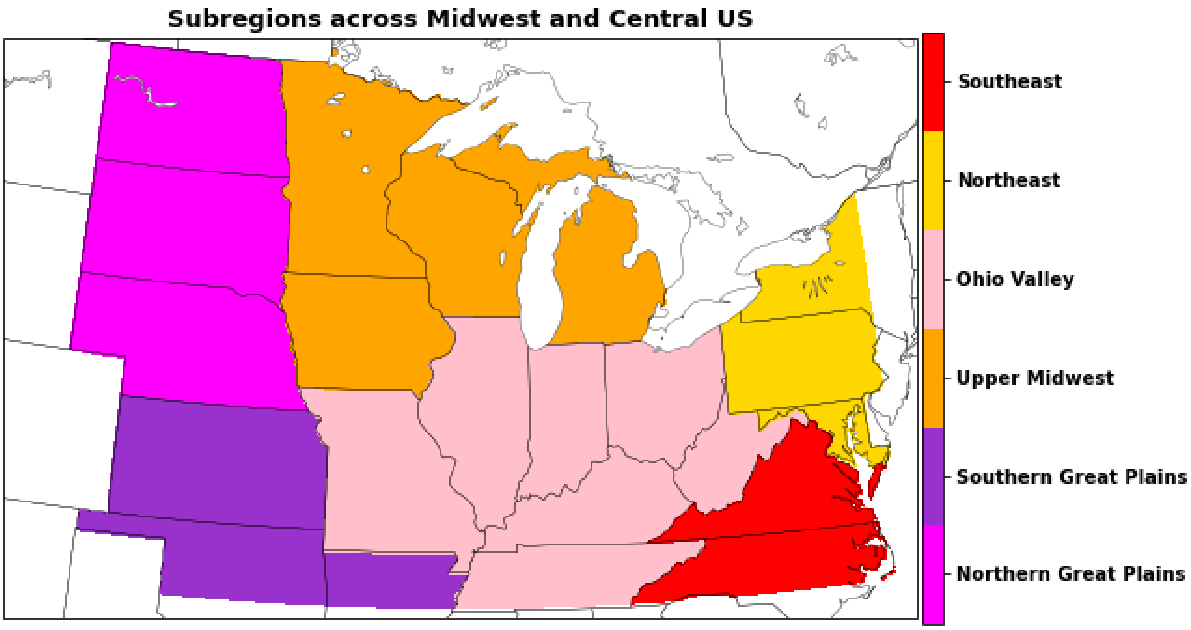

Figure 3.3: *Subset regions defined in Karl and Knight (1998).*

suffer from freezing risks. The monthly FAP values could be explained as the number of freezing days occurring in the defined region at some springtime month. Higher values of monthly FAP are observed in the northern subregions and the earlier months.

Figure 3.4 shows the time series of monthly aggregated FAP values. Larger values are shown in the northern regions, the Northern Great Plains, the Upper Midwest, and the Northeast. Throughout the whole study region, a noticeably low FAP value is in the year 2012 is sandwiched between two large values. We observed some interannual and interdecadal periodicity of the time series of monthly FAP values by spectral analysis (not shown here). Since the causes of springtime freezes could be related to large circulations, we later investigate the relationship between FAP values and some teleconnection indices.

We conduct trend analyses for monthly FAP values (Table 3.2). The results reveal decreasing trends of FAP in almost all regions for the three months, except for increasing trends in the Northern Great Plains and also the Upper Midwest in March and in the Northeast and Southeast in May. The trends for the accumulated springtime are downward with a significance in the Ohio Valley, which extends the findings in Easterling et al. (2002) from the period 1948-1999 into 1981-2019.

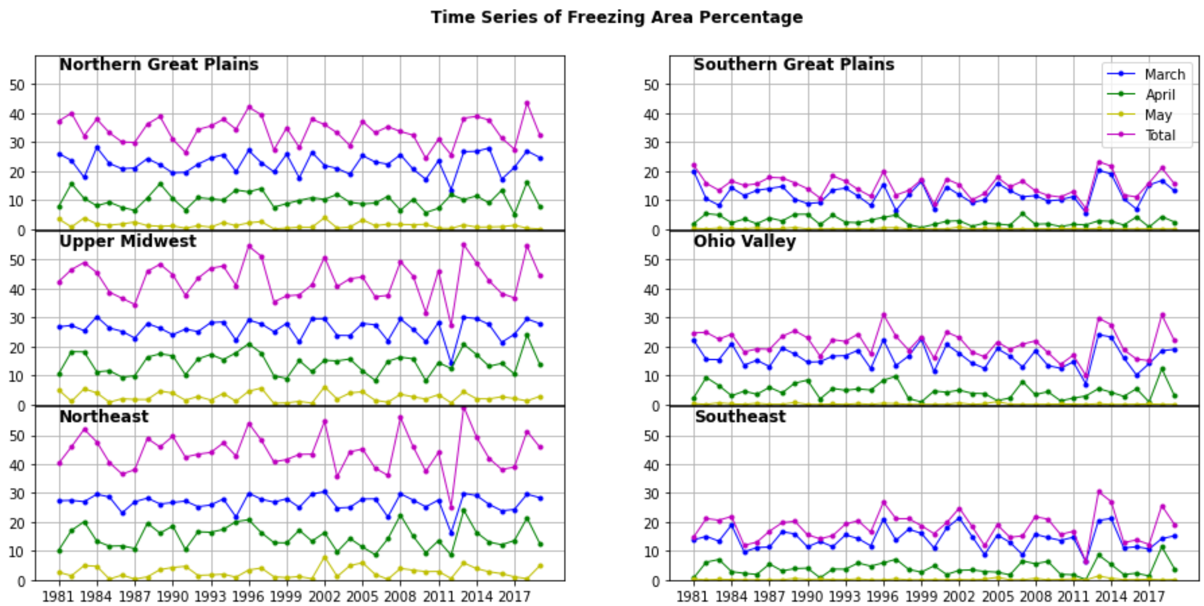

Figure 3.4: *Time series of monthly FAP values.*

Easterling et al. (2002) revealed a non-significant trend of -0.1 days per decade in the Ohio Valley for springtime from 1948 to 1999, while our results show a significant trend (p-value less than 0.1) of -0.113 days per year for springtime from 1981 to 2019, furthering indicating fewer freezing days occurring in the Ohio Valley during recent decades.

	Northern Great Plains	Southern Great Plains	Upper Midwest	Ohio Valley	Northeast	Southeast
March	22.641	12.173	26.135	16.387	26.724	14.154
April	10.06	2.699	14.416	4.6	14.884	3.92
May	1.312	0.135	2.58	0.163	2.639	0.175
Springtime	34.013	15.007	43.131	21.15	44.248	18.248

Table 3.1: *39-year mean of regional averaged monthly FAP.* Relationships with p values less than 0.10 are characterized with one star and those less than 0.05 are with two stars.

	Northern Great Plains	Southern Great Plains	Upper Midwest	Ohio Valley	Northeast	Southeast
March	0.027	-0.001	0.004	-0.031	-0.006	-0.004
April	-0.012	-0.037*	-0.03	-0.06	-0.041	-0.013
May	-0.031*	-0.002	-0.016	-0.001	0.005	0
Springtime	-0.065	-0.065	-0.016	-0.113*	-0.019	-0.003

Table 3.2: *Theil-Sen Slope for monthly FAP.* Relationships with p values less than 0.10 are characterized with one star and those less than 0.05 are with two stars.

To further investigate the periodicity of monthly FAP values, we relate them to some teleconnection indices, Niño-3.4, NAO, PNA, and PDO. The positive phase of the NAO reflects below-normal heights and pressure across the high latitudes of the North Atlantic and above-normal heights and pressure over the eastern United States. The pattern is reversed for the negative phase. The strong positive phase of NAO tends to be associated with above-normal temperatures in the eastern United States (CPC, 2012). Table 3.3 shows Pearson correlation values comparing monthly FAP values for the springtime months to NAO values with 0-3 months earlier. It is noteworthy that we observe a significantly strong negative correlation between FAP values and NAO in March from 1981 to 2019. This result leads to the conclusion that the positive phase of NAO is usually associated with less freezing risk in March across the study region. The Pearson correlation value could be as high as -0.469 in the Ohio Valley, indicating a highly significant correlation with the positive phase of NAO occurring during March for recent decades. Even though not significant, some positive correlations are occurring for monthly FAP values in April and May after the significant negative correlation in March, especially in the Southern Great Plains and Ohio Valley. This is likely because the effects of the polar jet stream become weaker in the late springtime. With lagging lengths increasing from 1 to 3 months, more positive correlations are observed. The monthly FAP values in April are positively correlated with NAO in February, indicating a positive phase of NAO in February is statistically associated with more freezing risks in April across the study region, especially in the Northern Great Plains, Upper Midwest, Ohio Valley, and Northeast. Also, when the positive phase of NAO in December occurs, fewer freezing risks in March are observed across our study region, especially in the Upper Midwest, Northeast, and Southeast.

	Northern Great Plains	Southern Great Plains	Upper Midwest	Ohio Valley	Northeast	Southeast
Lag 0						
March	-0.368**	-0.576**	-0.357**	-0.469**	-0.466**	-0.376**
April	-0.105	0.108	0.039	0.093	-0.096	-0.069
May	0.008	0.145	-0.029	0.047	-0.193	-0.08
Springtime	-0.016	-0.045	0.036	-0.05	-0.114	-0.206
Lag 1						
March	0.142	-0.159	0.129	0.028	0.055	0.08
April	0.226	0.294*	0.159	0.237	0.067	0.023
May	-0.116	-0.175	0.07	-0.089	0.005	0.02
Springtime	0.039	-0.172	0.134	-0.06	-0.021	-0.188
Lag 2						
March	0.178	0.075	0.138	0.239	-0.07	0.081
April	0.494**	0.251	0.416**	0.317**	0.289*	0.089
May	-0.176	0.041	-0.015	-0.128	-0.102	-0.343**
Springtime	0.166	-0.244	0.19	0.042	0.071	-0.064
Lag 3						
March	-0.125	-0.085	-0.346**	-0.179	-0.443**	-0.418**
April	0.07	-0.158	0.093	-0.087	0.176	-0.011
May	-0.216	0.009	0.137	-0.098	0.053	0.005
Springtime	0.233	-0.055	0.125	0.082	0.042	-0.067

Table 3.3: *Pearson correlation values (r) comparing monthly FAP for the months of March, April, and May to NAO values 0-3 months earlier.* Relationships with p values less than 0.10 are characterized with one star and those less than 0.05 are with two stars.

Table 3.4 shows 0-3 month lagged Pearson correlation values between the monthly FAP values for each of the three months to PNA values. The positive phase of the PNA pattern is associated with above-average temperatures over western Canada and the extreme western United States and below-average temperatures across the south-central and southeastern United States (Dixon et al., 2007). The correlations between PNA and FAP are overall negative. Nevertheless, FAP values in May are significantly positively associated with PNA in May, especially in the Northern Great Plains and the Upper Midwest. This indicates that the positive phase of PNA in May could lead to more freezing risks across most of our study regions in May. Also, we notice that the total springtime FAP values are always significantly negatively correlated with PNA values 1-3 months earlier, except in the Southern Great Plains region. This relationship provides forecast tools for predicting springtime freezing risks across relevant areas for up to three months ahead.

	Northern Great Plains	Southern Great Plains	Upper Midwest	Ohio Valley	Northeast	Southeast
Lag 0						
March	-0.17	0.121	-0.228	0.01	-0.197	-0.124
April	-0.205	-0.08	-0.299*	-0.185	-0.266	-0.12
May	0.356**	0.267	0.343**	0.304*	0.148	0.272*
Springtime	-0.153	0.073	-0.198	-0.102	-0.158	-0.163
Lag 1						
March	-0.350**	-0.217	-0.338**	-0.26	-0.315*	-0.185
April	-0.465**	-0.249	-0.362**	-0.397**	-0.17	-0.243
May	0.058	-0.105	-0.174	0.017	-0.175	-0.223
Springtime	-0.407**	-0.184	-0.429**	-0.358**	-0.324**	-0.271*
Lag 2						
March	-0.067	0.125	-0.133	-0.041	-0.086	-0.138
April	-0.191	-0.229	-0.238	-0.286*	-0.134	-0.223
May	0.166	-0.144	-0.041	0.061	-0.136	-0.035
Springtime	-0.397**	-0.111	-0.430**	-0.362**	-0.358**	-0.322**
Lag 3						
March	-0.142	-0.095	-0.269*	-0.085	-0.245	-0.16
April	-0.232	-0.097	-0.357**	-0.267	-0.436**	-0.302*
May	0.157	-0.003	-0.064	0.015	-0.044	-0.058
Springtime	-0.285*	-0.147	-0.429**	-0.299*	-0.401**	-0.320**

Table 3.4: *Pearson correlation values (r) comparing monthly FAP for the months of March, April, and May to PNA values 0-3 months earlier.* Relationships with p values less than 0.10 are characterized with one star and those less than 0.05 are with two stars.

El Niño events usually occur with above-normal temperatures in the northern regions of the United States (CPC, 2008). Since the positive PNA is often associated with an El Niño event (CPC 2007), the overall relationships between FAP values and Niño-3.4 are negative as well. It is noteworthy that the FAP values across the Northern Great Plains in March show significant negative correlations with Niño-3.4 0-3 months earlier. Our results also reveal general positive relationships between monthly FAP and PDO values. In May, the FAPs are positively correlated with PDO, especially in the Northern Great Plains, the South, the Upper Midwest, and the Ohio Valley.

3.3.3 Result of EOF analysis for freezing days in springtime months

Empirical Orthogonal Function (EOF) analysis is performed to identify the dominant spatial patterns of interannual variability of freezing days in March, April, and May, respectively. We discuss here the results of the leading two modes for each month.

For freezing days in March (Figure 3.5), the first EOF mode explains 61.97% of the total variance with in-phase fluctuation across our study region. The first EOF spatial pattern shows a relatively large variation in the Ohio Valley and the first EOF time series shows substantial interannual variability. We conduct the spectral analysis to identify major periods, which reveals prominent periods of 2.5 to 4.5 year, indicating that the in-phase fluctuation pattern of freezing days across the region in March occurs every 2.5 to 4.5 years. The second mode only contributes to 8.3% of the total variance. The second EOF spatial pattern shows opposite phases between the region encompassing the Ohio Valley, the Southeast, and the Northeast, and the region covering the Northern Great Plains and the Upper Midwest. The spectral analysis of the second EOF time series reveals a major period of 6.5 years.

To further understand how the frequency of these patterns associated with large circulations, we also relate the EOF time series to some teleconnection indices. The result reveals that the first EOF time series is significantly correlated with positive phase NAO in March as well as December of the previous year. This indicates that if we observe a positive phase of NAO in the aforementioned months, the in-phase fluctuation across our study region with a higher intensity over the Ohio Valley

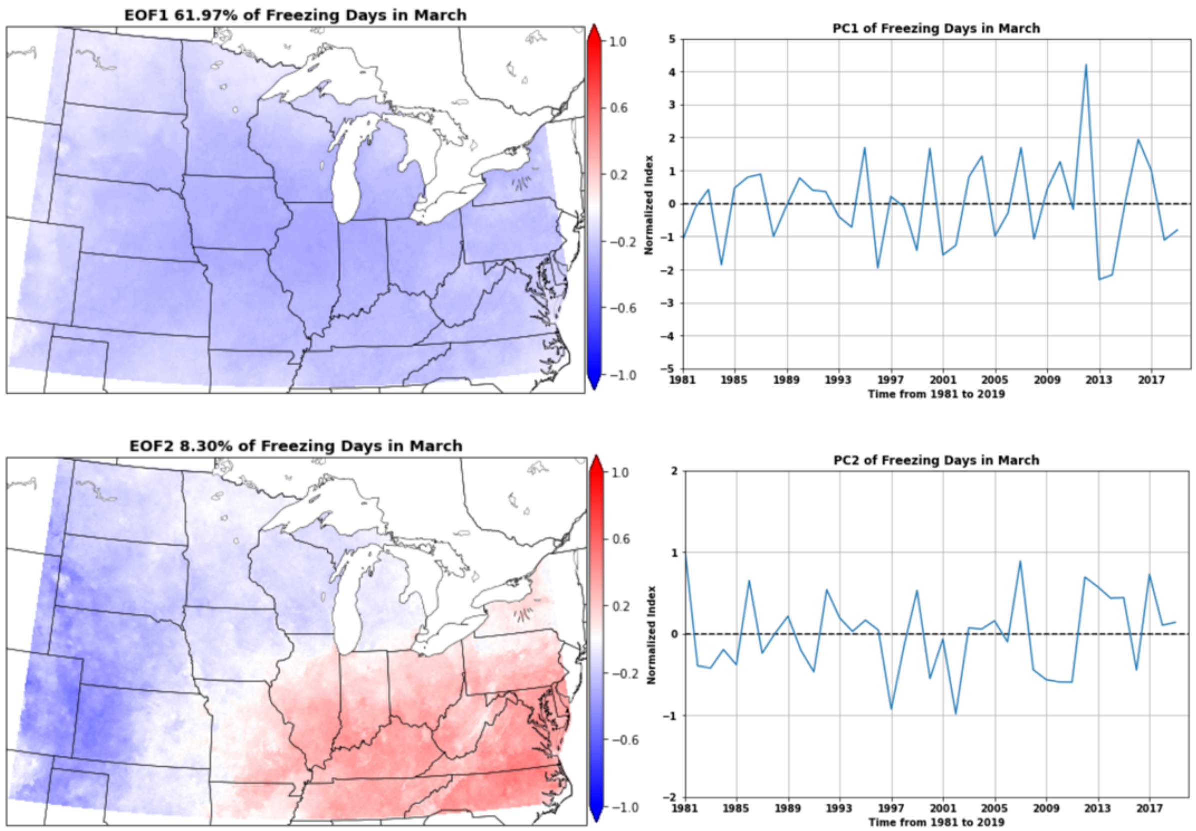

Figure 3.5: *The leading two EOF modes and PC times series for freezing days in March.*

is likely to occur in March.

For freezing days in April (Figure 3.6), the first mode of in-phase fluctuations over the domain explains 56.242%. The first spatial pattern also shows a larger variation across the Northern Great Plains. The first EOF time series shows inter-decadal variability with major periods of 5 to 7 years. The second mode accounts for 12.33% of the total variance. The spatial pattern of the second mode shows out-of-phase variability between the Northern Great Plains and the rest of our study region, and the time series of it shows interannual variability with major periods of 2.5 to 3.5 years. The correlation of coefficients between freezing days in April and the three teleconnection indices reveal that the first EOF time series is significantly correlated to positive phase NAO in February and negative phase PNA in March and December of the previous year.

For freezing days in May (not shown here), the first mode explains 57.8% of the total variance. Since in May, some southern areas are in frost-free season, we only observe in-phase fluctuation

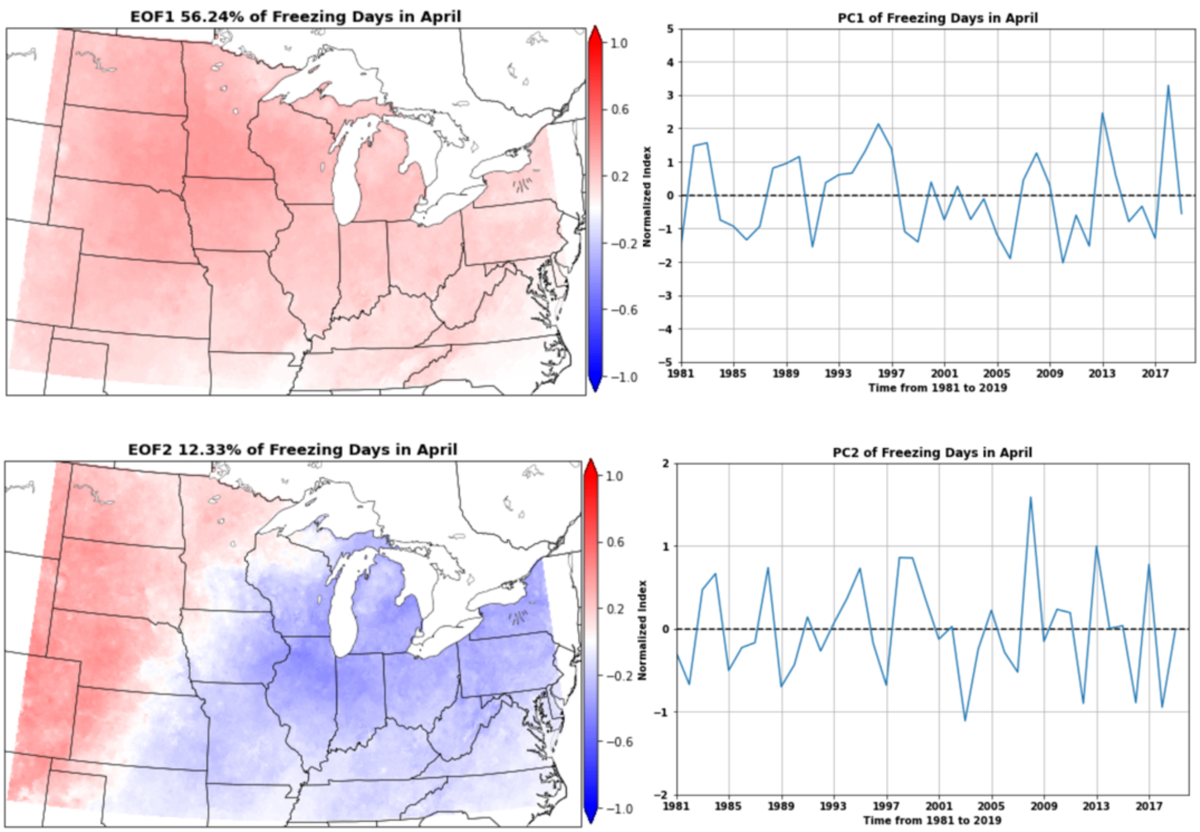

Figure 3.6: *The leading two EOF modes and PC times series for freezing days in April.*

in the northern part of the study region. And the time series for it shows major periods of 3 to 7 years. The second mode explains 10.71% of the total variance and shows opposite phases between the Northern Rockies and Plains and the rest of our study region. The time series for it reveals interannual variability. The relation to teleconnection indices shows that the second mode time series is significantly related to both positive phases of NAO, PNA, and PDO in May.

To understand the spatial patterns of the two leading EOF modes of freezing days in different months across our study region in the context of atmospheric circulation anomalies, we regress the time series of the first two EOF modes of freezing days in March to several monthly anomalous atmospheric variables, including the 500 hPa geopotential height (H500), 1000 hPa geopotential height (H1000), the 500-1000 hPa thickness, and the 1000 hPa wind.

The anomalous 500-hPa geopotential height regressed on normalized PC1 in March shows that this variable is negatively correlated with normalized PC1 throughout our study region, while

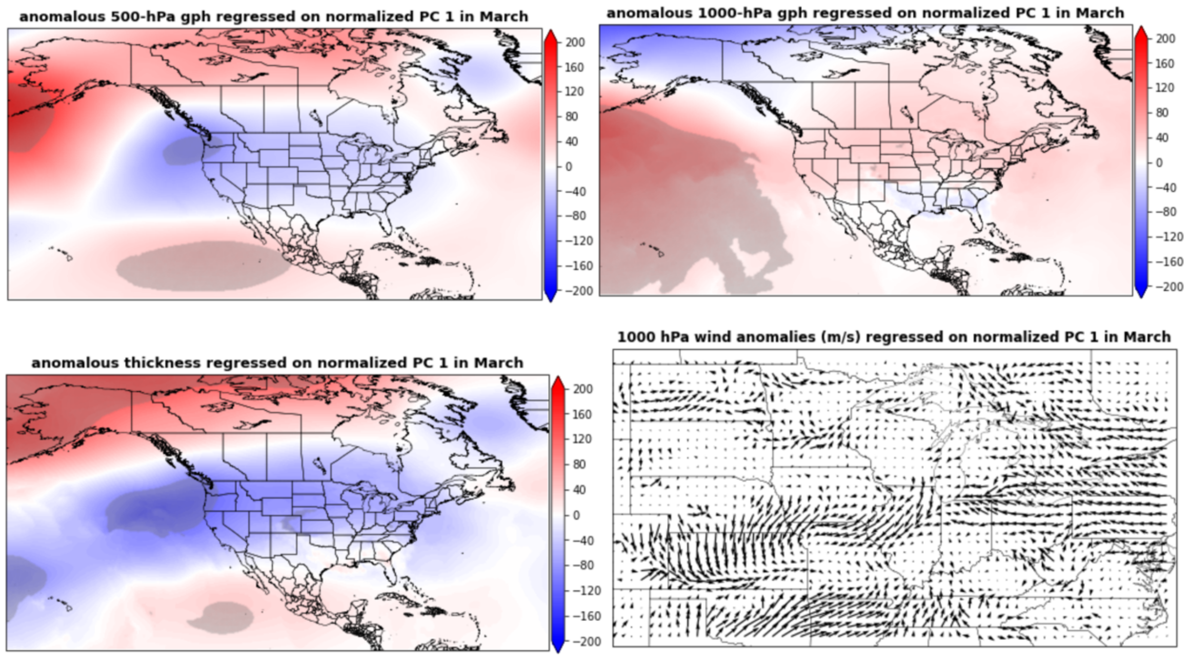

Figure 3.7: *The first PC times series for freezing days in March related to atmospheric variables.*

anomalous 1000-hPa geopotential height is positively correlated (Figure 3.7). This result indicates that the overall negative freezing day anomalies over the entire study domain (Figure 3.5) are associated with lower- (higher-) than-normal 500-hPa (1000 hPa) height and shallower-than-normal thickness between the two levels. The results for PC2 tells a different story (Figure 3.8) that when PC2 of freezing days in March is positive, which is associated with the out-of-phase variability EOF2 spatial pattern in Figure 3.5, the geopotential height is lower than average at the upper level and below normal at the surface, resulting in a thickness thicker than normal. The regression results between the anomalous atmospheric variables and NAO in March reveal significant Rossby wave patterns. The thickness regression pattern of PC1 is similar to that of NAO, which is consistent with the above conclusion that freezing days in March are significantly correlated to NAO (Figure 3.9). The 1000 hPa wind anomalies regressed on normalized PC1 and PC2 show similar results, which are both similar to the result of NAO. This anomalous wind field is characterized by an anomalous cyclone over the Southern Great Plains and an anomalous easterly wind from the Atlantic to the Ohio Valley.

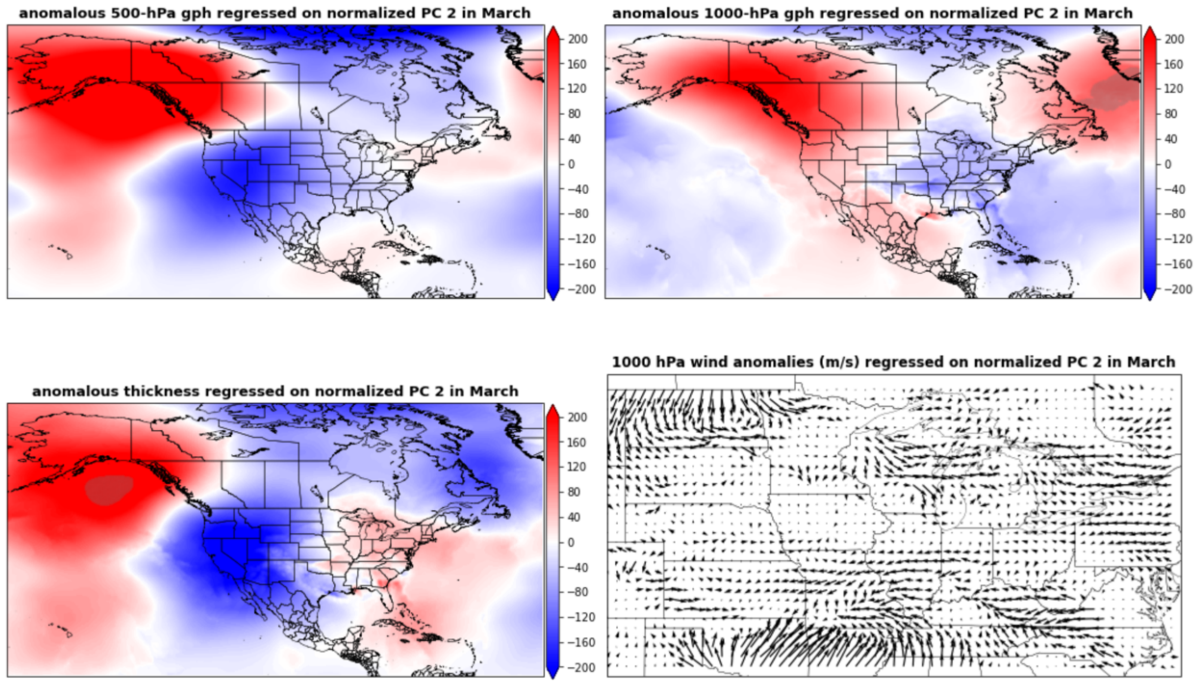

Figure 3.8: *The second PC times series for freezing days in March related to atmospheric variables.*

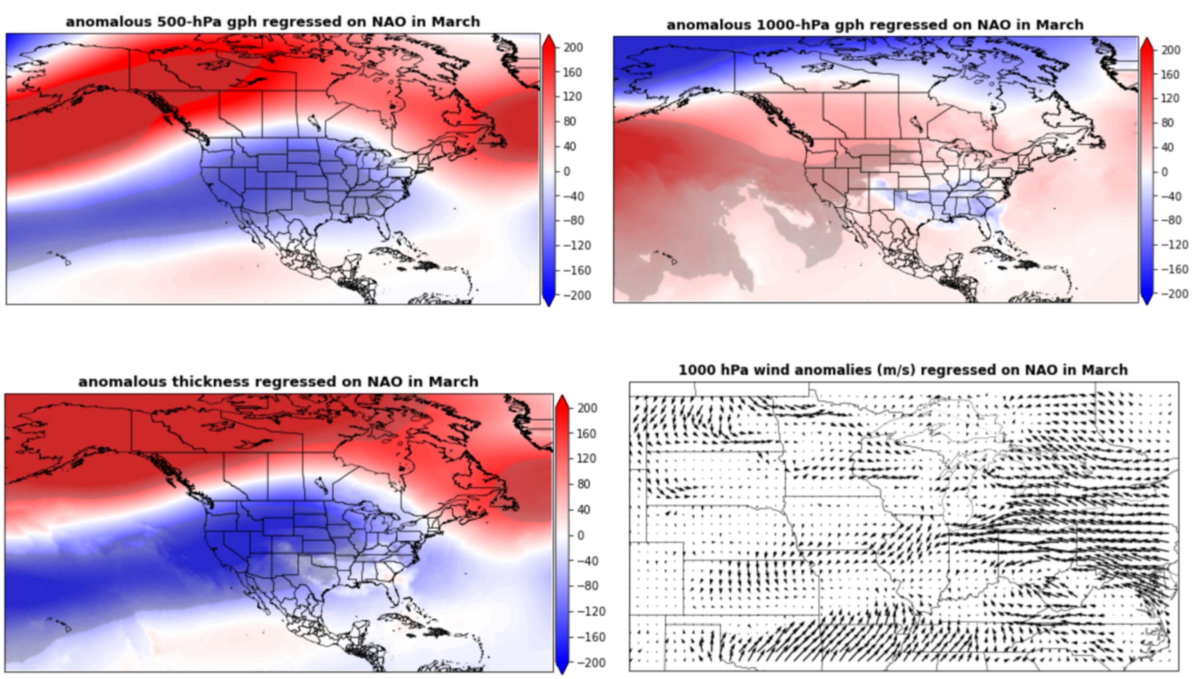

Figure 3.9: *Times series of NAO in March related to atmospheric variables.*

3.4 Summary

This study investigates the frequency, severity, and climate background of springtime freeze event occurrences. We conduct trend analysis for freezing days at each grid point and also at the region-averaged level. We also use the EOF technique to identify the spatial pattern and corresponding trend of freezing days each springtime month. And we also use climate variables to explain these results. The major findings are as follows.

1) Trend analysis at each grid point reveals that freezing days in March show a decreasing trend across the central and Midwestern US. Trend analysis over the spatially averaged springtime freeze events, which is significantly correlated to spatially averaged daily minimum temperature, also reveals a general decreasing trend across the study region. Although the years 2007 and 2012 show a low frequency of freeze events, considerable crop damage was observed in these two years, as a consequence of false springs exposing the earlier developed crops to the subsequent freeze events.

2) We then define a variable, freezing area percentage (FAP), over the regions of interest. The trends for the accumulated springtime are downward with a significance in the Ohio Valley, which extends the findings in Easterling et al. (2002) from the period 1948-1999 into 1981-2019. To further investigate the periodicity of monthly FAP values, we relate them to some teleconnection indices, Niño-3.4, NAO, PNA, and PDO. We conclude that the positive phase of NAO is usually associated with less freezing risk in March across the study region and the total springtime FAP values are always significantly associated with the negative phase of PNA values 1-3 months earlier, except in the Southern Great Plains region.

3) EOF analysis of freezing days in March shows a relatively larger variation in the Ohio Valley, and the first EOF time series shows substantial interannual variability. And when a positive phase of NAO in March and December of the previous year occurs, the in-phase fluctuation across our study region with a higher intensity over the Ohio Valley is expected to occur in March. And this pattern is likely associated with the geopotential height lower than average at the upper level and higher than average at the surface and a thickness shallower than normal.

The analysis work done in this study has some limitations. First, to gain better results at the subregion level, the study region should be extended to the contiguous United States. We only get limited parts of the defined subregions of the Northeast, the Southeast, and the Southern Great Plains. Therefore, the freezing days averaged across these defined regions in this study could not represent the general trend of the whole region defined in Karl and Knight (1998). Second, to understand the weather conditions of freeze event formation, specific case studies could be done. For example, we could select a couple of freeze events that profoundly impact crops' growth to investigate the particular weather conditions of wind, temperature, and humidity.

In spite of the limitations of this study, the implications of trends and causes of springtime freeze events are important for fruit growers in the central and midwestern United States. NAO is an excellent index to indicate the freeze event occurrences in March. Although the freeze event occurrences tend to decrease in recent decades, crops are exposed to higher false spring risks, which will be investigated in the next chapter.

CHAPTER 4

SPRINGTIME FREEZE EVENTS IMPACTS ON AGRICULTURE

4.1 Background

4.1.1 Springtime freeze types and their impacts on perennials

Different types of freeze events could cause different levels of damage to perennials. Consequently, it is important to understand when and how these freeze events occur and thus find ways to minimize the impacts of these adverse weather events on crops. Although the terms frost and freeze are often used interchangeably, they represent two kinds of weather events. The term freeze is typically used to describe an invasion of a large, frigid air mass from the Arctic or Canadian regions, which is commonly called the advective freeze (Powell et al., 2000). The advective freezes tend to occur in a well-mixed boundary layer with strong winds associated with cold fronts or with the leading edges of polar-origin high-pressure systems (Winkler et al., 2012). Frosts, also known as the radiative freeze, usually occur under calm, clear conditions on cold nights where the ground or plant canopy surface cools radiatively more quickly than the air above it, which is usually associated with high-pressure systems. (Winkler et al., 2012). There are two types of frost: hoar frost and black frost. Hoar frosts are visible with ice formation, and black frosts are invisible due to insufficient water vapor (Powell et al., 2000). Empirically, radiative freezes happen more frequently, and advective freezes result in colder and more extended periods. Both advective freezes (intrusion of chilled air) and radiative freezes (negative heat energy balance) could significantly decrease agricultural production. Radiative freezes occur more frequently and are associated with temperature inversion and are comparatively easier to predict. On the contrary, advective freezes are less frequent and occur without inversion developing and thus are difficult to predict.

Knowing the type of freeze could help suggest ways of managing crop plantation distributions since the two types of freeze events produce different damage patterns across the growing region.

Research has shown that freeze event that damage plants are more often radiative than advective (Charrier et al., 2015). Radiative freezes typically occur after sunset when the weather conditions are calm. Since there is no incoming solar radiation adding heat to the system, the outgoing long-wave infrared radiation cools the ground and thus makes the heat energy balance negative (Charrier et al., 2015). Therefore, radiative freezes occur more frequently in narrow valleys, in concave or flat locations, and less regularly in elevated and convex areas more exposed to wind (Lindkvist et al., 2000). Consequently, proper crop site selection is an effective way to avoid freezing injury caused by radiative freezes. Hilltops and slopes are considered as good orchard sites from which relatively cold air can flow downslope away from the orchard site, while landscape depressions are regarded as poor sites where cold air accumulates at night due to air drainage (Winkler et al., 2012). In contrast, advective freezes may cause more significant damage by enhancing the heat loss and cooling of plant tissue (Perry 1998) at those good sites under radiative freezes (elevated and convex areas more exposed to wind), which are more exposed to wind with subfreezing temperatures (Winkler et al., 2012). Therefore, the combination of both types of freezes could result in crop site selection failures. In addition, local topography complexity and variations play an important role in leading to freezes events formation by influencing temperature and wind in valley or lake systems (Lindkvist et al., 2000).

4.1.2 False spring occurrences and impacts on crops

Extreme temperature fluctuations during the springtime can have enormous impacts on the growth of vegetation, and many agricultural and horticultural crops. An extended period of warmer temperatures, identified as a "false spring", could cause perennial crops to break dormancy and start their growing season earlier than usual (Kistner et al., 2018). As a result, when the cold air comes back, these crops are especially vulnerable and susceptible during their bud stages, and, hence, spring freezes have profound impacts on crops. In 2002, sour cherry production in Michigan was reduced by at least 95% from the previous annual yields due to springtime freeze events following the unexpected extended warm spells (NASS, 2002). In April 2007, after an extended warmth prompting early growth of vegetation and crops, cold arctic air infiltrated southward into the central and eastern US, causing temperatures to drop to freezing and thus leading to an estimated $2 billion of yield reductions for crops such as winter wheat, corn, and forage legumes due to frost burn and plant mortality (Marino et al., 2011; Kral-O'Brien et al., 2019). During March 2012, a persistent upper air ridging feature resulted in the warmest temperature anomalies at many locations across the Midwestern US since 1900 for that month, which brought many crops out of dormancy (Labe et al., 2015). Near the end of March and throughout April 2012, average temperatures returned to these regions, resulting in a series of crop yield loss due to freeze damages, including the loss of approximately 85% of apple crop yields and 90% of tart cherry crop yields for the year in Michigan (Kistner et al., 2018).

Global climate change has sparked considerable research on extreme weather events and their impacts on vegetation growth. Nevertheless, research focused on the occurrences, immediate effects, and long-term consequences of false spring events have been limited, despite their potential for extreme environmental and economic consequences (Kral-O'Brien et al., 2019). False springs are related to global warming in the way that the onset of spring has generally shifted earlier in the year over the past several decades due to rising average temperatures (Allstadt et al., 2015). False springs, which usually happen in late winter or early spring, are sufficiently mild and long to bring vegetation out of dormancy earlier, rendering the vegetation vulnerable to later freeze events (Ault et al., 2013). The later the freeze occurs after growth begins, the more damage is likely to be caused since plants are in a more vulnerable phenological stage (Marino et al., 2011). Additionally, it is projected that false spring risks might increase in portions of the Midwestern US (Allstadt et al., 2015).

4.1.3 Influence of phenology on freeze damage

Freeze events that occur at a different time could result in different injuries to crops. Usually, freeze events after false springs could cause severe damage to growing crops. Also, phenological processes are particularly crucial for freeze events avoidance in spring and autumn (Charrier et al., 2015). Microclimate factors that affect crop development include chill units, growing degree hours, and minimum temperatures, varying in diversified topography (Logan et al., 2000). Since phenological processes are strongly dependent on temperature, microclimate could affect crop stages by delaying development with cooling and accelerating growth with warming. During winter, fruit trees in the stage of dormancy are very resistant to cold temperatures. During the annual cycle of growth and dormancy, the transition periods in autumn and spring are the riskiest since there is a moderate probability of freezing when plants are most vulnerable (Charrier et al., 2015). The temperatures that cause damage in spring are much lower than the temperatures that trees encounter damage in autumn (Larcher et al., 2010). Therefore, moderately low temperatures in spring could result in deadly impacts on crops. As fruit trees develop in the spring and buds start to swell, they lose the ability to withstand cold winter temperatures (Longstroth et al., 2012). The stage of bud development determines how susceptible any given fruit crop is when freeze events occur (Longstroth et al., 2012). When a spell of unexpected warm weather in the spring occurs, the plants will develop quickly. And when the temperatures return to normal, these developing crops that are very vulnerable would suffer significant damages.

4.1.4 Study objectives

This study aims to investigate the historical impacts of springtime freeze event damage on crops in the Midwestern US from 1981 to 2018. In particular, the study focuses on the first green dates, bloom dates, poor pollination days, and the bud survival chance of the year for apples using crop simulation models with input datasets from PRISM. Also, damage days of the year, daily minimum temperature, and damage occurring dates for each phenology growing stage are included to explore the impacts of false springs.

4.2 Dataset and methods

4.2.1 PRISM dataset

PRISM, a gridded analysis dataset provided by the PRISM climate group from Oregon State University, offers estimates for six essential climate elements: precipitation (ppt), minimum temperature (tmin), maximum temperature (tmax), mean dew point (tdmean), minimum vapor pressure deficit (vpdmin), and maximum vapor pressure deficit (vpdmax). PRISM has an excellent spatial resolution of 4 km. Evaluations have been done in the second chapter, and conclusions reveal that the PRISM analysis dataset generally agrees well with the observations and could represent the freeze events. As inputs for our apple yield simulation model, we obtained three variables from PRISM, daily minimum temperature, daily maximum temperature, and daily precipitation.

4.2.2 Apple yield simulation model

A primary cause of year-to-year yield fluctuations in tree fruit production across the United States and international production areas is bud loss associated with the cold injury that typically occurs either during the spring or winter seasons (Andresen and Baule, 2018). Bud sensitivity to cold environmental temperatures is strongly dependent on the phenological stage of development and generally increases from full dormancy through vegetative into reproductive stages. In this study, potential seasonal yield losses for apple production associated with cold temperatures were estimated following the approach of Zavalloni et al. (2006), in which phenological development and cold sensitivity are simulated on a daily basis using observed maximum and minimum air temperatures. Estimation of phenological development of apple was based on the methodology of Rijal (2017) using summed seasonal totals of base 4°C growing degree days from March 1st. Ten and ninety percent damage threshold temperatures for apples at a number of phenological stages were obtained from Ballard et al. (1998). In general, the damage threshold temperatures vary from -34.4ºC during dormancy to -2.2ºC during late vegetative stages through full bloom. Assuming a linear relationship between the damage severity level and the critical freezing temperatures (Dennis and Howell, 1972), daily percent damage estimates based on observed minimum temperatures were developed for each phenological stage dormancy through full bloom. Potential yield losses due to cold temperatures were then generated seasonally at each location as the cumulative sum of daily cold damage simulated during the season.

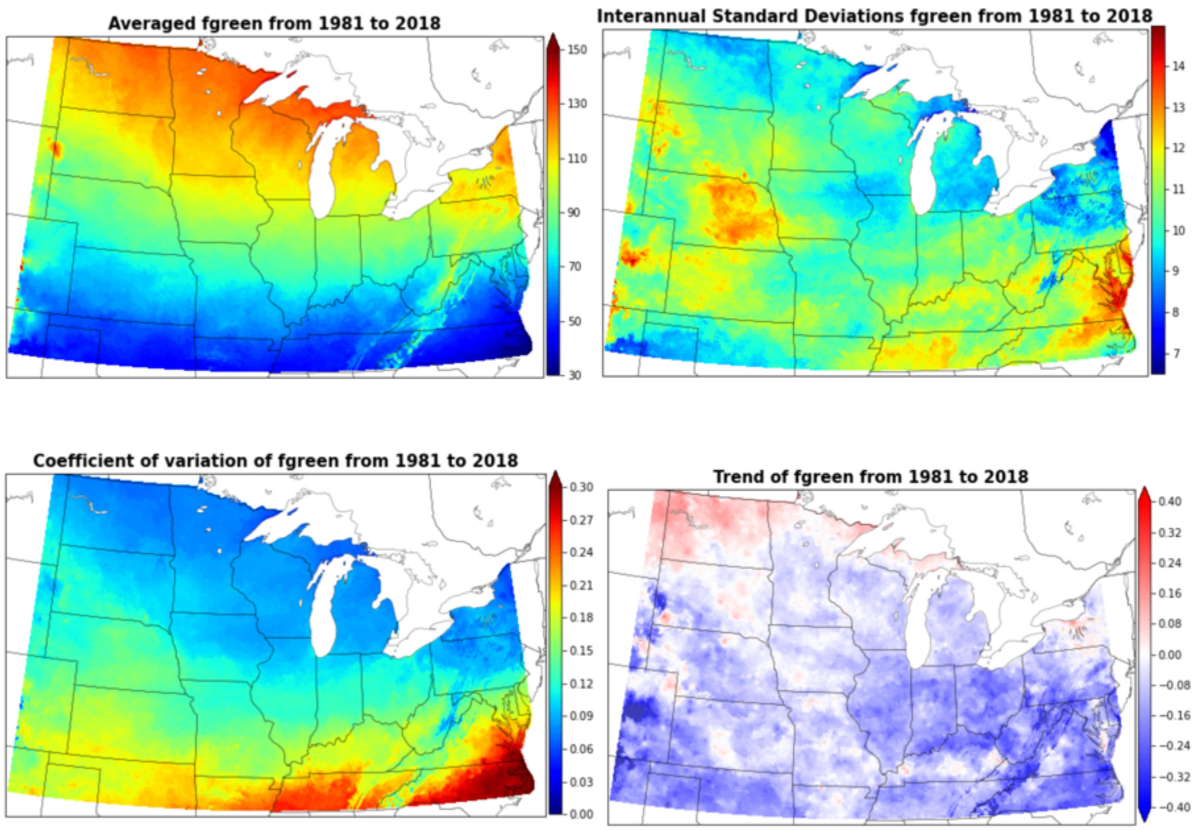

Figure 4.1: *Average, absolute variation, relative variation, and trend of the first green date (Julian date) from 1981 to 2018.*

4.3 Results

4.3.1 Characteristics of the yearly results

The crop simulation model outputs two files at each grid point, daily results and yearly results. The yearly results contain the first green date ('fgreen' in Figure 4.1, referred to as leaf out in some literature), the bloom dates, the poor days (in terms of pollination), and the yield (i.e., bud survival chance). And the daily results provide information about the Growing Degree Day (GDD), the phenological stage of apples, and the freeze damage.

Figure 4.1 shows characteristics of the first green date, including annual mean, absolute and relative variation, and the trend. The values are the Julian dates of the year. For example, 60 means the date of March 1st, which is the early springtime. The average values are latitude-dependent with later dates in the northern region and earlier dates in the southern region, similar to the averaged temperature pattern. For Michigan, we observe a gradual increase from the south to the north. The first green date in northern Michigan could be around early April, but that in the upper peninsula could be as late as the middle of May. The interannual standard deviation shows the absolute variation, while the coefficient of variation is the relative variation calculated as the absolute variation divided by the mean values. Therefore, the absolute variation of the first green date indicates that the northern regions have generally smaller variations than the southern regions. The highest absolute variation is observed in the Southeast of the study region and the lowest in the Northeast. So the first green date is more variable in warmer regions compared to cold regions. Since the absolute variation values are generally small compared to the mean values of the first green date, the relative variations are dominated by the averages, resulting in an opposite pattern to the mean values. The values in the trend graph are the slopes of the regression of the first green date on the 18 years, with negative values indicating earlier dates and positive values indicating later dates. Also, the significant trend is indicated by the grey shades. The results reveal that the first green dates are becoming earlier in most areas except for some northernmost regions of the northern plains and Michigan's Upper Peninsula.

Similar patterns are found for the bloom date (Figure 4.2) that occurs later in the year than the first green dates. The absolute variations of the bloom date are overall smaller than those of the first green date, especially across the entire Northeast, where the variations are small. The mean values still dominate the relative variations. The general trend of the bloom date is still becoming earlier. However, more areas of the Northern Great Plains and the Upper Midwest show later bloom dates. Also, more significant points are shown in the Southern Great Plains, the Northeast, and the Southeast.

The patterns for the poor pollination days, however, are different (Figure 4.3). The mean value pattern is not latitude-dependent. Most areas of our study region show values from 2 to 3 days. And large values are observed across the Ohio Valley and part of the Northern Great Plains. Most of the areas show an interannual standard deviation of fewer than two days. However, the large mean

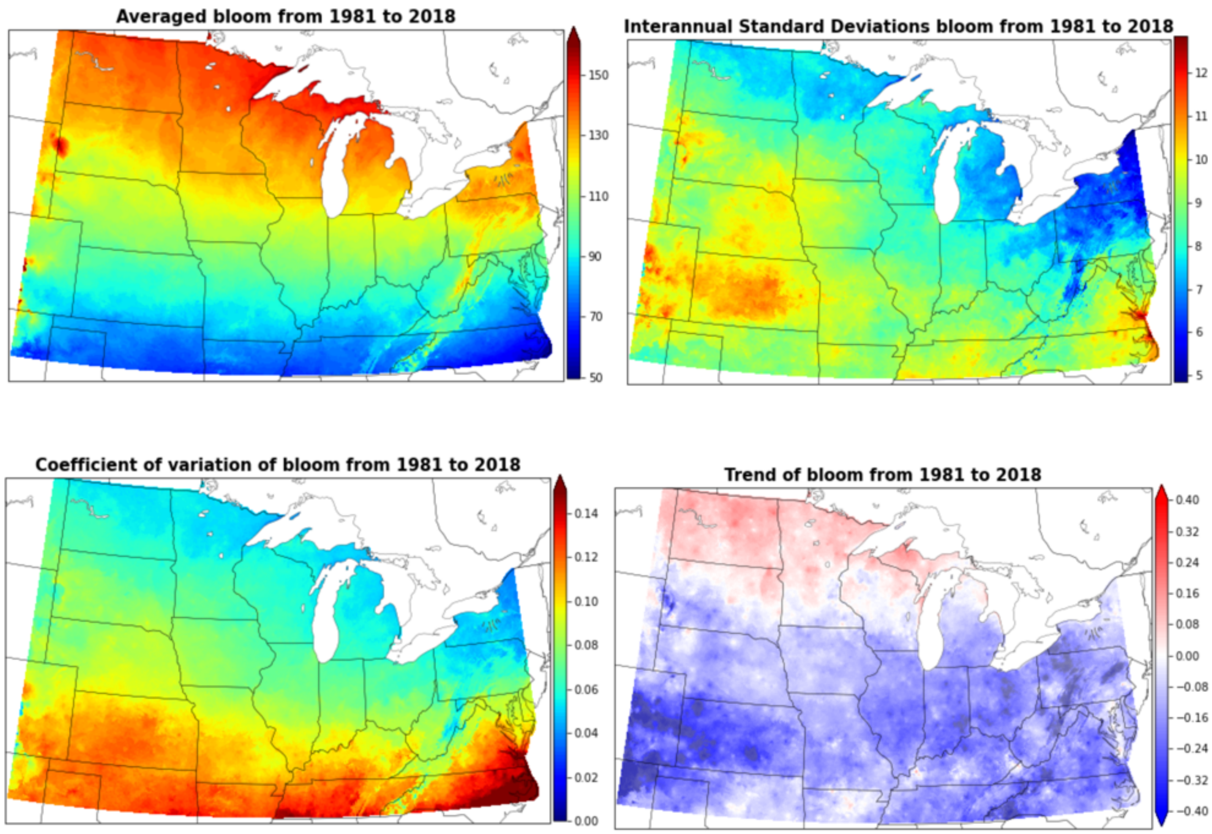

Figure 4.2: *Average, absolute variation, relative variation, and trend of the bloom date (Julian date) from 1981 to 2018.*

value areas also show larger absolute variations of around three days. The relative variation shows an exactly different pattern, which reveals large values in the Northern and the Southern Great Plains. Also, since the absolute variation values are in the same magnitude as the mean values, the relative variations are not dominated by the mean values. Regression of poor pollination days over the years reveals that the poor days increase across most of our study regions from 1981 to 2018, with noticeable significance in the Northern Great Plains, the Upper Midwest, and the Northeast. On the contrary, the poor days in the northern part of the Ohio Valley and the southern part of the Southern Great Plains significantly decrease throughout our study period.

Similar to poor pollination days, the pattern for the mean bud survival chance is also not latitude-dependent (Figure 4.4). The values are larger in the Upper Midwest and the Northeast than in the rest of the regions. It is noteworthy that the mean values around lakeshores are consistently

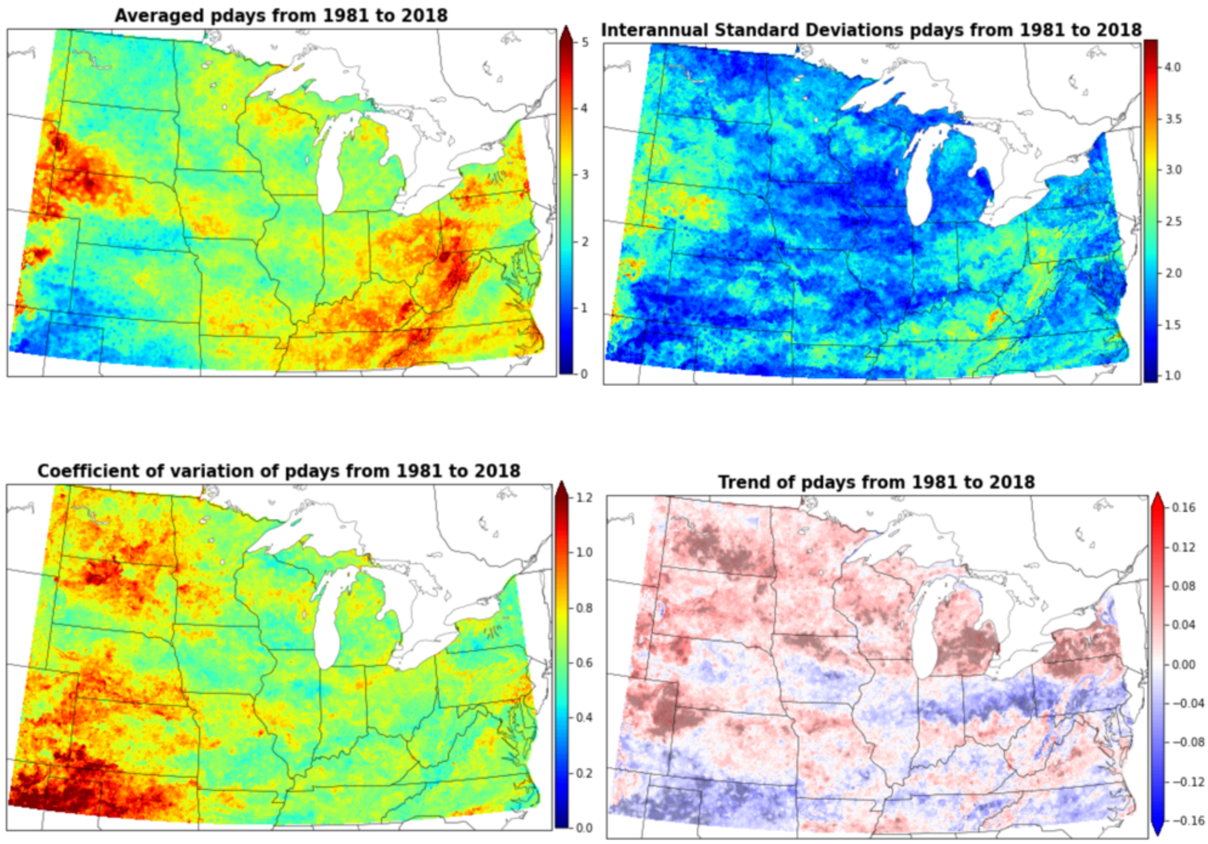

Figure 4.3: *Average, absolute variation, relative variation, and trend of the yearly poor pollination days from 1981 to 2018.*

high throughout the study period, which could be a result of the large bias in the input PRISM data in lake-modified areas, as discussed in Chapter 2. The large bias in the input data may also explain the small values in the interannual standard deviation in areas along the shorelines. The largest absolute variations are observed in the Northern Great Plains. Southern Michigan and the west of the Southern Great Plains show smaller absolute variations compared to other areas. It is also noticeable that there's a highlight region in the upper part of Michigan, which shows smaller bud survival chances and larger standard deviations compared to other parts of Michigan. Since the absolute variation pattern is consistent with the mean pattern, the relative variation pattern is still consistent, which is the opposite of the mean pattern. Regression of bud survival chance over the years reveals that most areas of our study region increase throughout our study period. And Wisconsin and the southern part of the Ohio Valley show significant increases.

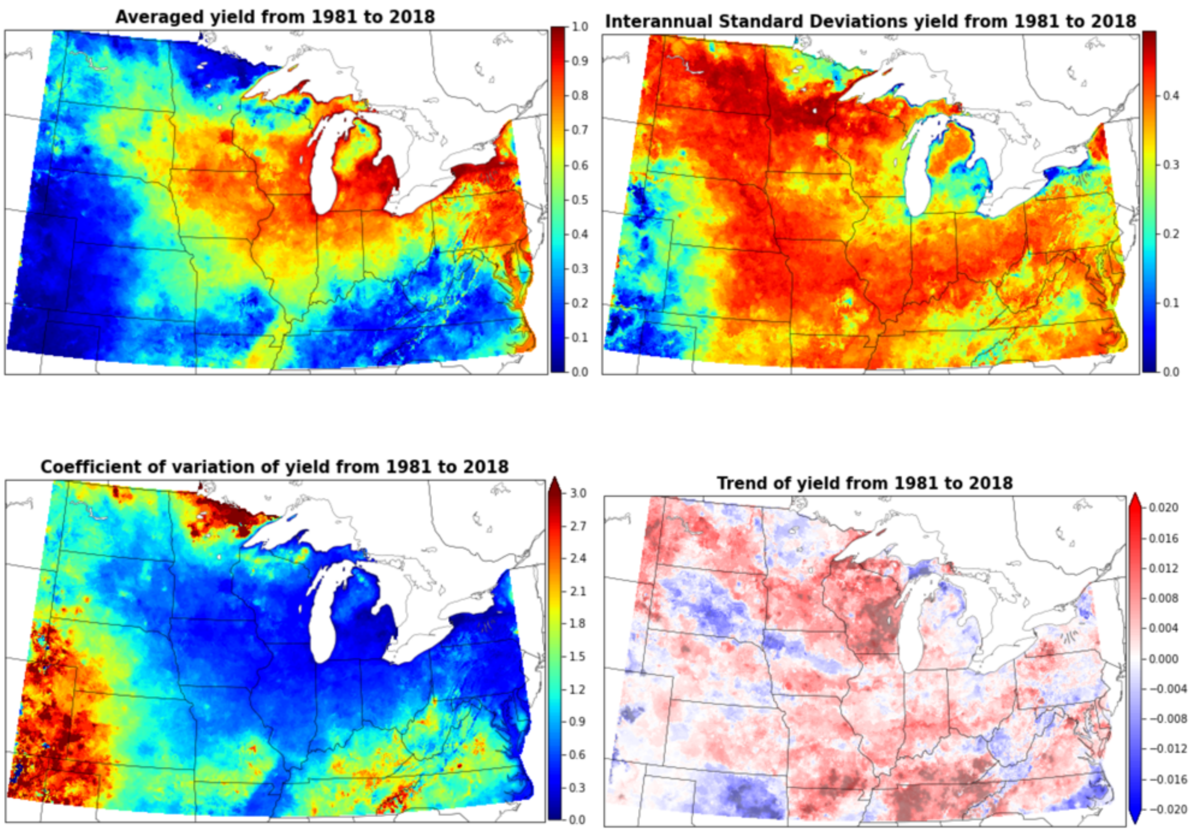

Figure 4.4: *Average, absolute variation, relative variation, and trend of the yield (bud survival chance) from 1981 to 2018.*

4.3.2 Daily Results and some derived indices

Freeze damage on each day is characterized by a fraction number less than 1.0 in the daily output files. Therefore, we could know the days when damage occurs and also the intensity of the damage. Also, we could know the date when the damage occurs, the phenological stage of the plant when damage occurs, in addition to the daily minimum temperature when damage occurs. We conduct some analyses based on these results.

Figure 4.5 shows the results for yearly accumulated damage days. Since the bud survival chance and the damage fraction numbers add up to 1.0, the mean pattern of damage days is the opposite of that of the bud survival chance. In contrary to the yield values, damage days around the Great Lakes Regions are fewer compared to other areas. The interannual standard deviation graph tells us that the areas where more damage days occur also show higher amplitudes of perturbations.

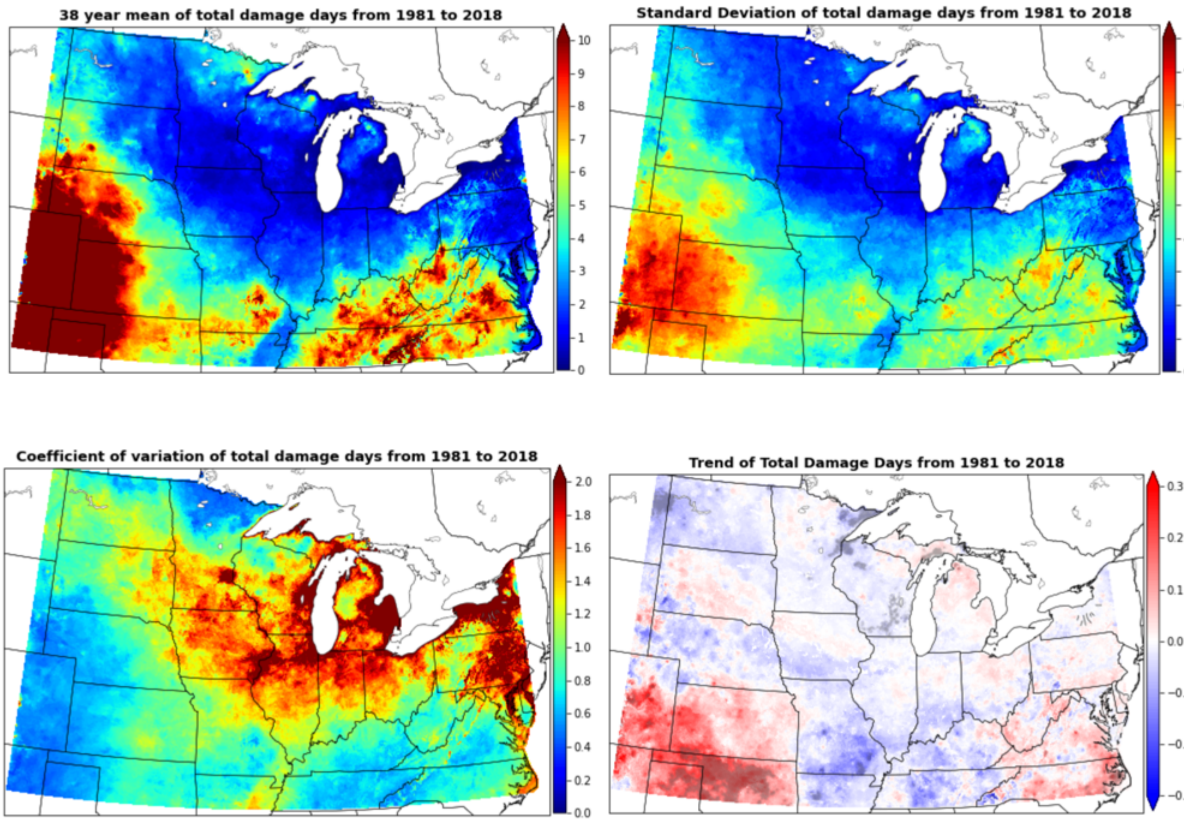

Figure 4.5: *Average, absolute variation, relative variation, and trend of damage days from 1981 to 2018.*

The results are characterized by lower variability in the Upper Midwest and the Northeast versus higher variability in the Southern Great Plains, the southern Ohio Valley, and the Southeast. The relative variation pattern tells a different story. Divided by the averages, the amplitudes around the Great Lakes Regions and the Northeast are larger than other areas. The trend of damage days across our study region is overall downward, which is the opposite of the bud survival chance. And significant increases are observed in the Southern Great Plains. It is also noteworthy that most areas of Michigan show a slight upward trend of damage days.

Figure 4.6 shows the average damage days at each growth stage. Stages are defined according to the running total of base 4 oC growing degree days each year, calculated based on temperature. By definition, we have Stage 0 and from 2 till 9 without Stage 1. In Stage 0, damage only occurs in the northernmost regions near the US and Canada border, which is expected because of the

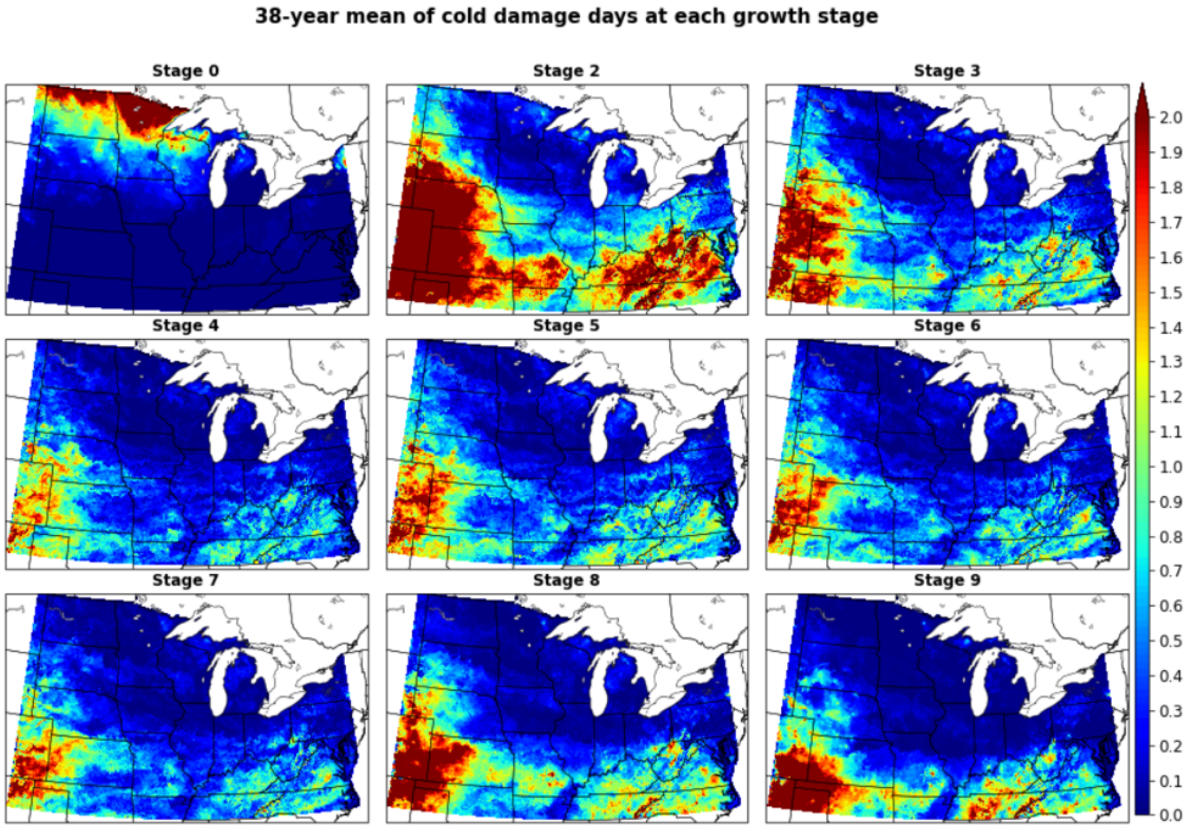

Figure 4.6: *Average of damage days at each growth stage from 1981 to 2018.*

temperature-dependence. In Stage 2, damages occur over large areas of the Southern Great Plains and in parts of the southern Ohio Valley and the Southeast. Damage areas stay in these regions through the rest of the stages, with the number of damage days and the areas influenced becoming smaller in Stages 3 -7, and larger again in Stages 8 and 9.

The trends of the damage days for each stage can be determined by regressing the time series of average damage days during each growth stage on the time series of the years over the study period (Figure 4.7). The damage days in Stage 0 that occur over the northern Plain exhibit a downward trend. On the contrary, the trends are generally upward in regions of the southern Plains, especially for Stage 2 and Stage 9.

Except for Stage 0, the dates when damage occurs during each growth stage show latitude-dependence with progressively later dates towards north. (Figure 4.8). In Stage 0, damage only occurs in the northern parts of the Great Plains and the Midwest as well as parts of the Ohio Valley.

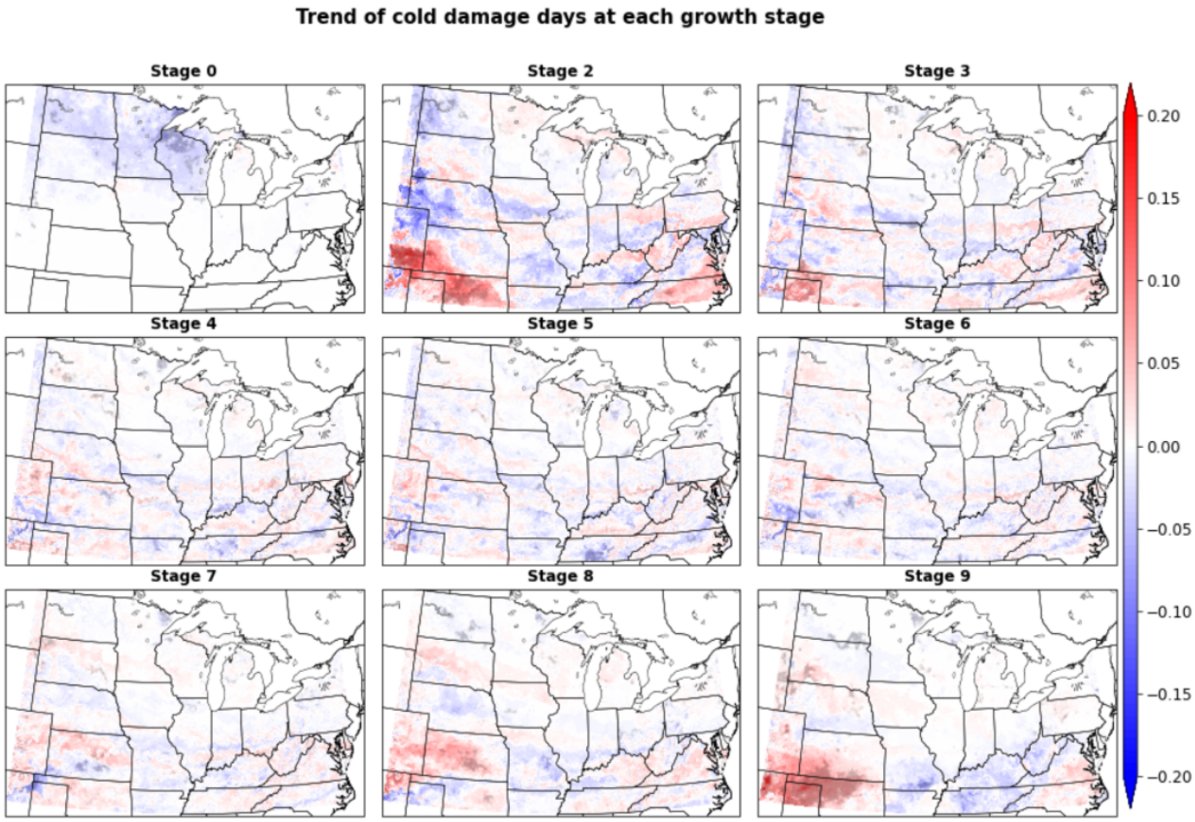

Figure 4.7: *The trend of damage days at each growth stage from 1981 to 2018.*

The damage across these regions happens around similar dates, with a slight delay in northern Michigan and Wisconsin, possibly due to the lake effect. In Stage 2, damage happens from late February in the southern edge of the study region to late March and early April in the southern Plains and the Ohio Valley, and from late April to early May in the northern Plains and upper Midwest. Similar delayed occurrence towards northern latitudes also occurs during other stages. The trend analysis (Figure 4.9) reveals that, in general, the occurring damage dates are becoming earlier across the study region over the 38-year study period, especially for Stage 9 when damage occurs much earlier across southern Michigan and northern Ohio. The only exception is Stage 0, during which damage in Michigan and Wisconsin happens significantly later.

The spatial patterns of the average damage days and the dates when damage occurs are consistent with the patterns of daily minimum temperature during the damage days (Figure 4.10). In Stage 0, the daily minimum temperatures during damage days are below -10 °C. Then in Stage 2,

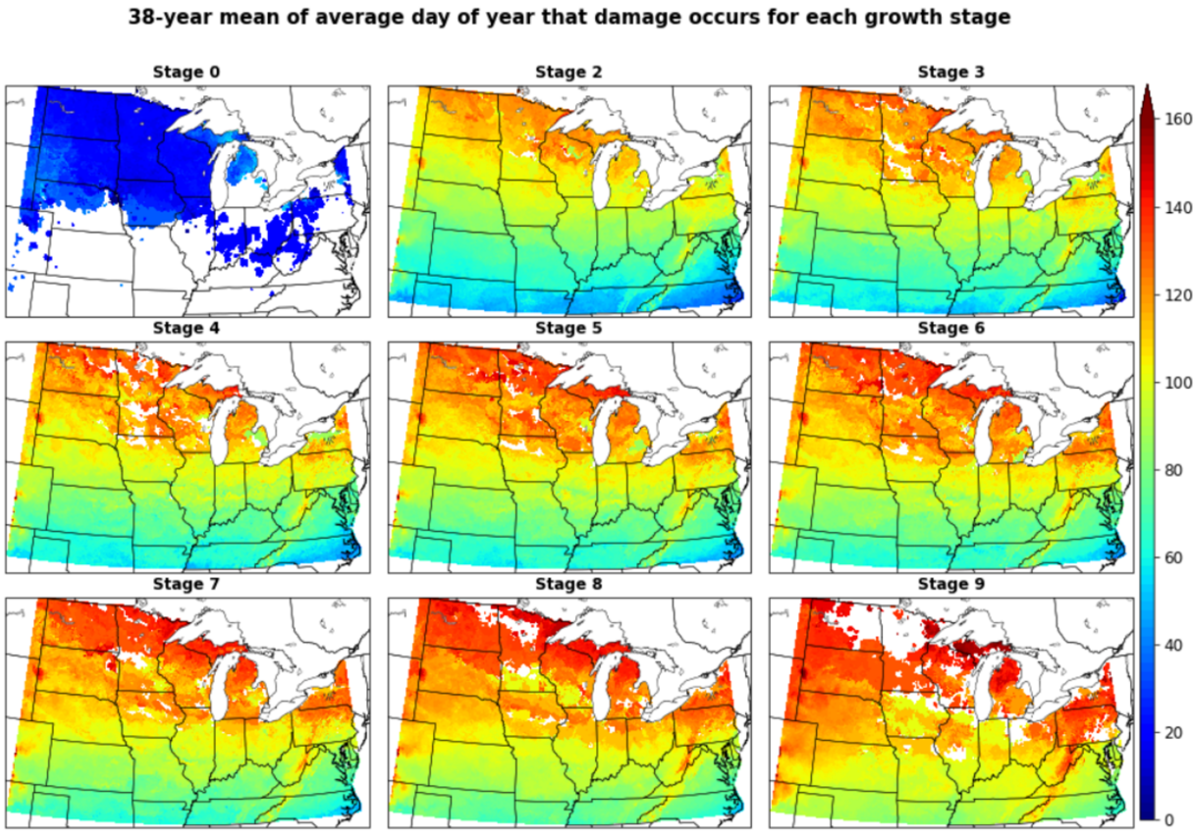

Figure 4.8: *The average of freeze damage occurring date at each growth stage from 1981 to 2018.*

most damage occurring in the Southern Great Plains with daily minimum temperature from -8 °C to -6 °C, while in the Upper Midwest with daily minimum temperature from -6 °C to -4 °C. Then the daily minimum temperatures for Stage 3 and Stage 4 are similar, from -5 °C to -3 °C across our study region. Then as the phenology marches into later stages, the daily minimum temperatures are higher. Generally, the damage occurring in the northern areas with higher daily minimum temperatures compared to the southern areas. The regression analysis (Figure 4.11) reveals that the daily minimum temperatures are overall becoming warmer during damage days. And larger trend values are only showing around the Great Lakes Region compared to other areas. It is noteworthy that the areas showing earlier damage occurring dates in Figure 4.9 show daily minimum temperature trends upward. Therefore, we conclude that damage is generally occurring on earlier and warmer days. This conclusion could be related to the 'False Spring' occurrences. False springs are related to the global warming trend in the way that the onset of spring has generally

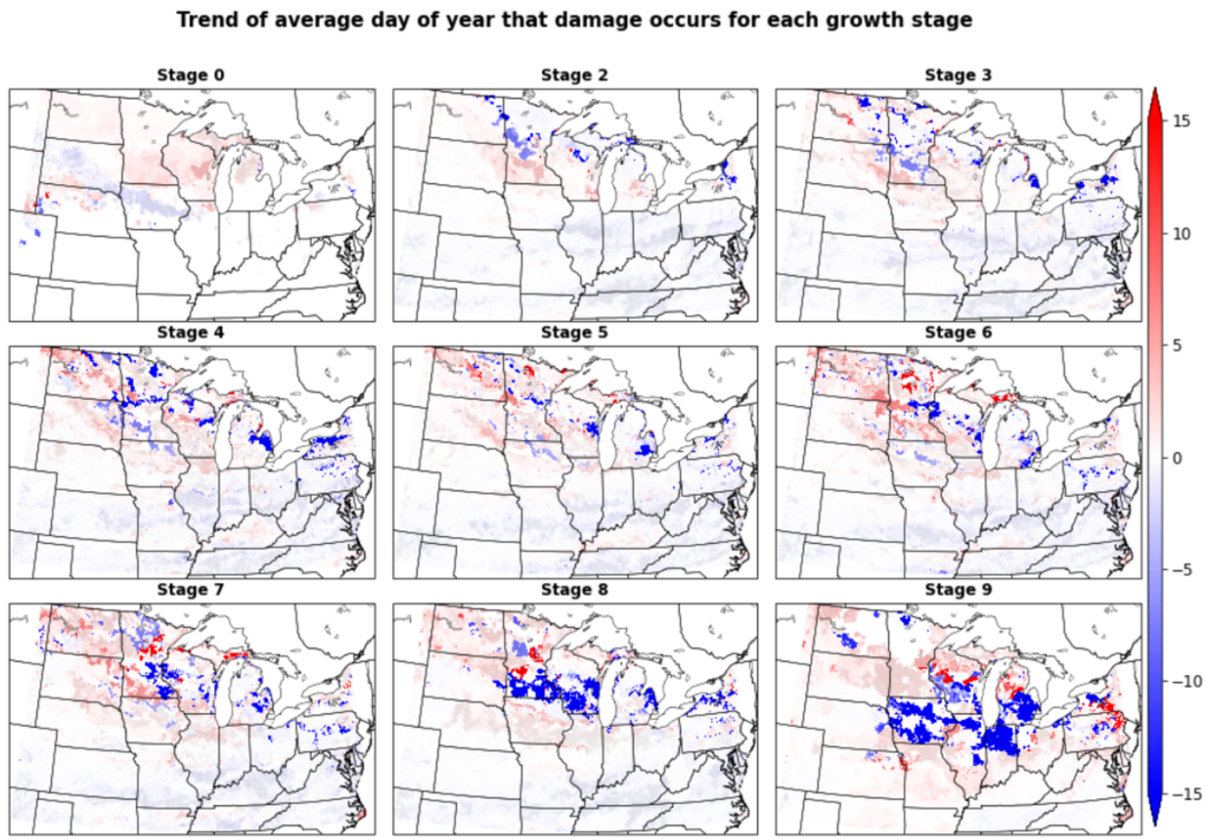

Figure 4.9: *The trend of freeze damage occurring date at each growth stage from 1981 to 2018.*

shifted earlier in the year with rising average temperatures. As a consequence of earlier springs and increasing temperatures, the damage is occurring earlier with warmer temperatures.

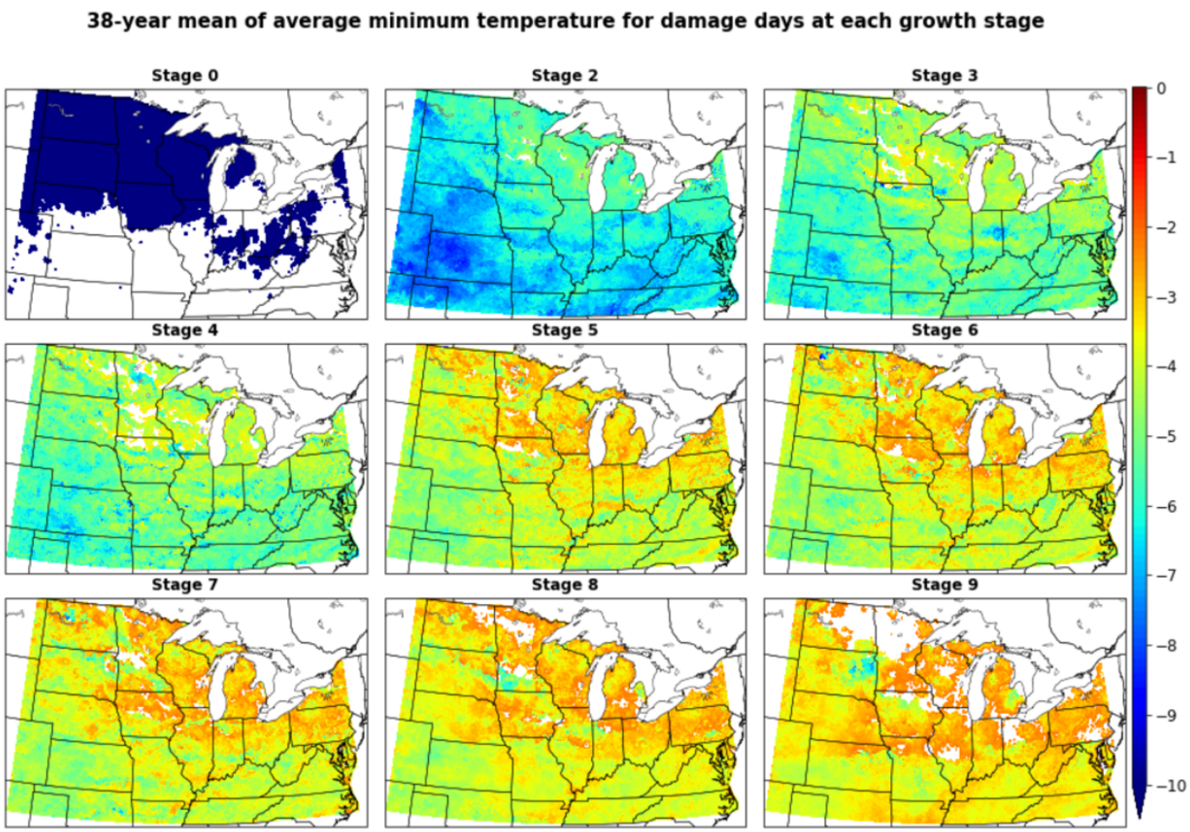

Figure 4.10: *The average daily minimum temperature during damage occurring date at each growth stage from 1981 to 2018.*

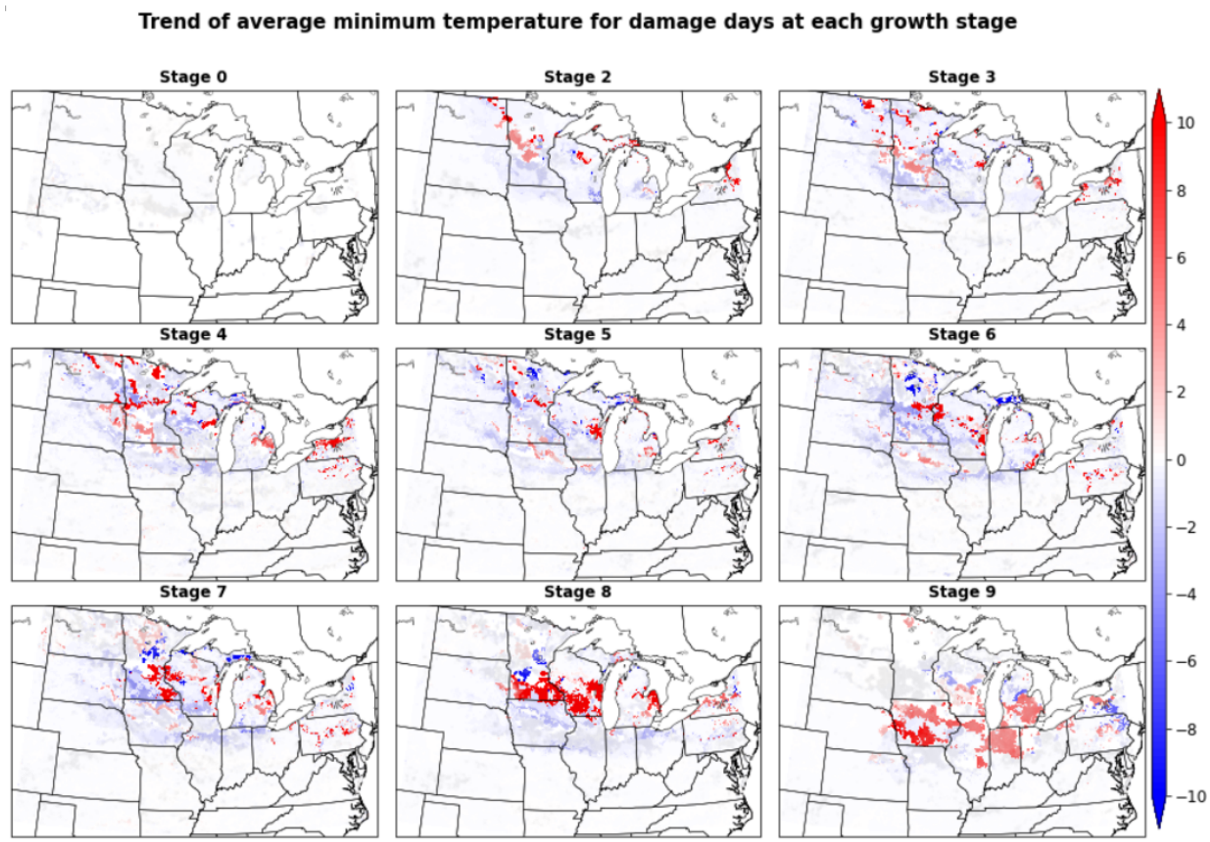

Figure 4.11: *The trend of daily minimum temperature during damage occurring date at each growth stage from 1981 to 2018.*

Following the division of the subregions in Chapter 3, we calculate the damage days averaged across different subregions (Figure 4.12). We first calculate the annual damage days at each grid point and then compute the spatial average in each subregion. Therefore, each subregion has a time series of damage days. We find damage days show an abrupt high value in 2012 in the Upper Midwest and the Northeast, which is consistent with the severe damage to crops reported during that year. The annual mean damage days and standard deviations range from 1.56 days yr-1 and 0.99 yr-1 over the Upper Midwest to 7.88 day yr-1 and 4.85 days yr-1 over the Southern Great Plains. The time series of damage days across different subregions suggests that the Southern Great Plains and the Southeast are not favorable for apple growth, whereas the Upper Midwest is most suitable for apple growth as far as the risk of freeze damage is concerned. Although only a small part of the Northeast is covered in our study, the result shows that the Northeast is also favorable for apple planting.

To further examine the regional differences of the damage days for each growth stage, we count the annual damage days over each growth stage at each grid point and average over all grid points in each subregion. We then sum the annual mean over the 38 years for each subregion, and the results are shown in Figure 4.13. First, the results reveal that there are more damage days occurring in the first two phenological stages since we know that crops are more vulnerable at early growing stages. The Upper Midwest and the Northeast show lower values for all nine stages compared to other regions. Also, there are no damage days during Stage 0 for the Southern Great Plains and the Southeast and almost no damage days during Stage 0 for the Ohio Valley and the Northeast. For most regions, the largest number of damage days occur during Stage 2, while for the Upper Midwest, most damage days occur during Stage 0. Damage days for other stages vary from region to region.

A similar calculation is done for annual damage values to understand how damage intensity varies with stage and region (Figure 4.14). It turns out that the Upper Midwest and the Northeast not only have fewer damage days but also show lower damage intensity, which is contrary to the Southern Great Plains and the Southeast. Also, the results reveal that Stage 2 and Stage 3 show the

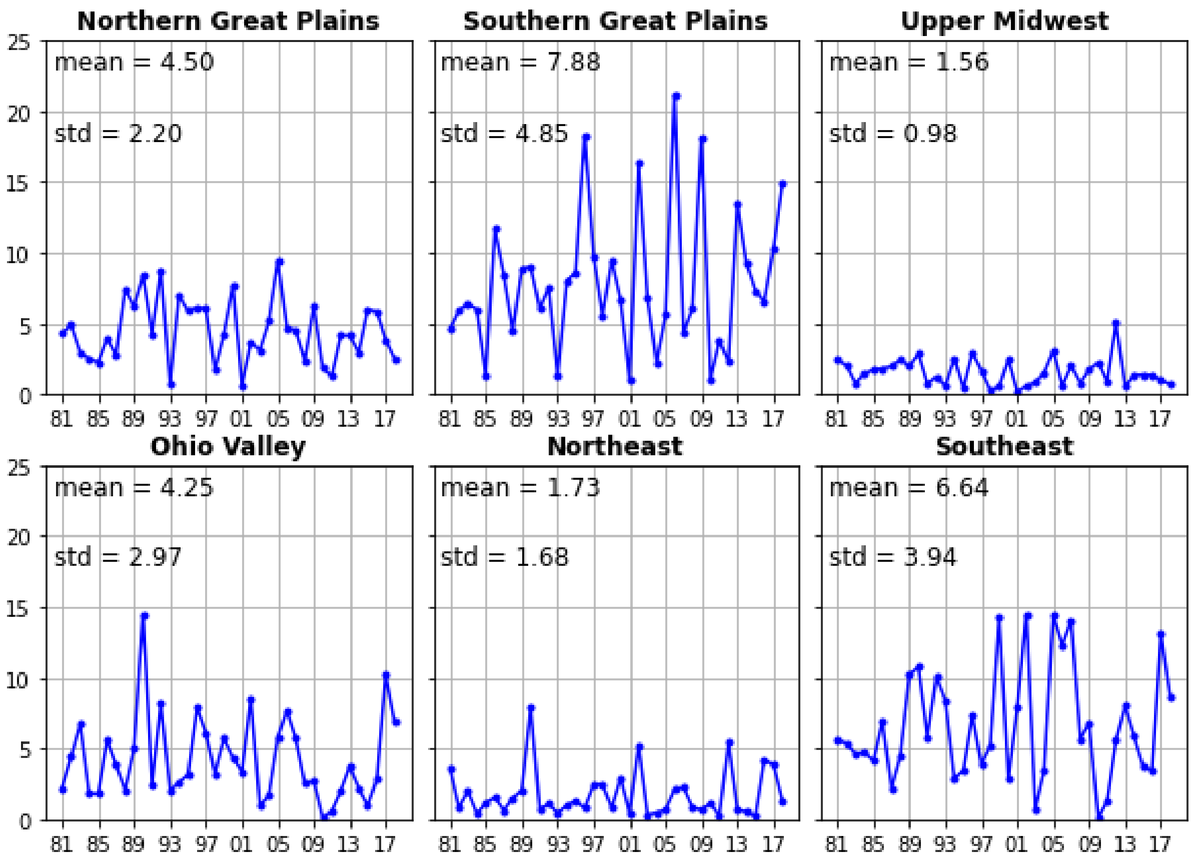

Figure 4.12: *The time series of area-averaged damage days in six subregions from 1981 to 2018.*

largest damage intensity of all nine stages for all our subregions. Therefore, for the six subregions except for the Upper Midwest, Stage 2 not only shows the most damage days but also shows the most intense damage. Although Stage 0 shows the most damage days in the Upper Midwest, the damage values for Stage 0 are not large. Hence, Stage 2 is the phenological stage that considerable damage might be most likely to occur.

The region- and stage-dependence of daily minimum temperature (Figure 4.15) shows a general increasing trend from the earlier stages to the later stages. However, for the Northern Great Plain and the Upper Midwest, the daily minimum temperatures during Stage 8 are higher than those during Stage 9. Also, for the two considerable damage occurring regions, the Southern Great Plains and the Southeast, the daily minimum temperatures during Stage 9 increase almost twice from Stage 8, indicating a significant temperature change. Combined with Figure 4.14, we conclude that nearly

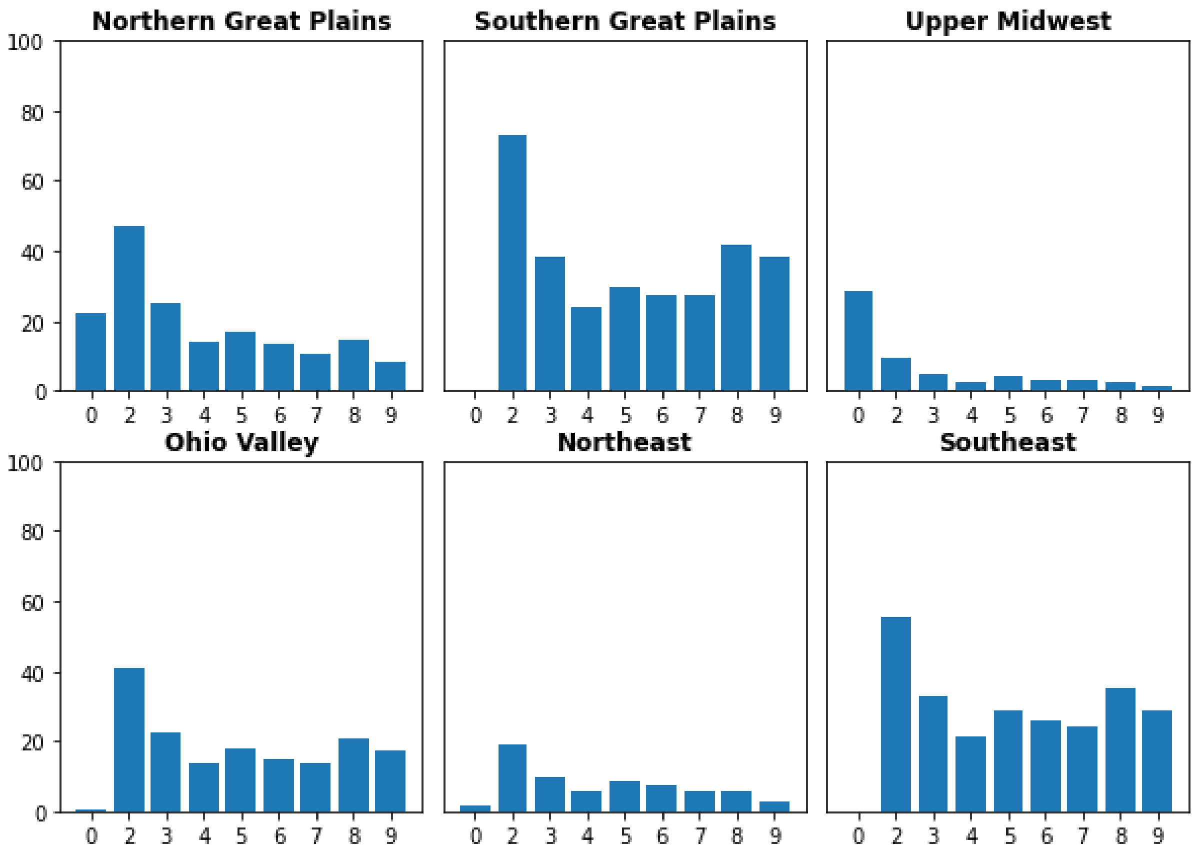

Figure 4.13: *The sum of damage days at each growth stage in six subregions from 1981 to 2018.*

no significant damage occurs during Stage 9 as the temperature increases.

The spatial and time-averaged daily minimum temperature on damage days only (Figure 4.16) reveal that the daily minimum temperatures during damage days of the Upper Midwest and the Northeast are generally higher than in other regions, consistent with the conclusion that these two regions have the least damage. At Stage 2, the phenological stage when the most severe damage occurs, the Upper Midwest and the Northeast show almost 1 Degree Celsius higher than the Southern Great Plain, where the most severe damage occurs. The daily minimum temperatures during damage days at Stage 2 for the two least freeze-damaged regions are above -6 °C, while those for other regions are all below -6 °C. There are sharp daily minimum temperature increases during damage days from Stage 2 to Stage 3 and from Stage 4 to Stage 5.

Finally, the spatial and time-averaged damage-occurring dates for each growth stage (Figure

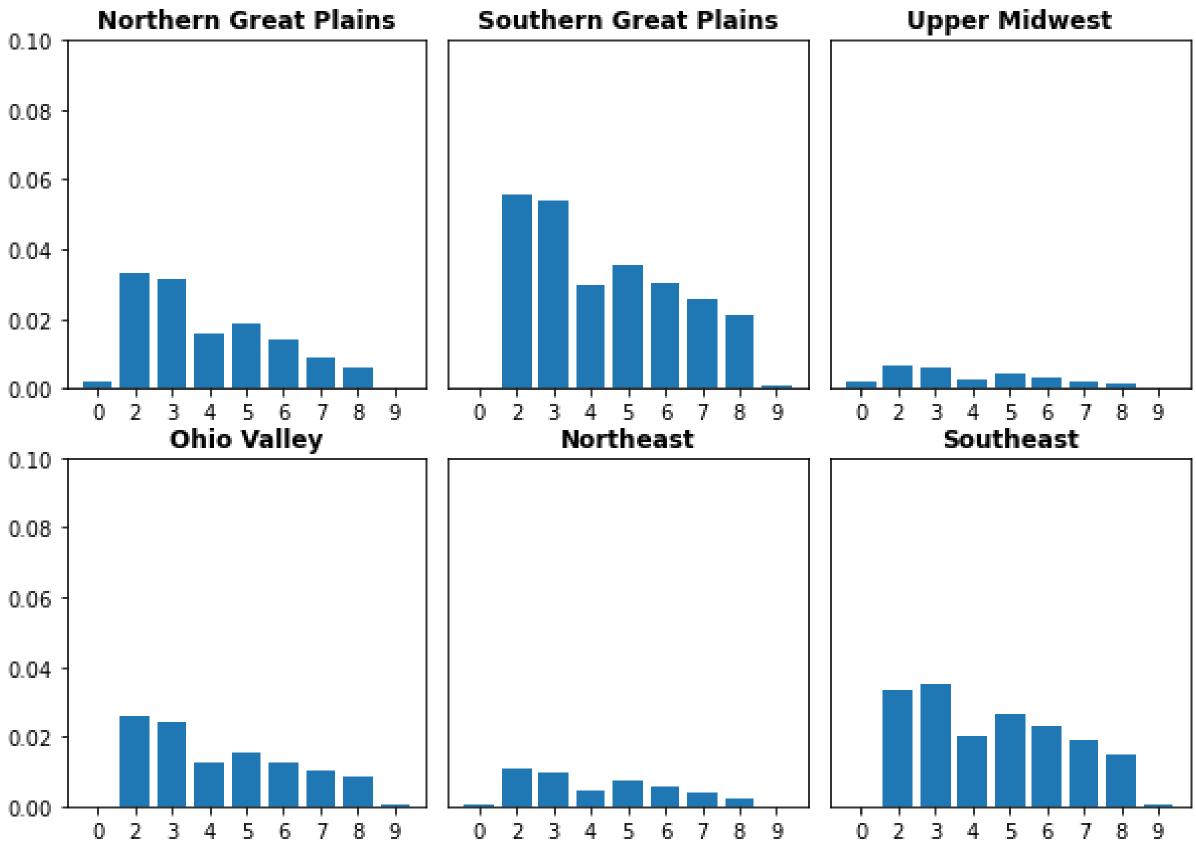

Figure 4.14: *The average of damage values at each growth stage in six subregions from 1981 to 2018.*

4.17) reveal a large increase from an average Julian date of 20 for Stage 0 to an average Julian date of more than 60 for Stage 2. Then from Stage 2 to Stage 9, the dates increase gradually. The two most severe damage-occurring regions, the Southern Great Plains and the Southeast show much earlier damage-occurring dates compared to other regions.

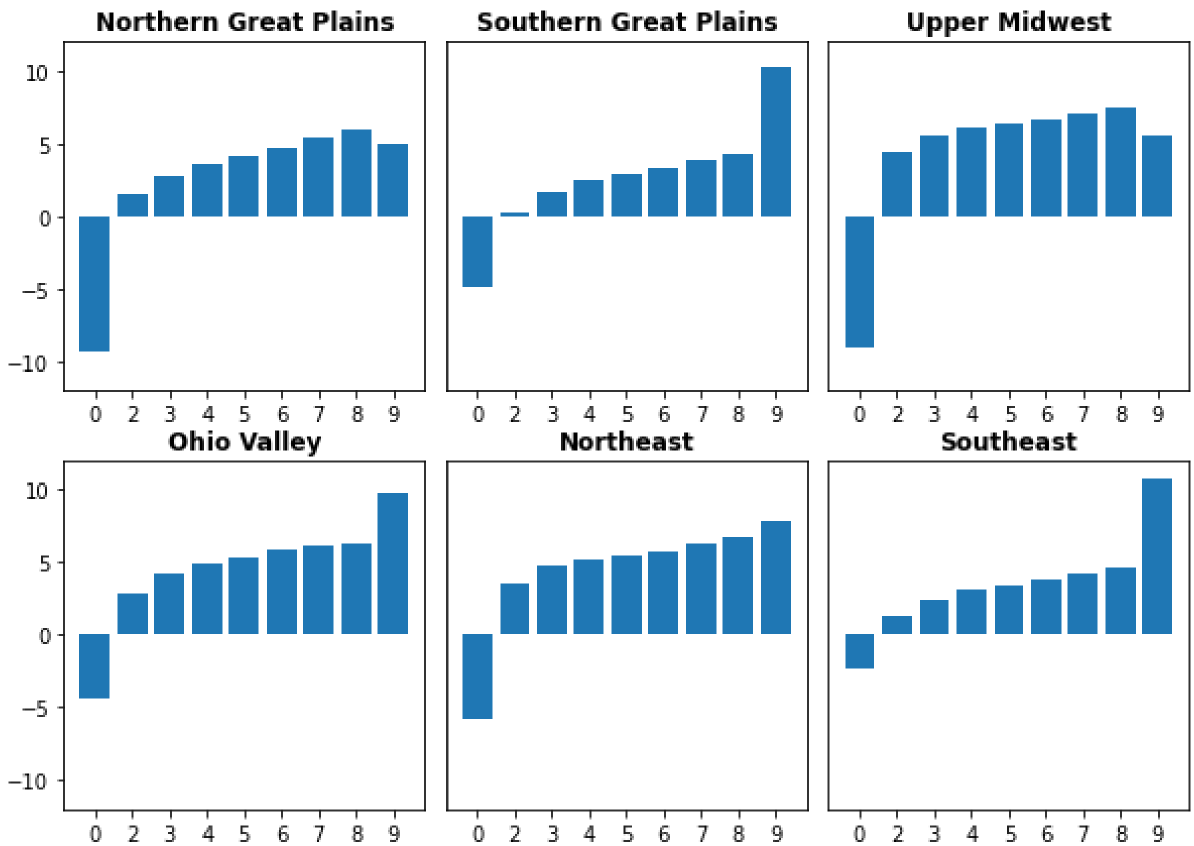

Figure 4.15: *The average daily minimum temperature at each growth stage in six subregions from 1981 to 2018.*

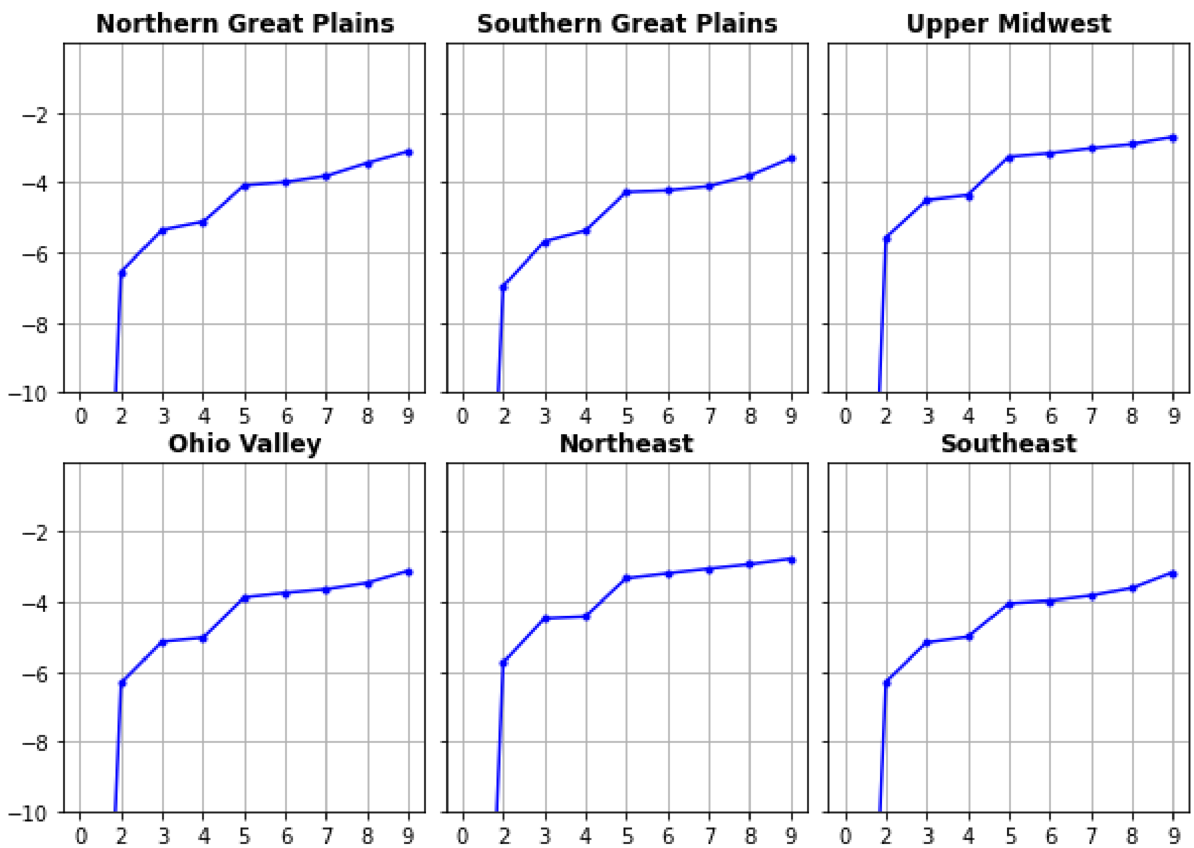

Figure 4.16: *The average daily minimum temperature during damage days at each growth stage in six subregions from 1981 to 2018.*

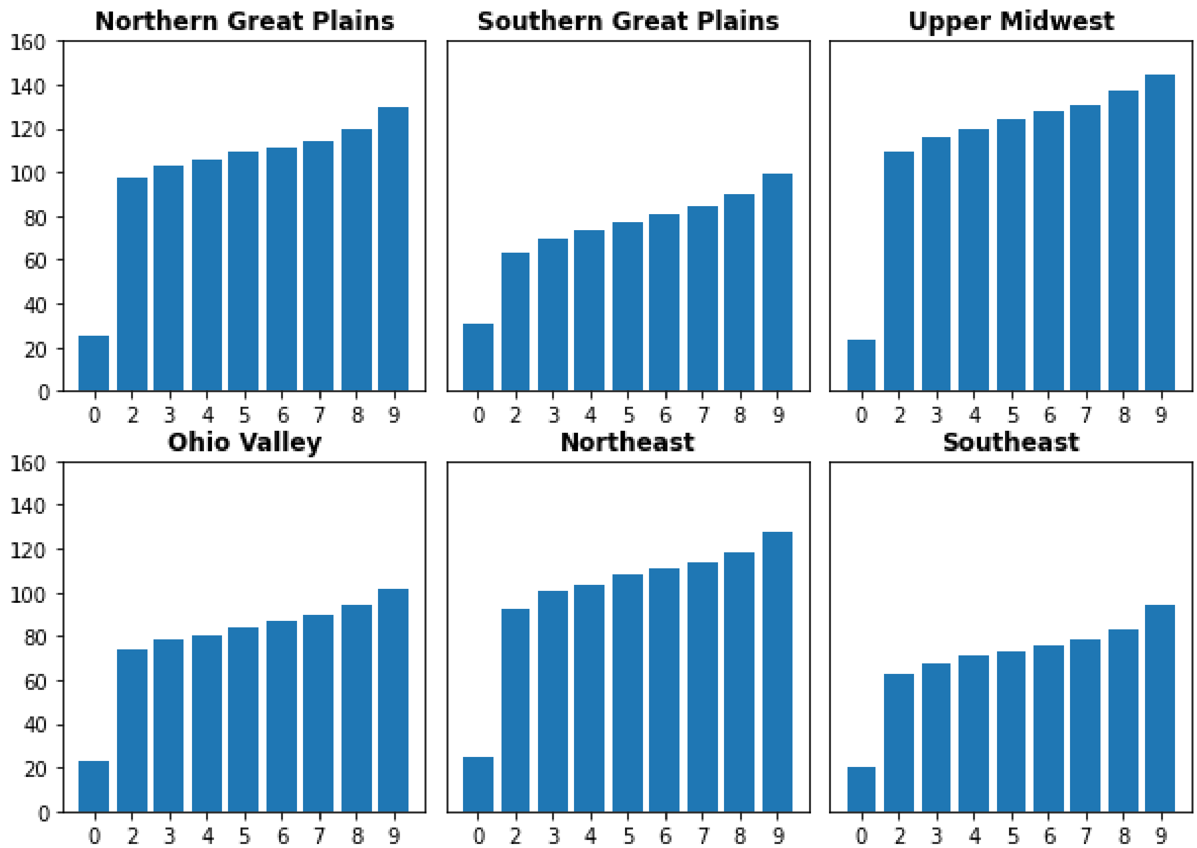

Figure 4.17: *The average damage-occurring dates at each growth stage in six subregions from 1981 to 2018.*

4.4 Summary

This study investigates the historical impacts of springtime freeze event damage on crops in the central and midwestern US from 1981 to 2018 using crop simulation models with input datasets from PRISM. In particular, the variables examined in this study include the first green dates, bloom dates, poor pollination days, and the bud survival chance of the year for apples. Also, damage days of the year, daily minimum temperature, and damage occurring dates for each phenology growing stage are included to explore the impacts of false springs. The major findings are as follows.

1) Trend analysis for the onset dates of springs reveals a tendency towards earlier first green dates and bloom dates during our study period, indicating earlier springs in recent decades. This earlier shift of springs could result in more frequent false spring occurrences. Also, the onset of spring dates is more variable in the warmer southern regions than the colder northern regions.

2) Higher bud survival chances and fewer poor pollination days with lower variation around the Great Lakes Region than other regions in the Midwestern and Central US are shown in our results, indicating the favorable growing conditions for apples in these areas. This result is consistent with the fewer freeze damage risks in the Upper Midwest and the Northeast with lower variability compared to the Southern Great Plains and the Southeast.

3) Damage is generally occurring on earlier and warmer days, which could be a consequence of more frequent 'False Spring' occurrences. As a result of the global warming trend, earlier springs and increasing temperatures lead to damage occurring earlier with warmer temperatures.

4) We also observe damage days show an abrupt high value in 2012 in the Upper Midwest and the Northeast, which is consistent with observed severe damage during then. This abrupt change is not observed in other defined regions.

5) There are more damage days in stage 2 with higher severity since apples are vulnerable during the early growing stages. This information suggests that if apples begin their growing seasons earlier, they could suffer from significant damage due to subsequent freeze events.

6) The Midwest and the Northeast are two regions favorable for apple planting since these two regions show fewer damage days with lower damage intensity and also higher daily minimum

temperature during damage occurring days, while the Southern Great Plains and the Southeast are in the opposite.

This study simulates the historical yields of apples to show the impacts of false springs with some limitations. First, the crop simulation model only takes inputs of temperatures and precipitation, which might be problematic since crop growth could be related to more complicated factors. Second, how this simulation model represents the observations needs to be evaluated. Some observational records could be used to testify the model's behavior. Also, if this model is reliable, some future projections could be made to provide some valuable predictions for apple planters. Despite the limitations, this study provides helpful information for apple planters about the damage occurring earlier with warmer temperatures due to false springs.

CHAPTER 5

CONCLUSION

This research focuses on the climatology of springtime freezes and their impacts on agriculture, especially for the central and eastern United States. Chapter 2 assesses ERA5 reanalysis and PRISM analysis datasets by comparing them to station observations at selected locations. Chapter 3 investigates the frequency, severity, and potential causes of springtime freeze event occurrences. The Impacts of false springs and subsequent freeze events are examined in Chapter 4.

In Chapter 2, ERA5 and PRISM reanalysis products are compared to station observations. The conclusion is that the PRISM dataset, demonstrating a better agreement of temperatures with observations, could be used as a proxy to represent observed freeze events. Root mean squared errors (RMSDs) and bias are calculated to evaluate how the gridded datasets agree with the station observations. Gridded reanalysis datasets tend to reduce the observed daily cycles. At a daily level, ERA5 underestimates daily maximum temperature while overestimates daily minimum temperature, resulting in reduced daily cycles. In contrast, PRISM tends to overestimate both daily minimum and maximum temperature. Since daily maximum temperatures are measured in more mixed conditions, the observations should agree with the area-averaged gridded datasets to a larger extent than daily minimum temperatures. Both gridded datasets show better results for daily maximum temperature than daily minimum temperature, as shown in the lower amplitudes of perturbations of the time series and the smaller values of RMSDs of daily maximum temperature. Lake effects are shown by large RMSDs and Bias and also large perturbations of time series of near-lake stations for both gridded datasets. PRISM shows excellent ability in capturing different types of freeze events for both wintertime and springtime. Generally, freeze events are caught in a better way during wintertime than other seasons.

In Chapter 3, we investigate the frequency, severity, as well as climate background of springtime freeze event occurrences. Trend analysis and EOF analysis are conducted to reveal the characteristics of freezing days during the springtime. Our results indicate a general decreasing trend in the frequency of springtime freeze events. Considerably damage years of 2007 and 2012 show a low frequency of freeze events, indicating the profound impacts of false springs that expose the earlier developed crops to the subsequent freeze events. By dividing our study region into six subregions, we observe significant downward trends for the total freezing days during the springtime in the Ohio Valley, which extends the findings in Easterling et al. (2002) from the period1948-1999 into 1981-2019. By relating the area-averaged freezing days to some teleconnection indices, we conclude that the positive phase of NAO is usually associated with less freezing risk in March across the study region. EOF analysis of freezing days in March shows a relatively larger variation in the Ohio Valley, and the first EOF time series shows substantial interannual variability. When a positive phase of NAO shows in March and December of the previous year, the in-phase fluctuation across our study region with a higher intensity over the Ohio Valley tends to occur in March. And this pattern is usually associated with the geopotential height lower than average at the upper level and higher than average at the surface and a thickness shallower than average.

Chapter 4 investigates the historical impacts of springtime freeze event damage on crops in the central and midwestern US from 1981 to 2018 using crop simulation models with input datasets from PRISM. Our results reveal that the onset of springs is shifted earlier in recent decades with the indicators of first green dates and bloom dates that are more variable in the warmer southern regions than the colder northern regions during our study period. This earlier shift of springs is associated with more frequent false spring occurrences. Results also reveal that the Upper Midwest and the Northeast are less vulnerable to freeze damage for apple planting than the Southern Great Plains and the Southeast indicated by higher bud survival chances, and fewer freeze damage risks with lower variability. Damage is generally occurring on earlier and warmer days as a consequence of more frequent 'False Spring' occurrences. There are more damage days in Stage 2 with higher severity since apple is vulnerable during the early growing stages.

There are some limitations in this research, as discussed in more detail in the individual chapters. Wind speed and direction that have profound impacts on freeze event formation are not evaluated in Chapter 2. Also, precipitation data needs to be assessed between the gridded datasets and stational observations. In Chapter 3, limited by our study region, our subregions could not exactly represent the regions defined in Karl and Knight (1998). Specifically, the Northeast, the Southeast, and the Southern Great Plains are only parts of the regions defined in Karl and Knight (1998), leading to a misrepresentation of the conclusions of freeze events over these regions. In addition, specific weather conditions need to be investigated to understand the causes of freeze event formation. In Chapter 4, the crop yield simulation model should be not only evaluated but also improved. Also, some future trends of damage risks could be projected to provide guidelines for fruit growers.

In conclusion, the most valuable information that could provide fruit growers is that associated with global warming, fewer springtime freeze events but more frequent false spring events occur in recent decades. The damage to crops occurs on earlier and warmer days in recent decades.

APPENDIX

A.1 Impacts of Soil Moisture on Springtime Freeze Events

The thermal conductivity of the soil depends on its mineralogical composition, texture, as well as its water content (DeVries et al., 1986). Since soil moisture change has a profound effect on soil temperature, soil reflectance, and soil heat storage (AL-KAYSSl et al., 1990), it is questionable how the soil moisture change affects the apparent temperature, which is closely related to the heat balance between the ground and above atmosphere. When soils hold more water, the ability to store and transfer heat during the night is enhanced. The results from AL-KAYSSl et al. (1990) reveal that an increase in soil moisture content decreases the soil temperature difference between day-time and night-time. And this decreased temperature change could protect plant root systems from sharp and sudden changes in soil temperature (AL-KAYSSl et al., 1990). Finally, plant growth rate and yield might increase due to the modification of plant climate at higher soil moisture content. This valuable information could provide crop growers with instructions on when and how to protect their crops confronting a predicted sudden and extreme freeze event.

This study investigates the impacts of increasing soil moisture content on 2m air temperature change. With the application of a deterministic regional-scale numerical forecast model, this study aims to investigate the extent of how the soil moisture change affects the daily minimum temperature change in the Great Lakes Region.

We use NAM (the North American Mesoscale Forecast System) analyses to initiate our model configuration. NAM is one of the major weather models run by the National Centers for Environmental Prediction (NCEP) for producing dozens of weather variables, from temperature and precipitation to turbulent kinetic energy. The NAM generates multiple grids (or domains) of weather forecasts over the North American continent at various horizontal resolutions (https://www.ncdc.noaa.gov/data-access/model-data/model-datasets/north-american-mesoscale-forecast-system-nam). We take input data from NAM analyses and then use WRF (Weather Research and Forecasting) model to forecast how the temperature is sensitive to soil moisture change.

Specifically, we conduct WRF sensitivity studies to investigate the sensitivity to changing vertical resolution and changing initial soil moisture settings. We observe two noticeable freeze events on the nights of May 8th and May 12th. Therefore, based on these two events, we conduct a series of studies. Before we modify any parameters, we first compare the WRF model outputs to observations to know the representation of the WRF outputs. As shown in Figure A.1.1, the WRF outputs measure soil moisture values at different layers compared to the observational data at Williamsburg. The results reveal that the WRF simulations consistently overestimate the moisture values at the upper soil levels and underestimate them at the bottom layer for both these two freeze events (May 8th and May 12th) at this location. Then we compare other weather variables at three stations, East Lansing, Gaylord, and Williamsburg. The results reveal that for both two freeze events, WRF outputs capture the daily cycles well for all three variables, air temperature, relative humidity, and wind speed, and the difference values vary by location. We compare WRF air temperatures at 2m to observational air temperatures at 1.5m (Figure A.1.2). The differences range from -5 degrees to 5 degrees. Generally, WRF outputs underestimate maximum air temperatures in the afternoon and overestimate minimum air temperatures during the night. This bias is just what we expect since WRF outputs are area-averaged results, which should reduce the daily cycle amplitudes. It is noteworthy that in the graph, we note the time from WRF outputs, which is the standard UTC that is four hours earlier than the local eastern time. WRF does not show excellent behavior in representing the relative humidity since relative humidity is sensitive to temperature values. For wind speed comparison, we also show that WRF outputs tend to overestimate the minimum velocity during the night while tend to underestimate the maximum velocity in the afternoon. Also, it is noteworthy that we are comparing WRF wind speed at 10m to observational wind speed at 3m.

Since PRISM has been evaluated in Chapter 2, we choose to use PRISM as a proxy to represent the observational daily minimum temperature values to assess WRF outputs' quality. As shown in Figure A.1.3, WRF captures the spatial variation on May 8th. We use a linear model, OLS (ordinary least squares) regression model, to quantitatively investigate how the WRF outputs fit the observation values from PRISM. Our results reveal that WRF outputs represent 68.3%, 27.1%, 31.8%, and 1.1%, respectively, for May 8th, May 9th, May 12th, and May 13th, as shown in the

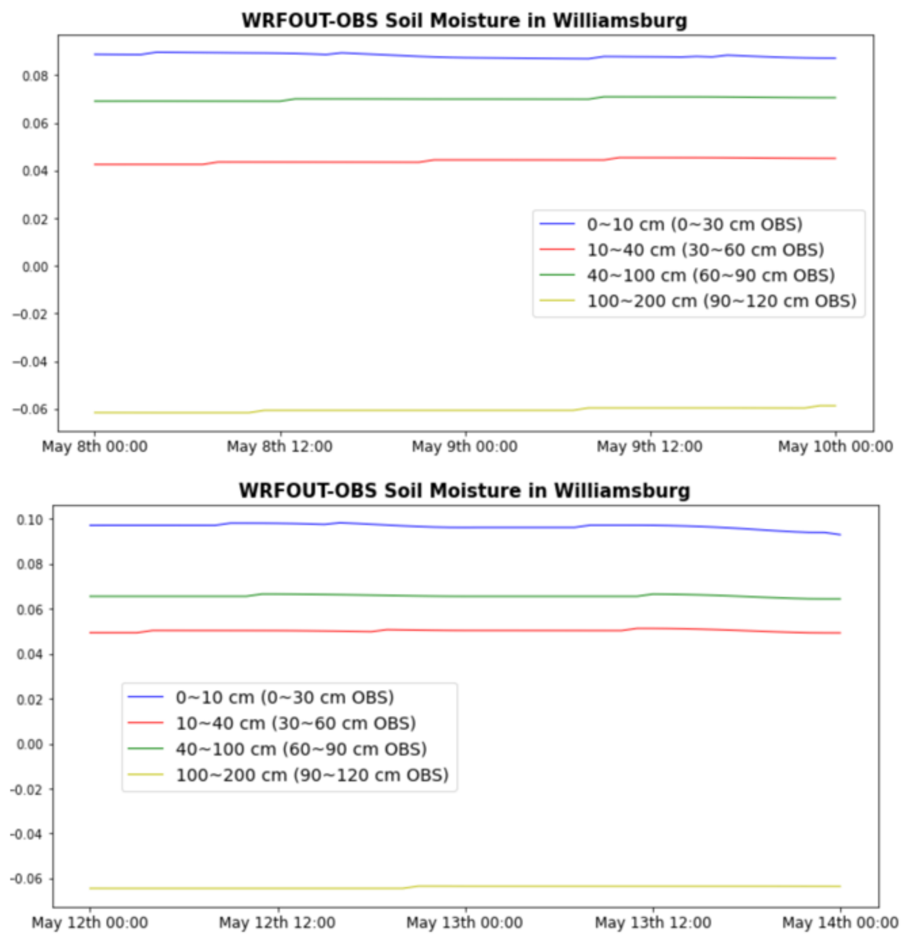

Figure A.1.1: *Differences of soil moisture between WRF outputs and observations at Williamsburg.*

	East Lansing	Gaylord	Williamsburg
30 levels	2.172	2.1566	1.898
38 levels	2.3653	2.0065	1.9866
40 levels	2.3213	2.068	1.3364
45 levels	2.3725	2.0733	1.3687

Table A.1.1: *RMSDs of air temperature between WRF and observations at three locations for 48 hours from May12th to May13th with different vertical resolutions.*

R squared values from the OLS model. Except for May 13th, WRF generally captures the spatial characteristics over the Great Lakes Region.

Then we try to understand how the higher vertical resolution affects the representation of WRF outputs. By modifying the initial vertical layer setting, we run WRF with 30 levels, 38 levels,

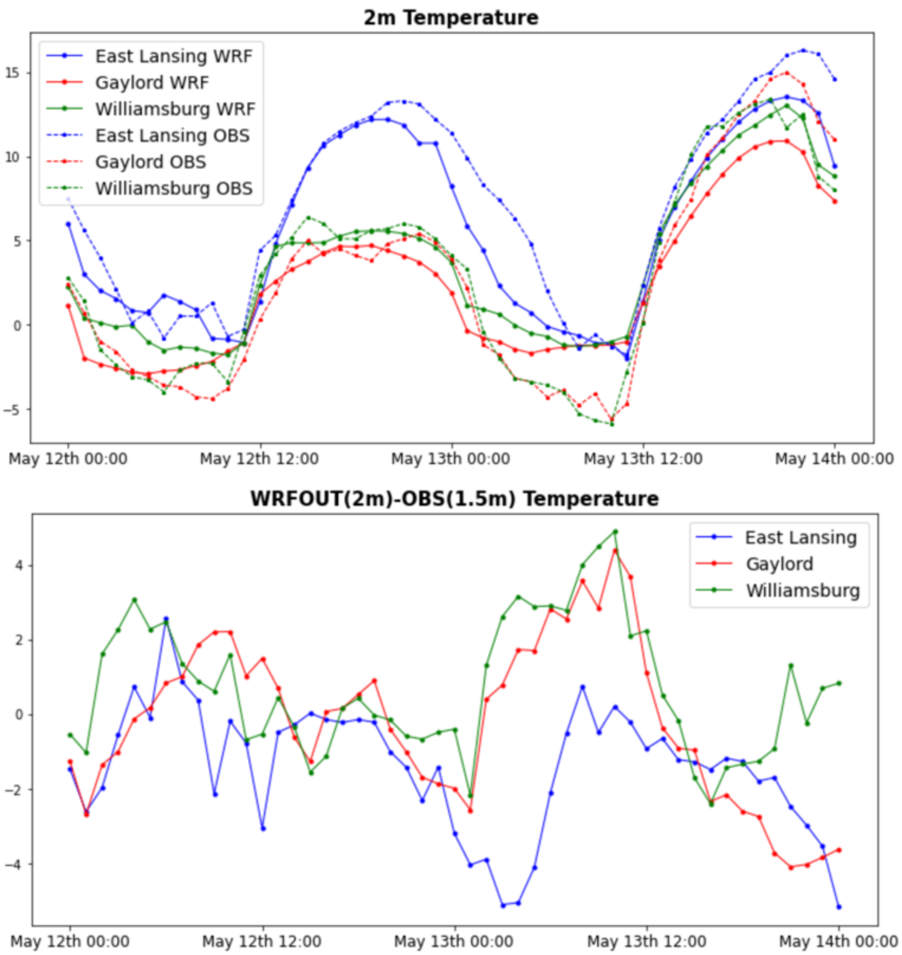

Figure A.1.2: *Differences of air temperature between WRF outputs and observations at three locations.*

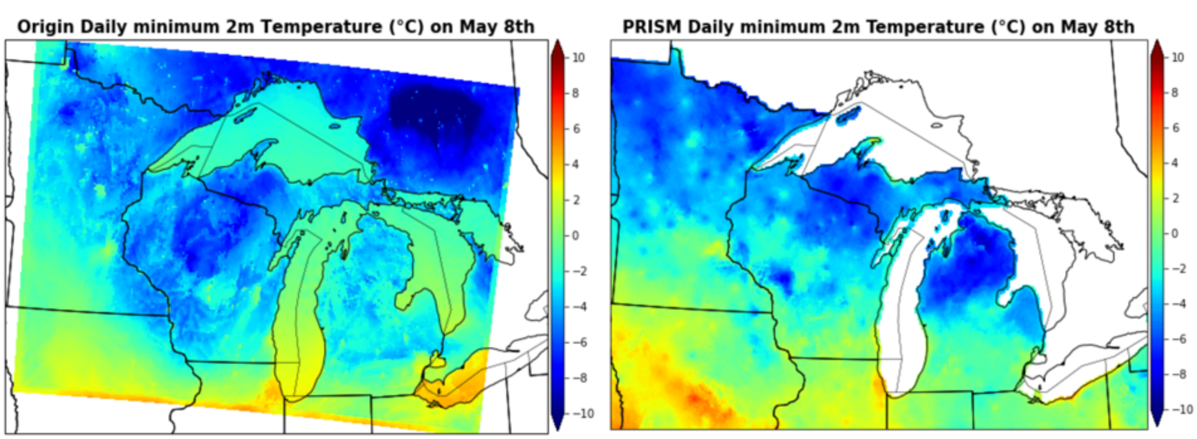

Figure A.1.3: *Comparison of daily minimum air temperature between WRF and PRISM on May 8th.*

	East Lansing	Gaylord	Williamsburg
30 levels	1.6087	1.6753	1.5199
38 levels	1.5629	1.6919	1.8894
40 levels	1.267	1.1656	1.6803
45 levels	1.3944	1.3109	1.8251

Table A.1.2: *RMSDs of wind speed between WRF and observations at three locations for 48 hours from May12th to May13th with different vertical resolutions.*

40 levels, and 45 levels. We increase the vertical resolution at lower levels. We do not observe a general improvement in the comparison between model outputs and observations at the three selected locations for air temperature and wind speed for 48 hours from May 12th to May 13th. Varying by location and variables, increasing the vertical resolved resolution improves temperature representation in Gaylord and Williamsburg and wind speed representation in East Lansing and Gaylord (Table A.1.1 and Table A.1.2). It is interesting to show that when increasing the layers from 40 to 45, usually the RMSDs are not becoming smaller; instead, larger RMSDs are observed in our simulations. From the results of the OLS model, we also reveal that increasing the vertical resolution does not necessarily improve the representation of the spatial characteristics of WRF.

Next, we examine how the air temperature is affected by an increase in soil moisture. We first run the WRF simulation without any changes in the initial input data. Then we get the original daily minimum air temperature for four days, as shown in the left column of Figure A.1.4. Then we change the soil moisture values in the input data by multiplying the original values by 1.05, increasing the initial soil moisture by 5 percent. The results are just as we expect; the daily minimum air temperatures on four different days are all increased less than 1 degree. However, it is not always physically reasonable to increase the soil moisture by multiplying a factor. As shown in Figure A.1.5, the maximum and minimum soil moisture values actually depend on the soil categories. For example, sandy loam is the type of soil that shows the best ability to store water. So we also change the soil moisture values to the maximum and minimum values based on the soil types (Figure A.1.6 and Figure A.1.7). The results reveal that decreasing soil moisture to the minimum values considerably decreases daily minimum temperatures with a maximum amplitude

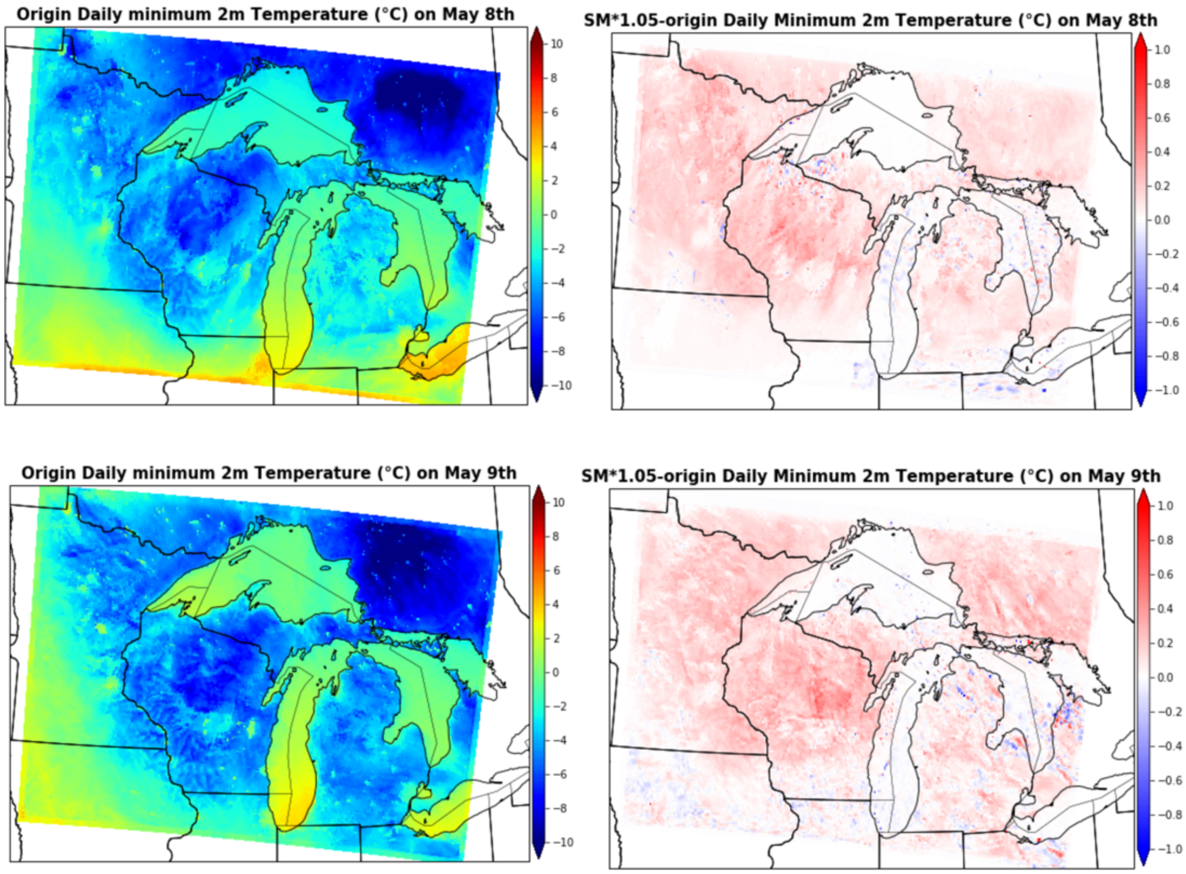

Figure A.1.4: *Daily minimum temperature changes in response to increased soil moisture by a factor of 1.05 on May 8th and May 9th.*

of 8 degrees, which is larger than the magnitude of changing soil moisture to maximum values.

In conclusion, this case study provides valuable information for crop growers that irrigation before predicted freeze events could help to protect crops from severe damage due to the positive response of temperature to increased soil moisture.

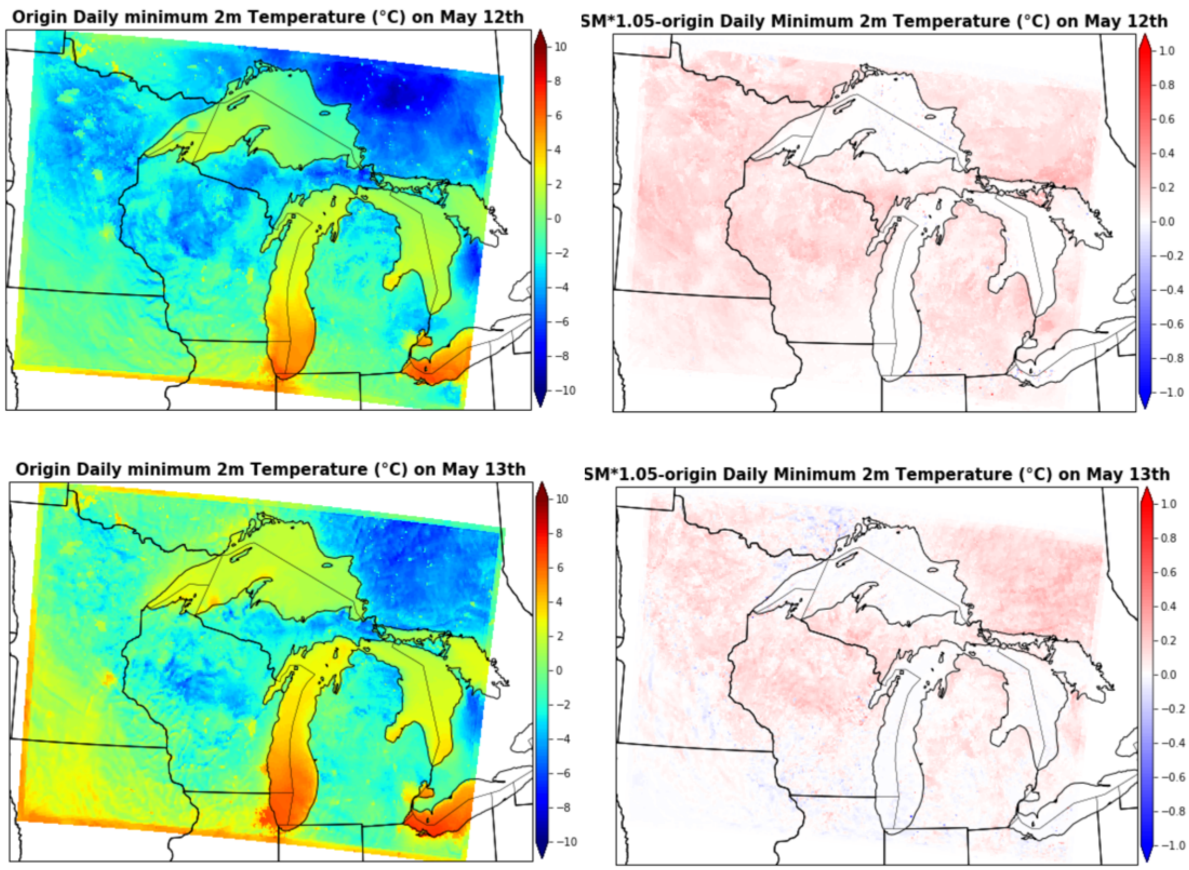

Figure A.1.5: *Daily minimum temperature changes in response to increased soil moisture by a factor of 1.05 on May 12th and May 13th.*

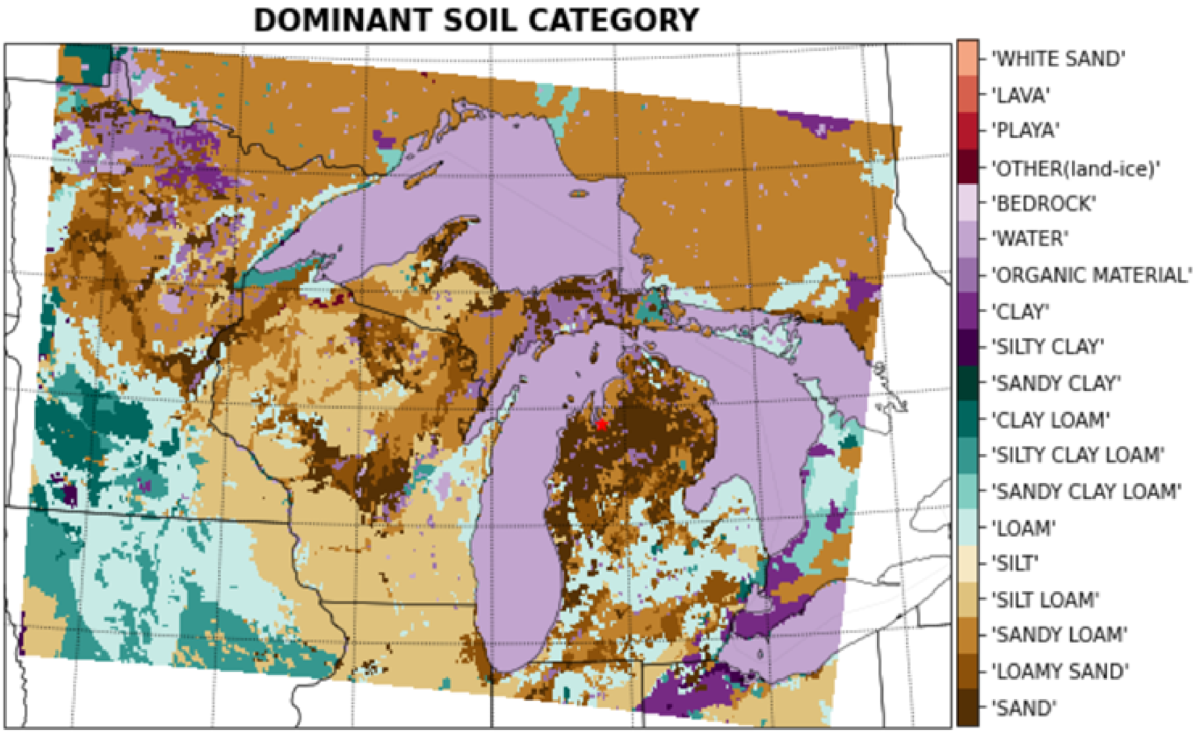

Figure A.1.6: *Major soil categories in our study region.*

May 8th

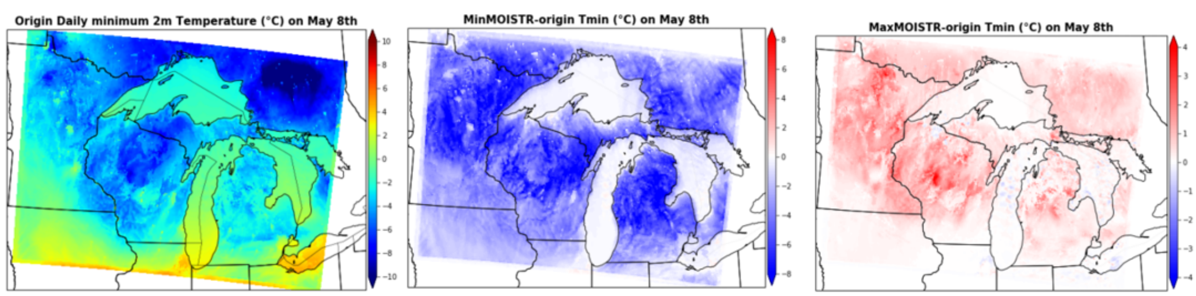

May 9th

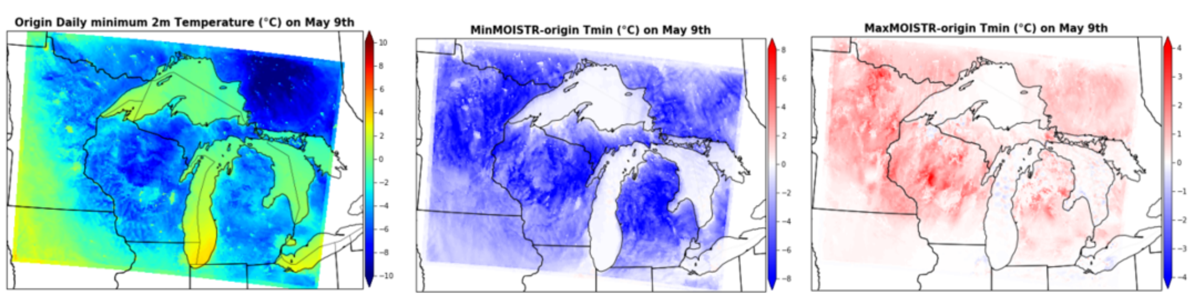

Figure A.1.7: *Soil moisture change based on soil types on May 8th and May 9th.*

May 12th

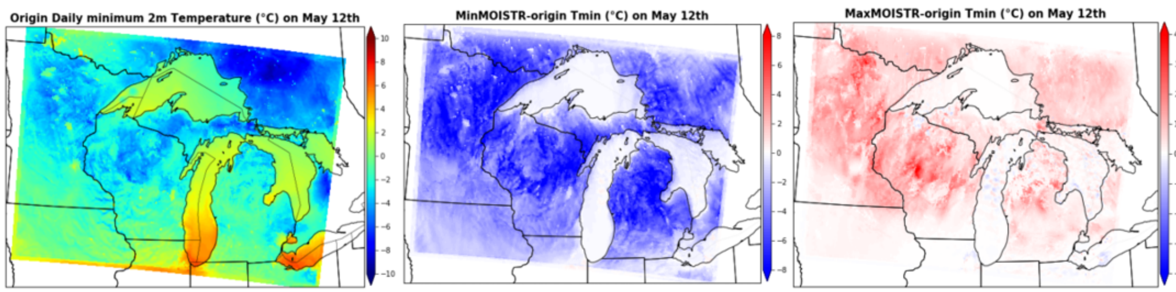

May 13th

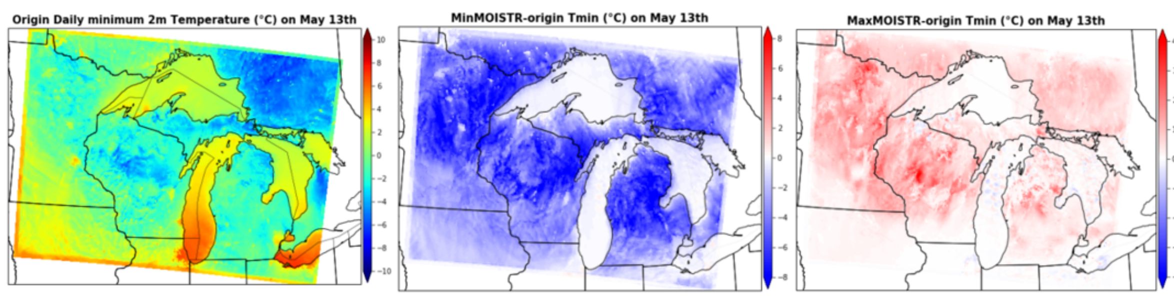

Figure A.1.8: *Soil moisture change based on soil types on May 12th and May 13th.*

BIBLIOGRAPHY

BIBLIOGRAPHY

Andresen, J.A. and W.J. Baule, 2018. Temperate Fruit Trees and Grapes. In: Agronomy Monographs, 60: Agroclimatology: Linking Agriculture to Climate. Eds.: J. Hatfield, M. Sivakumar, J. Prueger,. ASA, CSSA, and SSSA, Madison, WI. doi:10.2134/agronmonogr60.2014.0035.

"About Us - MSU Enviroweather - Weather for IPM Decisions." Accessed March 6, 2020. https://enviroweather.msu.edu/about.php.

Allstadt, Andrew J, Stephen J Vavrus, Patricia J Heglund, Anna M Pidgeon, Wayne E Thogmartin, and Volker C Radeloff. "Spring Plant Phenology and False Springs in the Conterminous US during the 21st Century." Environmental Research Letters 10, no. 10 (October 1, 2015): 104008. https://doi.org/10.1088/1748-9326/10/10/104008.

AL-KAYSSl, A W, A A Al-Karaghouli, and A M Hasson. "Influence of Soil Moisture Content on Soil Temperature and Heat Storage under Greenhouse Conditions," n.d., 12.

Augspurger, Carol K. "Reconstructing Patterns of Temperature, Phenology, and Frost Damage over 124 Years: Spring Damage Risk Is Increasing." Ecology 94, no. 1 (2013): 41–50. https://doi.org/10.1890/12-0200.1.

"Automated Surface Observing System (ASOS) | National Centers for Environmental Information (NCEI) Formerly Known as National Climatic Data Center (NCDC)." Accessed April 5, 2021. https://www.ncdc.noaa.gov/data-access/land-based-station-data/land-based-datasets/automated-surface-observing-system-asos.

———."Spring 2007 Warmth and Frost: Phenology, Damage and Refoliation in a Temperate Deciduous Forest." Functional Ecology 23, no. 6 (2009): 1031–39. https://doi.org/10.1111/j.1365-2435.2009.01587.x.

Ault, T. R., G. M. Henebry, K. M. de Beurs, M. D. Schwartz, J. L. Betancourt, and D. Moore. "The False Spring of 2012, Earliest in North American Record." Eos, Transactions American Geophysical Union 94, no. 20 (2013): 181–82. https://doi.org/10.1002/2013EO200001.

Ballard, J., E. Proebsting, and R. Tukey, 1998. Critical Spring Temperatures For Tree Fruit Bud Development Stages. Washington State University Extension Bulletin EB1128, Washington State University, Pullman, WA.

Bosilovich, Michael G., John Kennedy, Dick Dee, Rob Allan, and Alan O'Neill. "On the Reprocessing and Reanalysis of Observations for Climate." In Climate Science for Serving Society: Research, Modeling and Prediction Priorities, edited by Ghassem R. Asrar and James W. Hurrell, 51–71. Dordrecht: Springer Netherlands, 2013. https://doi.org/10.1007/978-94-007-6692-1-3.

Dennis FG and Howell GS, 1974. Cold hardiness of tart cherry bark and flower buds. Res. Rep. 220, Michigan State University, Ag. Exp. Stn., East Lansing, MI, USA.

Menzel, Annette. “Trends in Phenological Phases in Europe between 1951 and 1996.” International Journal of Biometeorology 44, no. 2 (August 1, 2000): 76–81. https://doi.org/10.1007/s004840000054.

Muñoz Sabater, J., (2019): ERA5-Land hourly data from 1981 to present. Copernicus Climate Change Service (C3S) Climate Data Store (CDS).

Cannon, D. J., D. J. Brayshaw, J. Methven, P. J. Coker, and D. Lenaghan. “Using Reanalysis Data to Quantify Extreme Wind Power Generation Statistics: A 33 Year Case Study in Great Britain.” Renewable Energy 75 (March 1, 2015): 767–78. https://doi.org/10.1016/j.renene.2014.10.024.

Cayan, Daniel R., Susan A. Kammerdiener, Michael D. Dettinger, Joseph M. Caprio, and David H. Peterson. “Changes in the Onset of Spring in the Western United States.” Bulletin of the American Meteorological Society 82, no. 3 (March 1, 2001): 399–416. https://doi.org/10.1175/1520-0477(2001)082<0399:CITOOS>2.3.CO;2.

Chai, T., and R. R. Draxler. “Root Mean Square Error (RMSD) or Mean Absolute Error (MAE)? – Arguments against Avoiding RMSD in the Literature.” Geoscientific Model Development 7, no. 3 (June 30, 2014): 1247–50. https://doi.org/10.5194/gmd-7-1247-2014.

Charrier, Guillaume, Jérôme Ngao, Marc Saudreau, and Thierry Améglio. “Effects of Environmental Factors and Management Practices on Microclimate, Winter Physiology, and Frost Resistance in Trees.” Frontiers in Plant Science 6 (2015). https://doi.org/10.3389/fpls.2015.00259.

Daly, Christopher. “Guidelines for Assessing the Suitability of Spatial Climate Data Sets.” International Journal of Climatology 26, no. 6 (2006): 707–21. https://doi.org/10.1002/joc.1322.

Daly, Christopher, Michael Halbleib, Joseph I. Smith, Wayne P. Gibson, Matthew K. Doggett, George H. Taylor, Jan Curtis, and Phillip P. Pasteris. “Physiographically Sensitive Mapping of Climatological Temperature and Precipitation across the Conterminous United States.” International Journal of Climatology 28, no. 15 (2008): 2031–64. https://doi.org/10.1002/joc.1688.

Dee, D. P., S. M. Uppala, A. J. Simmons, P. Berrisford, P. Poli, S. Kobayashi, U. Andrae, et al. “The ERA-Interim Reanalysis: Configuration and Performance of the Data Assimilation System.” Quarterly Journal of the Royal Meteorological Society 137, no. 656 (2011): 553–97. https://doi.org/10.1002/qj.828.

DeGaetano, Arthur T. “Recent Trends in Maximum and Minimum Temperature Threshold Exceedences in the Northeastern United States.” Journal of Climate 9, no. 7 (July 1, 1996): 1646–60. https://doi.org/10.1175/1520-0442(1996)009<1646:RTIMAM>2.0.CO;2.

DeVries D.A., Thermal properties of soils. Wijk W.R. (Ed.), Physics of Plant Environment, North-Holland Publishing Co., Amsterdam (1963), pp. 210-235

Dulière, Valérie, Yongxin Zhang, and Eric P. Salathé. "Extreme Precipitation and Temperature over the U.S. Pacific Northwest: A Comparison between Observations, Reanalysis Data, and Regional Models." Journal of Climate 24, no. 7 (January 7, 2011): 1950–64. https://doi.org/10.1175/-2010JCLI3224.1.

Easterling, David R. "RECENT CHANGES IN FROST DAYS AND THE FROST-FREE SEASON IN THE UNITED STATES," n.d., 6.

Essou, Gilles R. C., François Brissette, and Philippe Lucas-Picher. "The Use of Reanalyses and Gridded Observations as Weather Input Data for a Hydrological Model: Comparison of Performances of Simulated River Flows Based on the Density of Weather Stations." Journal of Hydrometeorology 18, no. 2 (February 1, 2017): 497–513. https://doi.org/10.1175/JHM-D-16-0088.1.

Fitchett, Jennifer M., Stefan W. Grab, Dave I. Thompson, and Gholamreza Roshan. "Increasing Frost Risk Associated with Advanced Citrus Flowering Dates in Kerman and Shiraz, Iran: 1960–2010." International Journal of Biometeorology 58, no. 8 (October 2014): 1811–15. https://doi.org/10.1007/s00484-013-0778-0.

MSU Extension. "Freeze Damage Depends on Tree Fruit Stage of Development." Accessed March 17, 2021. https://www.canr.msu.edu/news/freeze_damage_depends_on_tree_fruit_stage_of-_development.

"Freeze Protection Publication." Accessed February 11, 2020. https://ssl.acesag.auburn.edu/-department/peaches/freeze.html.

Gleixner, Stephanie, Teferi Demissie, and Gulilat Tefera Diro. "Did ERA5 Improve Temperature and Precipitation Reanalysis over East Africa?" Atmosphere 11, no. 9 (September 17, 2020): 996. https://doi.org/10.3390/atmos11090996.

Gu, Lianhong, Paul J. Hanson, W. Mac Post, Dale P. Kaiser, Bai Yang, Ramakrishna Nemani, Stephen G. Pallardy, and Tilden Meyers. "The 2007 Eastern US Spring Freeze: Increased Cold Damage in a Warming World?" BioScience 58, no. 3 (March 1, 2008): 253–62. https://doi.org/10.1641/B580311.

Hatfield, Jerry, and Maria Janowiak. "USDA Midwest and Northern Forests Regional Climate Hub: Assessment of Climate Change Vulnerability and Adaptation and Mitigation Strategies," n.d., 55.

Hufkens, Koen, Mark A. Friedl, Trevor F. Keenan, Oliver Sonnentag, Amey Bailey, John O'Keefe, and Andrew D. Richardson. "Ecological Impacts of a Widespread Frost Event Following Early Spring Leaf-Out." Global Change Biology 18, no. 7 (2012): 2365–77. https://doi.org/10.1111-

/j.1365-2486.2012.02712.x.

Integrated Pest Management. “Enviroweather Weather Data and Pest Modeling.” Accessed April 5, 2021. https://www.canr.msu.edu/resources/enviroweather_weather_data_and_pest_modeling.

Janowiak, Maria K, Daniel N Dostie, Michael A Wilson, Michael J Kucera, R Howard Skinner, Jerry L Hatfield, David Hollinger, and Christopher W Swanston. “ADAPTATION RESOURCES FOR AGRICULTURE,” n.d., 72.

JJ. “MAE and RMSD — Which Metric Is Better?” Medium, March 23, 2016. https://medium.com-/human-in-a-machine-world/mae-and-RMSD-which-metric-is-better-e60ac3bde13d.

Karl, Thomas R., and Richard W. Knight. “Secular Trends of Precipitation Amount, Frequency, and Intensity in the United States.” Bulletin of the American Meteorological Society 79, no. 2 (February 1, 1998): 231–42. https://doi.org/10.1175/1520-0477(1998)079<0231:STOPAF>2.0.CO;2.

Katz, Richard W., and Barbara G. Brown. “Extreme Events in a Changing Climate: Variability Is More Important than Averages.” Climatic Change 21, no. 3 (July 1992): 289–302. https://doi.org/10.1007/BF00139728.

Kidston, J., D. M. W. Frierson, J. A. Renwick, and G. K. Vallis. “Observations, Simulations, and Dynamics of Jet Stream Variability and Annular Modes.” Journal of Climate 23, no. 23 (2010): 6186–99.

Kistner, Erica, Olivia Kellner, Jeffrey Andresen, Dennis Todey, and Lois Wright Morton. “Vulnerability of Specialty Crops to Short-Term Climatic Variability and Adaptation Strategies in the Midwestern USA.” Climatic Change 146, no. 1–2 (January 2018): 145–58. https://doi.org/10.1007-/s10584-017-2066-1.

Kral-O’Brien, Katherine C., Peter L. O’Brien, and Jason P. Harmon. “Need for False Spring Research in the Northern Great Plains, USA.” Agricultural & Environmental Letters 4, no. 1 (January 2019): 1–5. https://doi.org/10.2134/ael2019.07.0025.

Kunkel, Kenneth E., David R. Easterling, Kenneth Hubbard, and Kelly Redmond. “Temporal Variations in Frost-Free Season in the United States: 1895–2000.” Geophysical Research Letters 31, no. 3 (2004). https://doi.org/10.1029/2003GL018624.

Kurlus, Robert, Lukasz Malarzewski, and Tadeusz Niedzwiedz. “Temperature Characteristics and Spring Frost Risk in the Sour Cherry (Prunus Cerasus L.) Blooming Period in 1985–2010.” Bulletin of Geography. Physical Geography Series 6, no. 1 (December 1, 2013): 99–115. https://doi.org/10.2478/bgeo-2013-0006.

Labe, Zachary, Toby Ault, and Raul Zurita-Milla. “Identifying Anomalously Early Spring Onsets in the CESM Large Ensemble Project.” Climate Dynamics 48, no. 11–12 (June 2017):

3949–66. https://doi.org/10.1007/s00382-016-3313-2.

Larcher, Walter, Christine Kainmüller, and Johanna Wagner. "Survival Types of High Mountain Plants under Extreme Temperatures." Flora - Morphology, Distribution, Functional Ecology of Plants 205, no. 1 (January 1, 2010): 3–18. https://doi.org/10.1016/j.flora.2008.12.005.

Lawhorn, Brandon, and Robert C. Balling. "Temporal and Spatial Variations in Freeze Warnings in the Conterminous United States: 2005–2018." Theoretical and Applied Climatology 139, no. 3 (February 1, 2020): 1379–84. https://doi.org/10.1007/s00704-019-03056-8.

León, José Andrés Pérez. "Global Reanalysis: Goodbye ERA-Interim, Hello ERA5." Text. ECMWF, April 15, 2019. https://www.ecmwf.int/en/newsletter/159/meteorology/global-reanalysis-goodbye-era-interim-hello-era5.

Lindkvist, L., Gustavsson, T., Bogren, J., 2000. A frost assessment method for mountainous areas. Agricultural and Forest Meteorology 102, 51–67. doi:10.1016/S0168-1923(99)00087-8

Lobell, David B., and Christopher B. Field. "California Perennial Crops in a Changing Climate." Climatic Change 109 (December 2011): 317–33. http://dx.doi.org.proxy1.cl.msu.edu/10.1007/s10584-011-0303-6.

Logan, Joanne, Marcella A. Mueller, and Michael J. Searcy. "Microclimates, Peach Bud Phenology, and Freeze Risks in a Topographically Diverse Orchard." HortTechnology 10, no. 2 (January 2000): 337–40. https://doi.org/10.21273/HORTTECH.10.2.337.

Longstroth, Mark. "Freeze Damage Depends on Tree Fruit Stage of Development." MSU Extension, March 2012. https://www.canr.msu.edu/news/freeze_damage_depends_on_tree_fruit_stage-_of_development.

Marino, Garrett P, Dale P Kaiser, Lianhong Gu, and Daniel M Ricciuto. "Reconstruction of False Spring Occurrences over the Southeastern United States, 1901–2007: An Increasing Risk of Spring Freeze Damage?" Environmental Research Letters 6, no. 2 (April 1, 2011): 024015. https://doi.org/10.1088/1748-9326/6/2/024015.

Maurer, E. P., H. G. Hidalgo, T. Das, M. D. Dettinger, and D. R. Cayan. "The Utility of Daily Large-Scale Climate Data in the Assessment of Climate Change Impacts on Daily Streamflow in California." Hydrology and Earth System Sciences 14, no. 6 (June 1, 2010): 1125–38. https://doi.org/10.5194/hess-14-1125-2010.

NASS, 2015. Cherry Production. National Agricultural Statistics Service, Agricultural Statistics Board, U.S. Department of Agriculture.

NASS, 2012. Cherry Production. National Agricultural Statistics Service, Agricultural Statistics Board, U.S. Department of Agriculture.

NASS, 2002. Cherry Production. National Agricultural Statistics Service, Agricultural Statistics Board, U.S. Department of Agriculture.

"North American Mesoscale Forecast System (NAM) | National Centers for Environmental Information (NCEI) Formerly Known as National Climatic Data Center (NCDC)." Accessed April 4, 2021. https://www.ncdc.noaa.gov/data-access/model-data/model-datasets/north-american-mesoscale-forecast-system-nam.

"NRCS National Water and Climate Center - Climate Products - PRISM." Accessed March 6, 2020. https://www.wcc.nrcs.usda.gov/climate/prism.html. Parker, Wendy S. "Reanalyses and Observations: What's the Difference?" Bulletin of the American Meteorological Society 97, no. 9 (September 1, 2016): 1565–72. https://doi.org/10.1175/BAMS-D-14-00226.1.

"Performance Metrics for Climate Models - Gleckler - 2008 - Journal of Geophysical Research: Atmospheres - Wiley Online Library." Accessed March 17, 2021. https://agupubs.onlinelibrary.wiley.com/doi/10.1029/2007JD008972.

Perry, K.B., 1998. Basics of frost and freeze protection for horticultural crops. HortTechnology 8, 10–15.

Peterson, Alexander G., and John T. Abatzoglou. "Observed Changes in False Springs over the Contiguous United States." Geophysical Research Letters 41, no. 6 (2014): 2156–62. https://doi.org/10.1002/2014GL059266.

Powell, Arlie A. and Himelrick, David G."Freeze Protection Publication." Accessed April 5, 2021. https://ssl.acesag.auburn.edu/department/peaches/freeze.html.

"Precipitation over Monsoon Asia: A Comparison of Reanalyses and Observations in: Journal of Climate Volume 30 Issue 2 (2017)." Accessed March 12, 2021. https://journals.ametsoc.org/view/-journals/clim/30/2/jcli-d-16-0227.1.xml.

"PRISM Climate Group, Oregon State U." Accessed March 30, 2020. http://www.prism.oregonstate.edu/.

Qu, Michael, Joe Wan, and Xianjun Hao. "Analysis of Diurnal Air Temperature Range Change in the Continental United States." Weather and Climate Extremes 4 (August 1, 2014): 86–95. https://doi.org/10.1016/j.wace.2014.05.002.

"Reanalyses.Org Home Page | Advancing Reanalysis." Accessed March 30, 2020. https://reanalyses.org/reanalysesorg-home-page.

Rigby, J. R., and Amilcare Porporato. "Spring Frost Risk in a Changing Climate." Geophysical Research Letters 35, no. 12 (2008). https://doi.org/10.1029/2008GL033955.

Rijal, I., 2017. Use Of Water Mist To Reduce The Risk Of Frost Damage In Tree Fruits. Ph.D. Dissertation, Dept. of Geography, Michigan State University, East Lansing, MI.

Rodrigo, J. "Spring Frosts in Deciduous Fruit Trees – Morphological Damage and flower Hardiness." Scientia Horticulturae, 2000, 19.

Rowe, Clinton M., and Logan E. Derry. "Trends in Record-Breaking Temperatures for the Conterminous United States." Geophysical Research Letters 39, no. 16 (2012). https://doi.org/10.1029/-2012GL052775.

Skaggs, Kari E., and Suat Irmak. "Long-Term Trends in Air Temperature Distribution and Extremes, Growing Degree-Days, and Spring and Fall Frosts for Climate Impact Assessments on Agricultural Practices in Nebraska." Journal of Applied Meteorology and Climatology 51, no. 11 (November 1, 2012): 2060–73. https://doi.org/10.1175/JAMC-D-11-0146.1.

Tarek, Mostafa, François P. Brissette, and Richard Arsenault. "Evaluation of the ERA5 Reanalysis as a Potential Reference Datasetfor Hydrological Modeling over North-America." Hydrology and Earth System Sciences Discussions, July 10, 2019, 1–35. https://doi.org/10.5194/hess-2019-316.

Tetzner, Dieter, Elizabeth Thomas, and Claire Allen. "A Validation of ERA5 Reanalysis Data in the Southern Antarctic Peninsula—Ellsworth Land Region, and Its Implications for Ice Core Studies." Geosciences 9, no. 7 (June 29, 2019): 289. https://doi.org/10.3390/geosciences9070289.

Toreti, A., A. Maiorano, G. De Sanctis, H. Webber, A. C. Ruane, D. Fumagalli, A. Ceglar, S. Niemeyer, and M. Zampieri. "Using Reanalysis in Crop Monitoring and Forecasting Systems." Agricultural Systems 168 (January 1, 2019): 144–53. https://doi.org/10.1016/j.agsy.2018.07.001.

"U.S. Surface Climate Observing Reference Networks." Accessed April 5, 2021. https://www.-ncdc.noaa.gov/crn/.

Walton, Daniel, and Alex Hall. "An Assessment of High-Resolution Gridded Temperature Datasets over California." Journal of Climate 31, no. 10 (May 15, 2018): 3789–3810. https://doi.org/10.1175/JCLI-D-17-0410.1.

"What Are the Different Methods of Statistical Downscaling and What Are the Strengths/Weaknesses? | The Climate Workspace." Accessed March 4, 2020. http://www.glisaclimate.org/faqs/what-are-the-different-methods-of-statistical-downscaling-and-what-are-the-strengthsweaknesses.

"What Is ERA5 - Copernicus Knowledge Base - ECMWF Confluence Wiki." Accessed March 6, 2020. https://confluence.ecmwf.int/display/CKB/What+is+ERA5.

Winkler, J., Andresen, J.A., Bisanz, J.M., Guentchev, G., Nugent, J., Piromsopa, K., Rothwell, N., Zavalloni, C., Clark, J., Min, H.K., Pollyea, A., Prawiranata, H., 2012. Ch. 8 Michigan's Sour Cherry Industry: Vulnerability to Climate Variability and Change, in: Pryor, S.C. (Ed.), Climate

Change in the Midwest: Impacts, Risks, Vulnerability, and Adaptation. Indiana University Press, Bloomington, IN, pp. 69–81.

Winkler, J.A., Cinderich, A.B., Ddumba, S.D., Doubler, D., Nikolic, J., Perdinan, Pollyea, A.M., 143 Young, D.R., Zavalloni, C., 2013. 2.04 - Understanding the Impacts of Climate on Perennial Crops, in: Climate Vulnerability: Understanding and Addressing Threats to Essential Resources. Elsevier, pp. 37–49.

Yu, Lejiang, Shiyuan Zhong, Xindi Bian, Warren E. Heilman, and Jeffrey A. Andresen. "Temporal and Spatial Variability of Frost-Free Seasons in the Great Lakes Region of the United States." International Journal of Climatology 34, no. 13 (November 2014): 3499–3514. https://doi.org/10.1002/joc.3923.

Zavalloni, C., J. A. Andresen, and J.A. Flore J.A. Winkler J.R. Black and T.L. Beedy, 2006. The Pileus Project: Climatic Impacts on Sour Cherry Production in the Great Lakes Region in Past and Projected Future Time Frames. Acta Hort 707: 101-108.